

Utah State University

DigitalCommons@USU

---

All Graduate Theses and Dissertations, Spring  
1920 to Summer 2023

Graduate Studies

---

8-2023

## A Scalable, Cost-Oriented Approach for Computing Charge Plans for Electric Bus Fleets

Daniel T. Mortensen  
*Utah State University*

Follow this and additional works at: <https://digitalcommons.usu.edu/etd>



Part of the [Electrical and Computer Engineering Commons](#)

---

### Recommended Citation

Mortensen, Daniel T., "A Scalable, Cost-Oriented Approach for Computing Charge Plans for Electric Bus Fleets" (2023). *All Graduate Theses and Dissertations, Spring 1920 to Summer 2023*. 8861.  
<https://digitalcommons.usu.edu/etd/8861>

This Dissertation is brought to you for free and open access by the Graduate Studies at DigitalCommons@USU. It has been accepted for inclusion in All Graduate Theses and Dissertations, Spring 1920 to Summer 2023 by an authorized administrator of DigitalCommons@USU. For more information, please contact [digitalcommons@usu.edu](mailto:digitalcommons@usu.edu).



A SCALABLE, COST-ORIENTED APPROACH FOR COMPUTING CHARGE PLANS  
FOR ELECTRIC BUS FLEETS

by

Daniel T. Mortensen

A dissertation submitted in partial fulfillment  
of the requirements for the degree

of

DOCTOR OF PHILOSOPHY

in

Electrical Engineering

Approved:

---

Jacob Gunther, Ph.D.  
Major Professor

---

Todd Moon, Ph.D.  
Committee Member

---

Greg Droge, Ph.D.  
Committee Member

---

Kevin Moon, Ph.D.  
Committee Member

---

John Edwards, Ph.D.  
Committee Member

---

D. Richard Cutler, Ph.D.  
Vice Provost of Graduate Studies

UTAH STATE UNIVERSITY  
Logan, Utah

2023

Copyright © Daniel T. Mortensen 2023

All Rights Reserved

## ABSTRACT

A Scalable, Cost-Oriented Approach for Computing Charge Plans for Electric Bus Fleets

by

Daniel T. Mortensen, Doctor of Philosophy

Utah State University, 2023

Major Professor: Jacob Gunther, Ph.D.  
Department: Electrical and Computer Engineering

Recent attention for reduced carbon emissions has pushed transit authorities to adopt battery electric buses (BEBs). One challenge experienced by BEB users is extended charge times, which create logistical challenges and may force BEBs to charge when energy is more expensive. Furthermore, BEB charging leads to high power demands, which can significantly increase monthly power costs and may push electrical infrastructure beyond its present capacity, requiring expensive upgrades. This work presents a novel method for minimizing the monthly cost of BEB charging while meeting bus route constraints. This method extends previous work by incorporating a more novel cost model, effects from uncontrolled loads, differences between daytime and overnight charging, and variable rate charging. We propose using mixed integer linear programs, to encode the charging action space, physical bus constraints, and battery state of charge dynamics. We also consider results for three scenarios: uncontested charging, which uses equal numbers of buses and chargers, contested charging, which has more buses than chargers, and variable charge rates. We desire to show that BEBs can be added to the fleet so that both the runtime of the planning framework and monthly cost increase linearly with the number of buses so that the charge planning framework is scalable.



## PUBLIC ABSTRACT

A Scalable, Cost-Oriented Approach for Computing Charge Plans for Electric Bus Fleets

Daniel T. Mortensen

Recent attention for reduced carbon emissions has pushed transit authorities to adopt battery electric buses (BEBs). One challenge experienced by BEB users is extended charge times, which create logistical challenges and may force BEBs to charge when energy is more expensive. Furthermore, BEB charging leads to high power demands, which can significantly increase monthly power costs and may push electrical infrastructure beyond its present capacity, requiring expensive upgrades. This work presents a novel method for minimizing the monthly cost of BEB charging while meeting bus route constraints. This method extends previous work by incorporating a more novel cost model, effects from uncontrolled loads, differences between daytime and overnight charging, and variable rate charging. We propose using mixed integer linear programs, to encode the charging action space, physical bus constraints, and battery state of charge dynamics. We also consider results for three scenarios: uncontested charging, which uses equal numbers of buses and chargers, contested charging, which has more buses than chargers, and variable charge rates. We desire to show that BEBs can be added to the fleet so that both the runtime of the planning framework and monthly cost increase linearly with the number of buses so that the charge planning framework is scalable.

To family and friends without whom I would not be here.

## ACKNOWLEDGMENTS

I am so happy that my advisor helped me and that my wife fed me.

I also want to express gratitude to the Space Dynamics Laboratory for their support through this experience. Finally, much of the research in this and future documents was also funded in part by the National Science Foundation through the ASPIRE Engineering Research Center under Grant No. EEC-1941524, the Department of Energy through a prime award with ABB under Grant No. DE-EE0009194, and PacifiCorp under contract number 3590.

Daniel T. Mortensen

## CONTENTS

	Page
ABSTRACT . . . . .	iii
PUBLIC ABSTRACT . . . . .	v
ACKNOWLEDGMENTS . . . . .	vii
LIST OF TABLES . . . . .	x
LIST OF FIGURES . . . . .	xi
1 Introduction . . . . .	1
2 A Discretized Approach to Compute Charge Plans . . . . .	5
2.1 Introduction . . . . .	5
2.2 Literature Review . . . . .	6
2.2.1 Battery Charging . . . . .	6
2.2.2 Cost Optimization . . . . .	8
2.2.3 Contributions . . . . .	8
2.3 Graph Based Problem Formulation . . . . .	9
2.3.1 Graph Formulation . . . . .	9
2.3.2 Graph Constraints . . . . .	13
2.3.3 Section Summary . . . . .	17
2.4 Battery State of Charge . . . . .	18
2.5 Multi-Graph Additions . . . . .	25
2.6 Objective Function . . . . .	26
2.6.1 Energy . . . . .	27
2.6.2 Power . . . . .	28
2.6.3 On/Off Peak Rates . . . . .	29
2.6.4 Objective Function . . . . .	31
2.7 Results . . . . .	32
2.7.1 Baseline and Setup . . . . .	32
2.7.2 Uncontested Results . . . . .	33
2.7.3 Contested Results . . . . .	36
2.7.4 Multi-Rate Comparison . . . . .	39
2.8 Conclusions and Future Work . . . . .	39
3 A Bin Packing Approach to Minimize Charging Cost for Electric Bus Fleets . . . . .	42
3.1 Introduction . . . . .	42
3.2 Bus Availability and Resource Contention . . . . .	44
3.2.1 Setup . . . . .	45
3.2.2 Constraints . . . . .	46
3.3 Battery State of Charge . . . . .	50

3.4	Integrating Uncontrolled Loads . . . . .	53
3.5	Objective Function . . . . .	62
3.5.1	Power Charges . . . . .	63
3.5.2	Energy Charges . . . . .	64
3.5.3	Cost Function and Final Problem . . . . .	65
3.6	Results . . . . .	65
3.6.1	Cost Comparison with Prior Work . . . . .	66
3.6.2	Scalability . . . . .	67
4	A Scalable Approach for Computing Charge Plans for Large Bus Fleets . . . . .	74
4.1	Introduction . . . . .	74
4.1.1	Energy Allocation and Group Assignment . . . . .	75
4.1.2	Session Time and Charger Assignment . . . . .	76
4.1.3	Final Optimization . . . . .	77
4.2	$p_1$ : Unconstrained Schedule . . . . .	77
4.2.1	Formulation . . . . .	79
4.2.2	Battery . . . . .	80
4.2.3	Cumulative Load Management . . . . .	81
4.2.4	Objective . . . . .	82
4.3	$p_2$ : Unconstrained Smooth Schedule . . . . .	83
4.4	$p_3$ : Group Assignment . . . . .	85
4.5	$p_4$ : Defragmentation . . . . .	87
4.6	$p_5$ : Charger Assignment . . . . .	89
4.7	$p_6$ : Optimizing Charge Schedules . . . . .	93
4.8	$p_7$ : Constrained Schedule . . . . .	95
4.9	$p_8$ : Constrained Smooth Schedule . . . . .	95
4.10	Results . . . . .	96
4.10.1	Overall Performance . . . . .	96
4.10.2	Optimality Gaps and Contention . . . . .	99
4.10.3	Contention: Sub-Optimal Schedules . . . . .	99
4.10.4	The Importance of Groups . . . . .	101
4.10.5	Effects of defragmentation . . . . .	102
4.10.6	Scalability . . . . .	103
4.11	Conclusions . . . . .	105
5	Conclusions . . . . .	112
6	Future Work . . . . .	114
	REFERENCES . . . . .	115
	CURRICULUM VITAE . . . . .	119

LIST OF TABLES

Table	Page
4.1 Description of the billing structure . . . . .	79

## LIST OF FIGURES

Figure	Page
2.1 Grid of nodes showing discrete timesteps advancing from left to right and charger states ascending vertically. . . . .	10
2.2 Grid of nodes displaying times when buses are available for charging. . . . .	10
2.3 Node to node connection. . . . .	11
2.4 Illustrates different types of edges: connect, disconnect, and charge edges. . . . .	12
2.5 Graph-based model of the complete decision-space. . . . .	12
2.6 A solution to a 2-bus 3-charger scenario. . . . .	13
2.7 A generic directed graph consisting of nodes and edges. . . . .	14
2.8 Network flow illustrating sources and sinks. . . . .	15
2.9 Example of groups in a network flow graph. . . . .	16
2.10 Incoming group edges. . . . .	17
2.11 Connect edge example for groups. . . . .	18
2.12 Depiction of which edges increase SOC for the single rate case . . . . .	18
2.13 Relationship between exit nodes (left) and entrance nodes (right) as $\delta$ . . . . .	19
2.14 Multi-Rate Charging . . . . .	20
2.15 Night and day graphs. . . . .	26
2.16 Bus SOC between night and day graphs. . . . .	26
2.17 Cost comparison between optimized and baseline algorithms. . . . .	35
2.18 15-Minute average power for one day. . . . .	36
2.19 Comparison between uncontrolled and bus loads. . . . .	36
2.20 Results for several single charger scenarios. . . . .	37

2.21	Comparison of the loads for a 5 and 11 bus scenario with one overhead charger.	38
2.22	Histogram of charge rates, where each rate is described by how much time it would take to charge a bus from 0% to 99%.	40
2.23	Scalability Analysis.	41
3.1	Bus Charging	46
3.2	Reserving time slots on chargers	49
3.3	Potential Overlap	49
3.4	State of Charge Variables	50
3.5	Placement for $\delta_i$	51
3.6	Discretization of continuous charging intervals	56
3.7	Description of the assumed billing structure	63
3.8	Cost comparison with prior work	67
3.9	15-Minute average power for one day	68
3.10	Comparison between uncontrolled and bus loads	68
3.11	Monthly Cost with 5 Chargers	68
3.12	Runtime with 5 Chargers at a 7% Gap	69
4.1	Overall Processing Chain	77
4.2	Processing chain for the energy allocation and group assignment problems	77
4.3	Processing chain for each group	78
4.4	Processing chain for the Final Optimization set	78
4.5	Descriptions of in which problems features are addressed	78
4.6	Demonstrates how bus power use is conceptualized	79
4.7	Bus schedule with availability	79
4.8	An example solution to a 3-bus, 2-charger scenario from $p_4$	89
4.9	Demonstrates how results from $p_4$ can be reexpressed in terms of continuous variables	89

4.10	Demonstrates the solution to $p_5$ . . . . .	89
4.11	Gives variables of optimization for $p_5$ . . . . .	90
4.12	Cost comparison with prior work . . . . .	97
4.13	Comparison between uncontrolled and bus loads . . . . .	98
4.14	15-Minute average power for one day . . . . .	98
4.15	Comparison of charge session duration vs average charge rate . . . . .	99
4.16	Comparison of Runtime for a 7-Charger Scenario . . . . .	100
4.17	Routes with a large gap in the route placement problem . . . . .	101
4.18	Routes with a small gap in the route placement problem . . . . .	101
4.19	Runtimes for a 18 bus 12 charger scenario at a 0.13% gap . . . . .	102
4.20	Routes with De-Fragmentation . . . . .	103
4.21	Routes without De-Fragmentation . . . . .	103
4.22	Cost comparison of different defragmentation thresholds in a pro-time optimization scheme. . . . .	104
4.23	Comparison of runtime for the uncontested and contested scenarios over different de-fragmentation criteria . . . . .	104
4.24	Runtime comparison for different numbers of buses . . . . .	105
4.25	Cost comparison for different numbers of buses . . . . .	106

## CHAPTER 1

### Introduction

Recent calls for a reduced carbon footprint have led transit authorities to adopt battery electric buses (BEBs). Replacing diesel and CNG buses with BEBs reduces environmental impact [1] as BEBs provide zero vehicle emissions [2], and can access renewable energy sources [3–5].

Charging BEBs draws power from electrical infrastructure. The combined effect of BEB charging with other necessary loads can exceed the capacity of local distribution circuits [6–8], leading to expensive infrastructure upgrades. Power providers pass the cost of upgrades on to customers. Thus, the benefits of large-scale electrified bussing seem appealing at first, but are only practical if infrastructural upgrades can be deferred or avoided altogether.

Prior literature has studied various methods for charging buses. One way in which charge times may be reduced is by charging a bus while it is in motion through dynamic charging. There are a number of ways to do this, including overhead [9] and inductive charging [10,11]. Overhead charging allows the bus to charge on overhead power lines while in motion. Inductive charging relies on specialized hardware in the roads that transfers energy to buses that pass overhead. Both methods remove the need to stop for service and allow an electric vehicle to stay in service indefinitely. Unfortunately, both methods require extensive infrastructure [12] that may not be available, or is cost prohibitive to install.

The authors of [13] and [14] propose a different approach to managing charge demands which exchanges depleted batteries for fresh ones. Such a method would eliminate both the logistical challenges of planning and the infrastructure dependence of dynamic charging. Unfortunately batteries are generally difficult to remove and require specialized hardware, technical expertise, or automation, all of which make exchanging batteries difficult in practice.

The focus of this dissertation is to manage a bus fleet’s charge needs with respect to two areas: operational impact and cost. Minimizing the operational impact means finding ways to meet each bus’s charge demands in a way that best imitates a conventional bus’s activity so that routes and bus assignments remain bus type-agnostic. Throughout this dissertation, we accomplish this by requiring that route arrival and departure times follow the schedules given for the existing bus fleets.

Throughout the remainder of this work, we consider a scenario where charging infrastructure is located at a central bus station and each bus is assumed to travel a single route periodically throughout the day. Each bus will spend time in the station after servicing its assigned route before departing once again. While in the station, each BEB may charge if a charger is available before departing on-route. Many authors have proposed methods for charging BEBs in the previously given scenario. The authors of [15–17] outline the first of many constraints we will consider in our work including a BEB’s state of charge, and battery capacity.

The second focus of this work is to best manage the cost of electricity. Because BEBs require more time to charge, it is tempting to begin with high charge rates to speed the refueling process. However doing so places large power demands on electrical infrastructure which may result in problems with network reliability and require additional maintenance and upgrades, which increase the cost of energy. Throughout this dissertation, we encode the cost of grid impacts into a fiscal rate schedule provided by Rocky Mountain Power [18] which assesses fees for energy based on time and speed of use.

Time of use is described in terms of on and off-peak periods. During off-peak hours, energy is billed with a lower cost per kWh than energy used during on-peak hours. Optimal charge schedules which manage cost with respect to on and off-peak times has been addressed by [19–21]. The speed of use is designed to penalize individuals who heavily tax the electrical grid when they use energy quickly by commanding high power values. Therefore, the measure for speed of use at any given time is computed as the average power for the previous 15 minutes and is used to compute cost in two separate charges: demand and

facilities where the demand charge is billed per kW of the maximum on-peak 15-minute average power during the month and the facilities charge is also assessed per kW of the maximum 15-minute average power for both on and off-peak hours.

Managing cost with respect to demand or fast charging has also received attention in the literature [22] although this literature selected management strategies that relied on batteries to reduce the demand on the grid. The authors of [23] and [24] propose simple, heuristic approaches to reduce power demands from BEB fleets. Work done by [25] uses a mixed integer linear program (MILP) to solve for a solution, which addresses both when buses should charge, and where they should deploy. Finally, a paper by [26] provides a MILP framework for minimizing the cost of demand power and both minimize the cost from time of use tariffs. Each of the aforementioned methods focus on demand power in relation to electric bus fleets, but do not account for external non-BEB activity on the grid.

One problem which previous work has not yet addressed is BEB charging with meter aggregation. Historically, power providers have separated consumers' energy needs into meters where each meter services a subset of a consumer's hardware such as BEBs, electric trains, buildings, etc. The power provider must constantly prepare to deliver the maximum contracted rate for each meter so that power will always be available, which introduces additional cost and effort. Aggregating meters would cause BEB chargers and other non-BEB loads to be billed in aggregate. For example, the Utah Transit Authority in Salt Lake City, UT may desire to place both an electric train which passes through the station and BEB chargers on a single meter, but are unable to because their joint energy demands exceed the limits of a single meter. An intelligent BEB charge schedule may allow for a single meter by accounting for the train load so that only one meter is needed. In our work, we allow for meter aggregation by incorporating non-BEB loads into our optimization method and refer to the non-BEB demands as "uncontrolled loads".

Another element which has gone largely unsolved is the ability to plan for large bus fleets which contain  $>100$  BEBs. For example, planning for relatively small fleets ( $<50$  BEBs) and less than 10 chargers with optimization problems from [17, 25, 26] yields for-

mulations with over  $10^5$  variables, including binary or integer variables, and over  $10^5$  constraints so that scaling to larger fleets and more chargers stresses computational resources and requires lengthy solve times.

This dissertation presents methods to compute daily charge strategies for electric bus fleets and presents the following contributions: cost function which encompasses the time and speed of use aspects from [18], the incorporation of uncontrolled loads, and the ability to plan for large bus fleets of over 100 buses. Because this dissertation follows a multi-paper format, Chapters 2 – 4 each constitute a separate journal paper on the topic. Chapter 2 computes a charge schedule which accounts for the various aspects of Rocky Mountain Power’s Schedule 8 in the presence of uncontrolled loads. One finding from 2 is that the discrete approach taken in Chapter 2 requires many variables for precise charge schedules. Chapter 3 adopts a bin packing approach so that the time variables are continuous instead of discrete, yielding precise charge plans without additional overhead. Unfortunately, the methods in both Chapters 2 and 3 cannot plan for large bus fleets without large compute resources. Chapter 4 reduces the number of computations by forming an eight-part multi-problem solution that can compute cost-oriented plans for bus fleets of 100+ buses.

## CHAPTER 2

### A Discretized Approach to Compute Charge Plans

#### 2.1 Introduction

Recent calls for a reduced carbon footprint have led transit authorities to adopt battery electric buses (BEBs). Replacing diesel and CNG buses with BEBs reduces environmental impact [1] as BEBs provide zero vehicle emissions and can access renewable energy sources [3, 4].

Charging BEBs draws power from electrical infrastructure. The combined effect of BEB charging with other necessary loads can exceed the capacity of local distribution circuits [6–8], leading to expensive infrastructure upgrades. Power providers pass the cost of upgrades on to customers. Thus, the benefits of large-scale electrified busing seem appealing at first, but are only practical if infrastructural upgrades can be deferred or avoided altogether.

One approach to deferring or avoiding upgrades is to intentionally manage when and at what rates buses should charge. An optimal charge plan must account for a number of physical constraints and operational realities. For example, buses must exceed a minimum charge level while adhering to route schedules, batteries must have sufficient time to charge, and buses must share a limited number of chargers. The focus of this work is to find an optimal charge schedule which meets these requirements and minimizes the cost of electricity and grid impacts in the presence of other uncontrolled loads. This problem is referred to hereafter as the “charge problem”.

The remainder of this paper is organized as follows: Section II describes prior related work and Section III outlines a graph-based framework for modeling the environment including buses, routes, chargers, and uncontrolled loads. Section IV incorporates the problem constraints involving battery charge dynamics and Section V extends the the graph framework to account for differences between day and night operations. Section VI translates

the rate schedule used for billing into an objective function. Finally, Sections VII and VIII present results and describe future work, respectively.

## 2.2 Literature Review

This section summarizes prior work related to the charge problem and includes discussion on battery charging and managing runtime costs. The final subsection discusses the contributions of this paper, and how they relate to prior methods.

### 2.2.1 Battery Charging

Recharging BEBs is more time consuming than refueling diesel and CNG buses [27]. A diesel or CNG engine can refuel in several minutes but an electric bus may require several hours to charge, making the extended charge time a primary concern for BEB conversion.

To circumvent long refuel times, [14] and [13] propose an approach which replaces batteries when the state of charge is low. The exchange would replace the current battery with one that was fully charged and recharge spent batteries afterward. Exchanging batteries reduces down time, but is non-trivial because battery swapping requires specialized tools and/or automation.

Another alternative is to inductively charge buses while they are in motion. Dynamic charging simplifies logistics because it eliminates the need for stationary charging. Both [11] and [10] propose methods that inductively charge BEBs using specialized hardware in the road. Furthermore, dynamic charging is supported by various planning algorithms such as [9, 12, 28].

Recharging BEBs at a station requires only the development of an intelligent charge schedule. Following a charge schedule requires minimal modifications to charging infrastructure and utilizes existing charging ports in the BEBs with no need for additional tools or automation. Algorithms for planning use foreknowledge of the runtime environment and battery dynamics to identify when and to which buses chargers should connect. Planning algorithms discussed in this review are considered on a scale from “reactive” to “global”,

where reactive methods respond to stimuli at the present, and global techniques assume complete knowledge about the operating environment to form a plan.

Because reactive planning generally focuses on present circumstances, it requires minimal knowledge of the operational environment, making reactive planning extremely versatile. Methods of this type are both computationally efficient and adapt to many use cases. One such example is illustrated in [5], which splits the total power draw between the grid and an external battery to regulate the instantaneous load. The authors of [24] give another approach which uses a Markov Decision Process to instantaneously make decisions.

Reactive algorithms can be enhanced by encoding details for future events to improve decision making. If only event details within a finite horizon are used, the algorithm becomes a hybrid, containing features of both reactive and global techniques. For example, [25] describes a technique for optimizing a charging schedule out to a scheduling horizon. Changing the horizon adjusts both the scope and computational complexity of the solution. In stochastic environments, a smaller window is beneficial as charge schedules must be frequently recomputed, whereas in more stable circumstances, longer windows can yield improved performance.

Global algorithms include all information from the beginning to the end. Because global algorithms assume complete foreknowledge of future events, they provide globally optimal plans and achieve the highest performance. Global algorithms can encompass a number of scenarios including hardware that is either distributed [29], or collocated although many times, a distributed scenario is not feasible due to added cost or scarce charger locations.

The authors in [15, 19, 26, 30, 31] present techniques that formulate constrained optimization problems which provide solutions in terms of binary charge decisions for each bus at each time-step while constraining the power use to comply with contractual obligations. Work from [32] even minimizes the total cost of power using a time of day pricing schedule. The authors in [33] take a somewhat different approach by encoding the bus constraints in a graph and solving for an optimal solution using a network-flow approach. The discrete nature of the graph based approach allows [33] to model a non-linear charge dynamic based

on the Constant Current, Constant Voltage model. The methods given by [19, 20, 30, 33] address the problem of scheduling buses while meeting constraints for power use, however this technique could be extended by considering non-BEB activity on the grid. In particular, results from [20] will be used as a comparison for this class of algorithms later in this paper.

The authors of [34] provide a technique which accounts for grid activity by assuming the external grid behavior is known apriori and incorporating its effects into a cost function.

### 2.2.2 Cost Optimization

In addition to physical constraints such as bus routes and charging dynamics, this paper focuses on minimizing the cost associated with charging and minimizes fees assessed for on and off-peak energy use, on and off-peak power demand, and facilities power charges [18]. Prior work has dealt with charge costs in various ways. The authors in [35] propose a method to forecast power use. Work done by [23] propose a method which reduces the demand charge by using power forecasts to plan charge times [35]. When forecasting is not possible, both [22] and [5] propose methods that decreases power demand by observing the load and drawing additional power from on-site battery packs. Additionally, [30] minimized over on/off peak energy as part of their work.

### 2.2.3 Contributions

This paper develops a novel charge schedule planning framework which extends the planner proposed by [33] to include multi-rate charging, uncontrolled loads, night/day charging, and the rate schedule given in [18]. Our method formulates the bus charge problem as a Mixed Integer Linear Program (MILP) and is unique because the objective function is the cost for the transit authority (bus fleet operator) and includes charges for on-peak and off-peak energy use, on-peak and off-peak power demand, and facilities demand. The proposed framework handles contention for charging resources in a globally optimal manner which guarantees charger availability even when chargers are scarce.

Prior work has also made assumptions for night time charge behavior. Our work

eliminates the need for such by including both day and night charging in the charge schedule. The modeling of night and day charging also includes their respective operational constraints such as charge rates, bus availability, and the number of available chargers.

Our work also seeks to understand how variable rate, as compared to single rate charging, affects the cost optimality and contributes a more accurate representation of battery charging dynamics.

Furthermore, because the proposed method includes operational characteristics such as the number of buses, the number of chargers, the battery capacity, and various route metadata in the constraints, it complements prior work which determines such parameters [36], [37].

The final contribution is recognizing that our framework is a tool that enables prediction of monthly costs for transit authorities and infrastructure demand for power providers. Optimized charging schedules reduce power demand and extend the lifetime of electrical infrastructure.

### 2.3 Graph Based Problem Formulation

This section formulates the charge problem as an optimization problem where the variables are defined in a graph. The first subsection describes the intuition behind this graph-based approach and the second develops a series of equality and inequality constraints resulting in a Mixed Integer Linear Program (MILP).

#### 2.3.1 Graph Formulation

A solution to the bus charge problem is a schedule of actions for charging equipment. A schedule states both *when* and *which* bus a charger should connect, suggesting a model with two dimensions. The first dimension represents time and is given discretely in a left-to-right fashion. The second dimension encodes the charger state and extends vertically as shown in Fig. 2.1. The charger may be in one of several possible states. For example, it may be connected to one of the  $N$  buses, or it may be unconnected, giving a total of  $N + 1$  different states. This (time, state) 2-D representation is encoded as a rectangular grid of

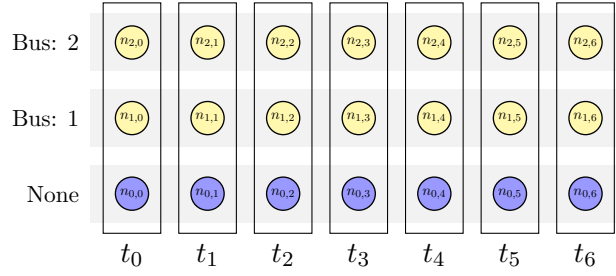


Fig. 2.1: Grid of nodes showing discrete timesteps advancing from left to right and charger states ascending vertically.

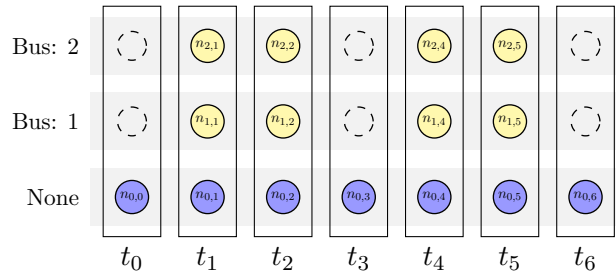


Fig. 2.2: Grid of nodes displaying times when buses are available for charging.

nodes. Node  $n_{i,j}$  represents the charger in  $i^{\text{th}}$  state during the  $j^{\text{th}}$  time index (see Fig. 2.1). For example,  $n_{1,0}$  from Fig. 2.1 represents a state where a charger is connected to Bus 1 at  $t_0$ .

We want the grid of nodes to encode the times at which each bus is at the station and available for charging. Therefore, let a nodes be present in the grid when the corresponding bus can connect to a charger, and delete from the grid nodes when a bus is away from the station. Consider the two bus scenario from Fig. 2.1 where buses 1 and 2 are away from the station at  $t_0$ ,  $t_3$ , and  $t_6$ . The schedule is encoded by removing  $n_{1,0}$ ,  $n_{2,0}$ ,  $n_{1,3}$ ,  $n_{2,3}$ ,  $n_{1,6}$ , and  $n_{2,6}$  to reflect the grid shown in Fig. 2.2.

The state of a charger at any time is represented by existing in a particular node. Changes in charger state over time are represented by the transitions from a node to multiple possible next nodes. These transitions are called edges (see Fig. 2.3) and represent four possible decisions: connect to a bus, charge a bus, remain idle, or disconnect from a bus. Edges are associated with actions and that action is determined by the nodes on either end. Consider the edge from  $n_{0,0}$  to  $n_{0,1}$  in Fig. 2.4. This edge represents a no-charge

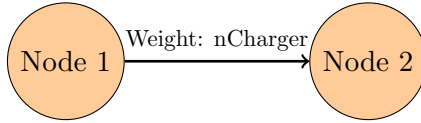


Fig. 2.3: Node to node connection.

decision because the nodes on both ends represent the disconnected charge state at times  $t_0$  and  $t_1$ . Chargers cannot charge while disconnected, so the edge decision is no-charge. Similarly, the edge between  $n_{1,1}$  and  $n_{1,2}$  indicates a decision to-charge as both  $n_{1,1}$  and  $n_{1,2}$  represent states where a charger is connected at times  $t_1$  and  $t_2$ . Both to-charge and no-charge decisions are represented by *horizontal* transitions in the graph and only reflect the passing of time as no changes to the physical hardware are made.

Conversely, diagonal transitions imply physical hardware changes because they represent decisions where chargers connect to or disconnect from a bus. One such example from Fig. 2.4 includes the edge from  $n_{0,0}$  to  $n_{1,1}$ . The state represented by  $n_{0,0}$  is disconnected. This edge represents an interval where a charger is disconnected at  $t_0$  and connected at  $t_1$ , implying a ‘to-connect’ decision. The same logic applies in reverse for the edge between  $n_{1,2}$  and  $n_{0,3}$ . Hence, the bus charge problem can be described in terms of nodes and edges (i.e. a graph) where nodes represent bus availability for charging and edges encode all possible charge decisions.

A charge schedule can be thought of as a list of charge decisions that govern charge behavior. Because decisions are represented by edges in the graph, a schedule is also represented by a sequence of connected edges that form a path through the graph. If an edge is selected, or active, it is considered part of the path. Active and inactive edges are represented edge weights equal to 1 and 0, respectively.

A graph with binary edge weights can only represent a plan for one charger. This representation can be expanded to represent an arbitrary number of chargers by using integer valued weights, where each weight gives the number of chargers in the transition.

Consider a three-charger scenario using the graph in Fig. 2.5. A solution where one charger is connected to Bus 1 from  $t_1$  to  $t_2$  and to Bus 2 from  $t_4$  to  $t_5$  would be expressed

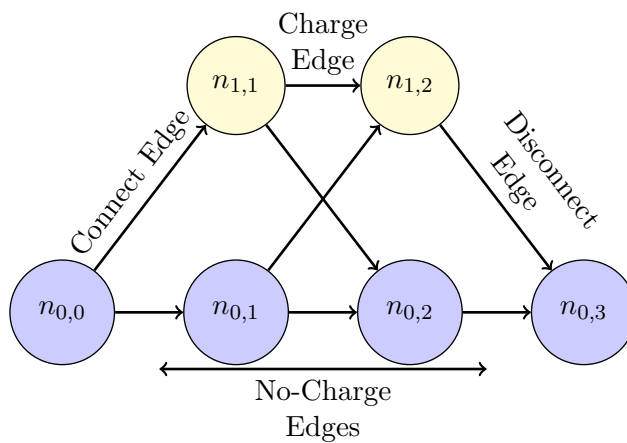


Fig. 2.4: Illustrates different types of edges: connect, disconnect, and charge edges.

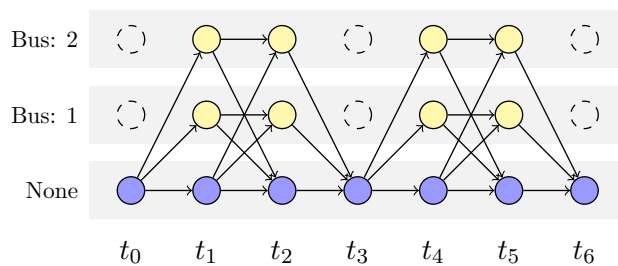


Fig. 2.5: Graph-based model of the complete decision-space.

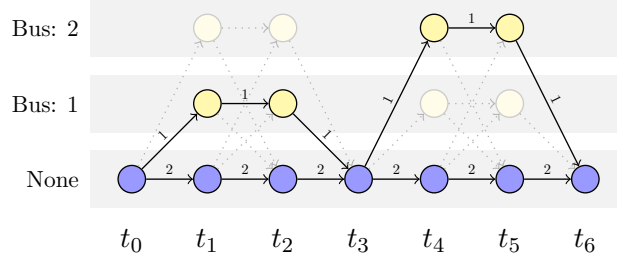


Fig. 2.6: A solution to a 2-bus 3-charger scenario.

by assigning unit weights to the appropriate connect, charge, and disconnect edges. The second charger remains idle as illustrated by the active edges along the bottom row of charger states (see Fig. 2.6).

In summary, the graph encodes bus availability with nodes, decisions with edges, and schedules with edge weights. Solving the bus charge problem becomes a matter of finding the optimal set of edge weights, where optimal is meant to denote the most cost effective charge plan.

### 2.3.2 Graph Constraints

Finding the optimal charge schedule can be expressed as an optimization problem, where the graph is used to derive equality and inequality constraints for a mixed integer linear program (MILP)

$$\begin{aligned} \min_{\mathbf{y}} \mathbf{r}^T \mathbf{y} \text{ subject to} \\ F\mathbf{y} = \mathbf{f}, Q\mathbf{y} \leq \mathbf{q}, \end{aligned} \quad (2.1)$$

where the equality and inequality constraints are encoded in  $F$ ,  $\mathbf{f}$ ,  $Q$  and  $\mathbf{q}$ . The variable  $\mathbf{y}$  is a vector containing the elements of the solution and has the form

$$\mathbf{y}^T = \left[ \mathbf{x}^T \ \mathbf{d}^T \ \mathbf{g}^T \ \mathbf{e}^T \ \mathbf{p}^T \ \hat{p} \ \hat{p}_{\text{off-peak}} \ \hat{p}_{\text{on-peak}} \right], \quad (2.2)$$

where each element of  $\mathbf{y}$  is defined later in this paper.

This subsection formulates two sets of constraints. The first represents the graph structure, enforces conservation of chargers, and defines the number of chargers through

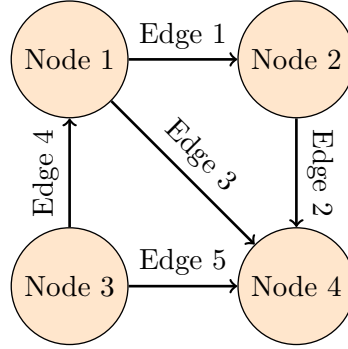


Fig. 2.7: A generic directed graph consisting of nodes and edges.

a set of net-flow constraints. The second prevents the charger from thrashing between connected/disconnected states and enforces one-bus/one-charger connectivity by enforcing what we call “group flow” constraints.

### Net-Flow Constraints

Network flow constraints are expressed in matrix-vector form as

$$\mathbf{A}\mathbf{x} = \mathbf{c}_f, \quad (2.3)$$

where  $A$  is the graph incidence matrix,  $\mathbf{x}$  is the  $n_E \times 1$  vector of edge weights and corresponds to  $\mathbf{x}$  in equation 2.2, and  $\mathbf{c}_f$  is  $n_N \times 1$  and equals the difference between incoming and outgoing edge weights, or *net-flow*. The parameter  $n_E$  is the number of edges and  $n_N$  is the number of nodes.

An incidence matrix organizes relationships between nodes and edges by describing which edges leave and enter which nodes. The matrix  $A$  is an  $n_N \times n_E$  matrix and expresses incoming connections between the  $i^{\text{th}}$  node and  $j^{\text{th}}$  edge by  $A_{i,j} = 1$ . Similarly, outgoing connections are given by  $A_{i,j} = -1$ , and no connection with  $A_{i,j} = 0$ . For example, the graph in Fig. 2.7 is represented as:

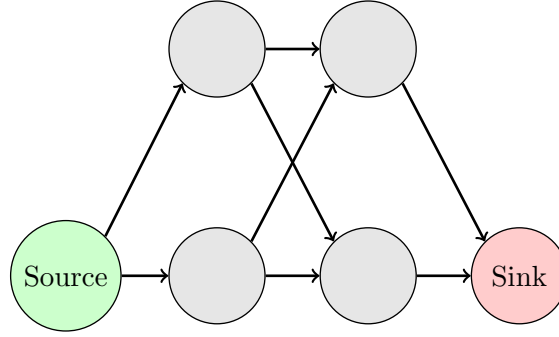


Fig. 2.8: Network flow illustrating sources and sinks.

$$\begin{bmatrix} -1 & 0 & -1 & 1 & 0 \\ 1 & -1 & 0 & 0 & 0 \\ 0 & 0 & 0 & -1 & -1 \\ 0 & 1 & 1 & 0 & 1 \end{bmatrix} \quad (2.4)$$

The difference between the number of chargers entering and leaving, or the *net-flow*, can be expressed in terms of  $A$  as seen in equation (2.3). Because the number of chargers does not change, the number of chargers entering and leaving a node must be equal. This is expressed in linear form as  $a_i^T x = 0$ , where  $a_i$  is the  $i^{\text{th}}$  row of  $A$ . The only exceptions occur at *source* and *sink* nodes.

A source node represents the beginning state for all chargers. Because edges originate here, there are no incoming edges and the net-flow will be minus the number of chargers. This is described in linear form as  $a_i^T x = -n_C$ , where  $n_C$  is the number of chargers.

Sink nodes represent the final state, where all edges terminate (see Fig. 2.8). Because sinks have no outgoing edges, they maintain a positive net-flow equal to the number of chargers and is expressed by  $a_i^T = n_C$ .

Therefore, the *flow constraints* require the elements of  $\mathbf{c}_f$  be equal to zero for all non-source and non-sink nodes as seen in equation (2.5).

$$Ax = \begin{bmatrix} 0 & \dots & -n_C & \dots & 0 & n_C & \dots & 0 \end{bmatrix}^T. \quad (2.5)$$

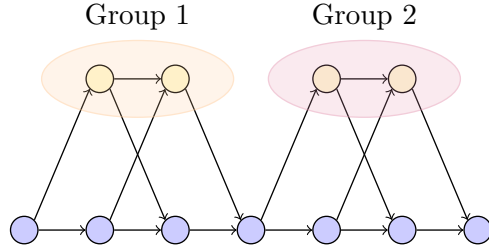


Fig. 2.9: Example of groups in a network flow graph.

Equation 2.5 can be formulated in terms of  $\mathbf{y}$  by appropriately zero-padding  $A$  such that

$$\begin{aligned} c_f &= \begin{bmatrix} A & 0 \end{bmatrix} \mathbf{y} \\ &= \tilde{A} \mathbf{y} \end{aligned} \tag{2.6}$$

### Group-flow Constraints

Another flow type, known as group flow, can be used to regulate the number of chargers entering a set of nodes. This is desired for two reasons. First, it prevents chargers from connecting multiple times during an interval when a bus is available for charging, and it limits the number of chargers connecting to a bus to be one at most.

Define a charge group as the set of all nodes for a given bus corresponding to one station visit as shown in Fig. 2.9. The *group flow* is the number of chargers that enter a group and is represented as the sum of all incoming edge weights (see Fig. 2.10).

Denote the  $n_G \times n_E$  group incidence matrix as  $B$ , where  $n_G$  is the number of groups and  $B_{i,j}$  is 1 if the  $j^{\text{th}}$  edge enters the  $i^{\text{th}}$  group and 0 otherwise. For example, the group incidence matrix corresponding to the graph in Fig. 2.11 contains 1 in the 7<sup>th</sup> and 10<sup>th</sup> columns for Group 1, and the 12<sup>th</sup> and 15<sup>th</sup> columns for group 2 as given in equation 2.7.

$$B = \begin{bmatrix} 0 & 0 & 0 & 0 & 0 & 0 & 1 & 0 & 0 & 1 & 0 & 0 & 0 & 0 & 0 & 0 \\ 0 & 0 & 0 & 0 & 0 & 0 & 0 & 0 & 0 & 0 & 0 & 1 & 0 & 0 & 1 & 0 \end{bmatrix} \tag{2.7}$$

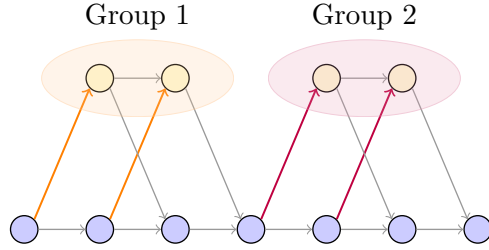


Fig. 2.10: Incoming group edges.

Let  $\mathbf{x}$  be the edge weights as before and  $\mathbf{c}_g$  be an  $n_G \times 1$  vector where the  $i^{\text{th}}$  element gives the group flow for group  $i$ . The group flow is then computed as

$$B\mathbf{x} = \mathbf{c}_g \quad (2.8)$$

But the group flow is required to be one at most to avoid connection thrashing. This is expressed by the inequality given in equation (2.9).

$$Bx \leq \mathbf{1}. \quad (2.9)$$

Similarly to (2.6), equation (2.9) can also be expressed in terms of  $\mathbf{y}$  with appropriate zero padding as

$$\begin{bmatrix} B & 0 \end{bmatrix} \mathbf{y} = \tilde{B}\mathbf{y} \quad (2.10)$$

so that

$$\tilde{B}\mathbf{y} \leq \mathbf{1}. \quad (2.11)$$

### 2.3.3 Section Summary

In summary, the bus charge problem can be formulated as a graph with nodes and edges, where charge plans are encoded as a path with unit edge weights. The charge problem aims to find a feasible path which minimizes the cost of power. Feasibility is defined through a set of net-flow and group-flow constraints. Net-flow constraints are encoded through an adjacency matrix and enforce both the conservation and total number of chargers. The group-flow constraints prevent connection thrashing and limit to one the number

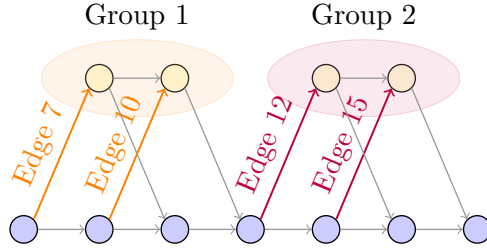


Fig. 2.11: Connect edge example for groups.

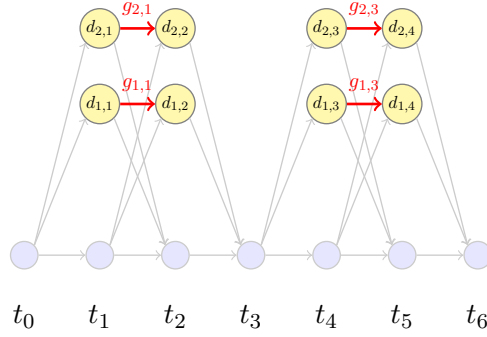


Fig. 2.12: Depiction of which edges increase SOC for the single rate case

of simultaneous charger-to-bus connections.

## 2.4 Battery State of Charge

Battery state of charge (SOC) plays a central role in the bus charge problem. Battery charge levels decay as a bus traverses a route. Solutions to the bus charge problem must account for bus routes and require that SOC values remain above a minimum threshold.

A SOC thresholding constraint requires that battery charge levels be modeled. The  $k^{\text{th}}$  SOC for bus  $i$  is denoted  $d_{i,k}$ , where  $k$  is the *node index*. The node indices used here are not directly tied to specific time steps. For example,  $d_{i,k+1}$  represents the bus SOC at the node in the graph following the node where  $d_{i,k}$  is the SOC as seen in Fig. 2.12. The set of all  $d_{i,k}$  can be organized as the vector  $\mathbf{d}$  from (2.2).

Because no charging is performed while on route,  $d_{i,k}$  will assume its lowest value when buses enter the charge station. Let  $d_{i,k+1}$  be the charge level for bus  $i$  as it enters the charge station, and  $\delta_i$  represent the power discharged while on-route. The entrance SOC can be

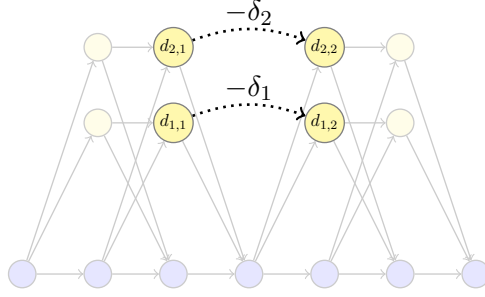


Fig. 2.13: Relationship between exit nodes (left) and entrance nodes (right) as  $\delta$

expressed as

$$d_{i,k+1} = d_{i,k} - \delta_i, \quad (2.12)$$

where  $d_{i,k}$  is the previous departure SOC for bus  $i$ . Consider the example in Fig. 2.13, where buses 1 and 2 leave the station at  $t_2$  and enter at  $t_4$ . The corresponding change in SOC is given as  $d_{1,2} = d_{1,1} - \delta_1$  and  $d_{2,2} = d_{2,1} - \delta_2$  for buses 1 and 2 respectively. The constraints from (2.12) can be expressed in linear standard form as

$$\begin{bmatrix} -1 & 1 \end{bmatrix} \begin{bmatrix} d_{i,k} \\ d_{i,k+1} \end{bmatrix} = \delta_i. \quad (2.13)$$

Equation (2.13) can be expressed in terms of  $\mathbf{y}$  with appropriate zero padding and expanded to account for the decrease in SOC for all buses outside the station. The expanded constraint is given as

$$\begin{bmatrix} 0 & \dots & -1_{d_{i,k}} & 0 & \dots & 1_{d_{i,k+1}} \end{bmatrix} \mathbf{y} = \mathbf{d}_\delta \quad (2.14)$$

$$D_\delta \mathbf{y} = \mathbf{d}_\delta,$$

where  $-1_{d_{i,k}}$  and  $1_{d_{i,k+1}}$  represent  $-1$  and  $1$  in locations corresponding to  $d_{i,k}$  and  $d_{i,k+1}$  respectively. Similar notation will be used throughout this paper as a means to imply a corresponding index for other variables.

Time periods between entrance and exit nodes represent time spent in the charge station and have the potential to charge the battery. An edge over which charging occurs

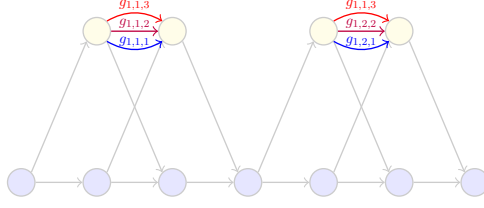


Fig. 2.14: Multi-Rate Charging

is referred to as  $x_{i,k}$ , where  $k$  gives the index of the edge's outgoing node, and  $i$  refers to the bus. When a charger occupies  $x_{i,k}$ , the resulting increase, or *gain*, in battery charge is denoted  $g_{i,k}$ , where  $i$  and  $k$  mirror the edge indices (see Fig. 2.12).

The value for  $g_{i,k}$  is computed using a single charge rate. Multiple charge rates can be encoded by connecting bus nodes with multiple edges, denoted  $x_{i,k,l}$ , where each edge has a distinct charge rate and gain denoted  $g_{i,k,l}$  (see Fig. 2.14). Having multiple charge rates gives the option for fast charging when necessary, and slow charging when possible to preserve battery health and decrease the electrical load [38].

The rate is selected by setting  $x_{i,k,l} = 1$ . All gains associated with unselected rates are set to zero. Gains that correspond to selected rates are computed using the constant current constant voltage (CCCV) model as derived in [33] which gives:

$$d_{i,k+1} = \bar{a}_l d_{i,k} - \bar{b}_l M, \quad (2.15)$$

where  $\bar{a}_l \sim (0, 1]$ , depends on the charge rate and is experimentally determined,  $M$  is the battery capacity in kWh, and  $\bar{b}_l = \bar{a}_l - 1$ . Equation (2.15) is used to show that

$$\begin{aligned} d_{i,k+1} &= \bar{a}_l d_{i,k} - \bar{b}_l M \\ d_{i,k+1} - d_{i,k} &= \bar{a}_l d_{i,k} - \bar{b}_l M - d_{i,k}, \end{aligned} \quad (2.16)$$

but the gain is equal to the difference in  $d_{i,k+1}$  and  $d_{i,k}$  such that  $g_{i,k,l} = d_{i,k+1} - d_{i,k}$ . So

$$\begin{aligned} g_{i,k,l} &= \bar{a}_l d_{i,k} - \bar{b}_l M - d_{i,k} \\ g_{i,k,l} &= (\bar{a}_l - 1) d_{i,k} - \bar{b}_l M. \end{aligned} \quad (2.17)$$

Therefore,

$$\begin{cases} g_{i,k,l} = d_{i,k}(\bar{a}_l - 1) - \bar{b}_l M & x_{i,k,l} = 1 \\ g_{i,k,l} = 0 & x_{i,k,l} = 0 \end{cases}. \quad (2.18)$$

The conditions given in (2.18) can be rewritten as

$$\begin{cases} g_{i,k,l} \leq d_{i,k}(\bar{a}_l - 1) - \bar{b}_l M & x_{i,k,l} = 1 \\ g_{i,k,l} \geq d_{i,k}(\bar{a}_l - 1) - \bar{b}_l M & \\ \\ g_{i,k,l} \leq 0 & x_{i,k,l} = 0 \\ g_{i,k,l} \geq 0 & \end{cases} \quad (2.19)$$

$$\begin{aligned} & g_{i,k,l} \leq d_{i,k}(\bar{a}_l - 1) - \bar{b}_l M - M(1 - x_{i,k,l}) \\ \Rightarrow & g_{i,k,l} \geq d_{i,k}(\bar{a}_l - 1) - \bar{b}_l M \\ & g_{i,k,l} \leq 0 + Mx_{i,k,l} \\ & g_{i,k,l} \geq 0, \end{aligned}$$

where  $M$  is the battery capacity. The results of (2.19) obtain a switching effect. When  $x_{i,k,l} = 1$ , (2.19) becomes

$$\begin{aligned} & \left. \begin{aligned} g_{i,k,l} &\leq d_{i,k}(\bar{a}_l - 1) - \bar{b}_l M \\ g_{i,k,l} &\geq d_{i,k}(\bar{a}_l - 1) - \bar{b}_l M \end{aligned} \right\} \text{Active} \\ & \left. \begin{aligned} g_{i,k,l} &\leq M \\ g_{i,k,l} &\geq 0 \end{aligned} \right\} \text{Inactive} \end{aligned} \quad (2.20)$$

The active constraints imply equality for  $g_{i,k,l} = (\bar{a}_l - 1)d_{i,k} - \bar{b}_l M$ . The inactive constraints imply that  $g_{i,k,l}$  is greater than zero and less than the battery capacity, which are trivially

satisfied. When  $x_{i,k,l} = 0$ , (2.19) becomes

$$\begin{aligned}
 & \left. \begin{aligned} g_{i,k,l} &\leq d_{i,k}(\bar{a}_l - 1) - \bar{b}_l M - M \\ g_{i,k,l} &\geq d_{i,k}(\bar{a}_l - 1) - \bar{b}_l M \end{aligned} \right\} \text{Inactive} \\
 & \left. \begin{aligned} g_{i,k,l} &\leq 0 \\ g_{i,k,l} &\geq 0 \end{aligned} \right\} \text{Active}
 \end{aligned} \tag{2.21}$$

where the inactive constraints are again trivially satisfied, and the active constraints imply equality for  $g_{i,k,l} = 0$ .

Equation (2.19) can be expressed in standard form as

$$\begin{aligned}
 -g_{i,k,l} + d_{i,k}(\bar{a}_l - 1) + x_{i,k,l} &\leq M(\bar{b}_l + 1) \\
 g_{i,k,l} - d_{i,k}(\bar{a}_l - 1) &\leq -\bar{b}_l M \\
 g_{i,k,l} - Mx_{i,k,l} &\leq 0 \\
 -g_{i,k,l} &\leq 0,
 \end{aligned} \tag{2.22}$$

and in matrix form as

$$\begin{bmatrix} -1 & \bar{a}_l - 1 & 1 \\ 1 & 1 - \bar{a}_l & 0 \\ 1 & 0 & -M \\ -1 & 0 & 0 \end{bmatrix} \begin{bmatrix} g_{i,k,l} \\ d_{i,k} \\ x_{i,k,l} \end{bmatrix} \leq \begin{bmatrix} M(\bar{b}_l + 1) \\ -\bar{b}_l M \\ 0 \\ 0 \end{bmatrix}. \tag{2.23}$$

Equation ((2.23)) can be expanded to include constraints for all  $g_{i,k,l}$ . Because each value for  $g_{i,k,l}$ ,  $d_{i,k}$ , and  $x_{i,k,l}$  is an element of  $\mathbf{y}$ , the constraints from (2.23) can be written as

$$\mathbf{G}\mathbf{y} \leq \mathbf{b}_g. \tag{2.24}$$

The value of  $d_{i,k}$  can be expressed as

$$d_{i,k+1} = d_{i,k} + \sum_l g_{i,k,l} \quad (2.25)$$

or

$$d_{i,k+1} - d_{i,k} - \sum_l g_{i,k,l} = 0, \quad (2.26)$$

because a non-zero element of  $g_{i,k,l}$  is only present for one corresponding  $l$ . This relationship is described in terms of an equality constraint such that

$$\begin{bmatrix} 1 & -1 & \dots & -1 \end{bmatrix} \begin{bmatrix} d_{i,k+1} \\ d_{i,k} \\ g_{i,k,1} \\ \dots \\ g_{i,k,l} \end{bmatrix} = 0. \quad (2.27)$$

Equation (2.27) can be appropriately zero padded to give

$$\begin{bmatrix} 1_{d_{i,k+1}} & -1_{d_{i,k}} & \dots & -1_{g_{i,k,l}} \end{bmatrix} \mathbf{y} = 0 \quad (2.28)$$

and expanded to define the values for all  $d_{i,k} \ni k > 0$  as

$$D_d \mathbf{y} = \mathbf{0}. \quad (2.29)$$

The values for  $d_{i,0}$  are defined with initial SOC conditions with additional equality constraints, denoted  $\mathbf{d}_0$  such that

$$\begin{bmatrix} 1_{d_{1,0}} & 0 & 0 & \dots & 0 \\ 0 & \dots & 1_{d_{2,0}} & 0 & 0 \\ \vdots & & \vdots & & \vdots \\ 0 & 0 & 0 & \dots & 1_{d_{i,0}} \end{bmatrix} \mathbf{y} = \mathbf{d}_0, \quad (2.30)$$

or

$$D_0 \mathbf{y} = \mathbf{d}_0. \quad (2.31)$$

Once all values for  $d_{i,k}$  are computed, they must be constrained to remain above a threshold  $\tau$ . The SOC thresholding constraint can be expressed as an inequality constraint such that

$$\begin{aligned} d_{i,k} &\geq \tau \\ \Rightarrow -d_{i,k} &\leq -\tau \\ \Rightarrow \begin{bmatrix} 0 & \dots & -1_{d_{i,k}} & \dots & 0 \end{bmatrix} \mathbf{y} &\leq -\tau. \end{aligned} \quad (2.32)$$

Equation ((2.32)) can be expanded to a matrix  $D_\tau$ , where each  $d_{i,k}$  contains a corresponding constraint row such that

$$\begin{aligned} D_\tau \mathbf{y} &\leq -\tau \mathbf{1} \\ &\leq \mathbf{d}_\tau. \end{aligned} \quad (2.33)$$

In summary, the minimum SOC for all feasible charge plans must exceed a given threshold. SOC values are computed while the bus is in the charge station. SOC values are updated when a bus enters by subtracting the discharged energy from the previous SOC estimate. SOC values are updated for in-station periods by adding the charge gains as given in (2.25). Gains are computed using a switching constraint which sets them to zero when not charging, otherwise they follow the CCCV model as set forth in (2.17). Initial SOC values are handled with the equality constraint given in (2.31) and the SOC is constrained to remain above the threshold  $\tau$  in (2.33). All constraints for  $d$  can be concatenated such that

$$\begin{bmatrix} D_0 \\ D_\delta \\ D_d \end{bmatrix} \mathbf{y} = \begin{bmatrix} \mathbf{d}_0 \\ \mathbf{d}_\delta \\ \mathbf{0} \end{bmatrix}, \quad \begin{bmatrix} D_g \\ D_\tau \end{bmatrix} \mathbf{y} \leq \begin{bmatrix} \mathbf{d}_g \\ \mathbf{d}_\tau \end{bmatrix} \quad (2.34)$$

and expressed as

$$D_{\text{eq}} \mathbf{y} = \mathbf{d}_{\text{eq}}, \quad D_{\text{ineq}} \mathbf{y} \leq \mathbf{d}_{\text{ineq}}. \quad (2.35)$$

## 2.5 Multi-Graph Additions

An additional contribution this work offers is the expansion to joint optimization of both night and day charging in a single optimization problem. Day and night operations differ in two aspects: number of chargers and bus availability. During the day, the buses can charge only at the charge station. The number of chargers in the station are limited, causing contention between buses. At night, each bus docks in a holding stall with one charger per stall, eliminating charger contention. Furthermore, nighttime charging is slow compared to daytime charging. Our model uses different rates for day and night charging.

Bus availability also changes because buses do not leave their stalls at night. This simplifies the charge problem because buses are always available for charging.

Equation (2.5) in section 2.3.2 describes the net-flow constraints which constrain the number of chargers in the source and sink nodes. Because the number of chargers are different from night to day, a separate graph is used at each transition as shown in Fig. 2.15.

Each graph is connected by equating the appropriate SOC values. Consider the multi-graph formulation given in Fig. 2.16. The morning graph is related to the day graph because  $d_{1,1}$  and  $d_{2,1}$  represent the same SOC values as  $d_{1,2}$  and  $d_{2,2}$  respectively. The same applies for the day and night graphs, where  $d_{1,5}$  and  $d_{2,5}$  represent the SOC values for  $d_{1,6}$  and  $d_{2,6}$ . This equality relationship can be expressed as an equality constraint where

$$\mathbf{d}_{\text{graph 1}} - \mathbf{d}_{\text{graph 2}} = \mathbf{0} \quad (2.36)$$

or by

$$D_{\text{multi-graph}}\mathbf{y} = \mathbf{0}, \quad (2.37)$$

where  $D_{\text{multi-graph}}$  is an  $n_{\text{Bus}} \times n_{\text{Var}}$  matrix such that

$$D_{\text{multi-graph}}\mathbf{y} = \mathbf{d}_{\text{graph 1}} - \mathbf{d}_{\text{graph 2}}. \quad (2.38)$$

Because all SOC values  $d$  are contained in  $\mathbf{y}$ , forming the matrix  $D$  amounts to placing 1

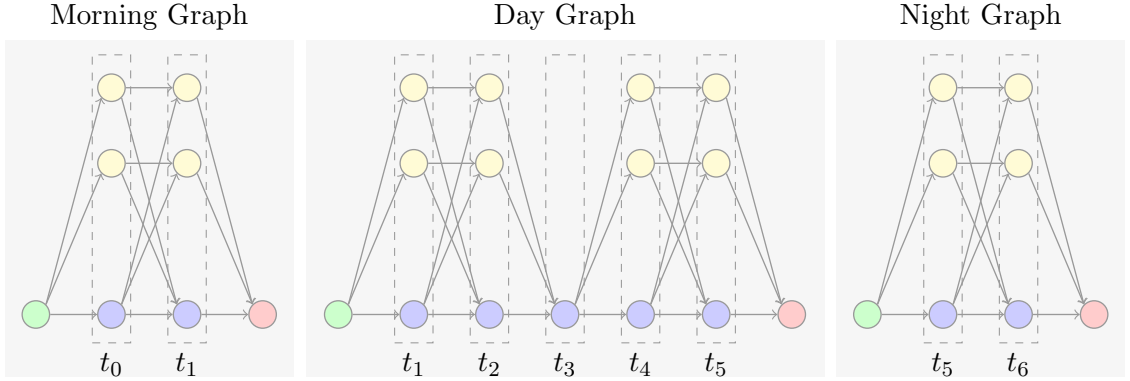


Fig. 2.15: Night and day graphs.

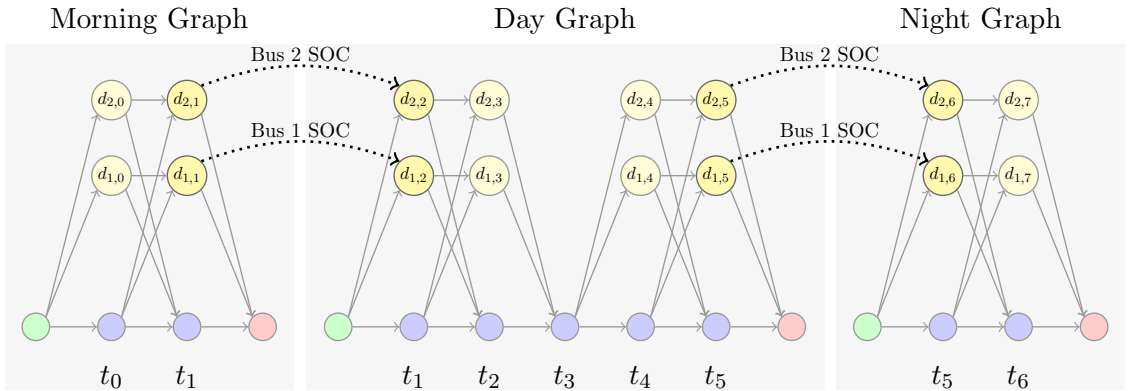


Fig. 2.16: Bus SOC between night and day graphs.

and  $-1$  at the indices corresponding to  $d_{\text{graph } 1}$  and  $d_{\text{graph } 2}$  respectively and zero otherwise.

## 2.6 Objective Function

The objective function in this work models the rate schedule used in [18], where the cost is modeled as the monthly charge a transit authority receives from the power provider. The objective function includes charges for energy, power, and facility use and implements both on and off-peak rates.

The objective function also includes effects and costs of uncontrolled loads. Uncontrolled loads might include the effects of patrons charging personal electric vehicles, electric trains passing through, CNG stations, etc. The loads used in this work were recorded at the

UTA Intermodal Hub station in Salt Lake City (SLC), Utah as the average power sampled at uniform time intervals.

### 2.6.1 Energy

Energy cost is assessed per Kilowatt-hour of energy consumed and includes energy consumed by uncontrolled loads and bus chargers. Let  $\mathbf{p}$  be the average external power used at each timestep, where  $\mathbf{p}_i$  is the average power draw between  $t_j$  and  $t_{j+1}$ . The energy consumed by external loads from  $t_j$  to  $t_{j+1}$  is computed as

$$e_j^l = \mathbf{p}_i \cdot \Delta_t, \quad (2.39)$$

where  $\Delta_t$  is the change in time from  $t_j$  to  $t_{j+1}$  in hours. The energy consumed by bus chargers for the same interval is computed as

$$e_j^b = \sum_{k \in t} g_{i,k,l}, \quad (2.40)$$

where  $k \in t$  represents all values for  $g$  that took place between  $t_i$  and  $t_{i+1}$  for every bus.

The total energy is computed as

$$e_j = e_j^l + e_j^b. \quad (2.41)$$

The expression in (2.41) can be written in standard form as

$$e_j - \sum_{k \in t} g_{i,k,l} = p_i \cdot \Delta_t$$

$$\begin{bmatrix} 1_{e_j} & -1_{g_1} & \dots & -1_{g_n} \end{bmatrix} \begin{bmatrix} e_j \\ g_1 \\ \vdots \\ g_n \end{bmatrix} = p_i \cdot \Delta_t. \quad (2.42)$$

Because power providers charge different rates for the total power consumed during the respective on and off-peak hours, equation (2.42) be modified to reflect the energy consumed

in arbitrary time periods. Let  $T$  be a set of  $t_j$ , or just  $j$ , which will later be used to denote on and off-peak periods as  $T_{\text{on}}$  and  $T_{\text{off}}$ . Equation (2.42) can be expanded to compute the total energy consumed in  $T$  as

$$e_T - \sum_{k \in T} g_{j,k,l} = \left( \sum_{j \in T} p_j \right) \cdot \Delta_t$$

$$\begin{bmatrix} 1_{e_T} & -1_{g_1} & \dots & -1_{g_n} \end{bmatrix} \begin{bmatrix} e_T \\ g_1 \\ \vdots \\ g_n \end{bmatrix} = e_T^{\text{load}}. \quad (2.43)$$

For multiple time periods, the constraint can be expanded in matrix form, where row  $i$  corresponds to the periods of time in  $T_i$ . Furthermore, by including the values for each  $e_{T_i}$  in  $\mathbf{y}$  and zero-padding appropriately, the expanded form of (2.43) can be written as

$$E\mathbf{y} = \mathbf{e}^{\text{load}}, \quad (2.44)$$

where row  $i$  in  $E$  reflects (2.43) for the time intervals in  $T_i$ , and  $\mathbf{e}_i^{\text{load}}$  contains the energy consumed by uncontrolled loads during  $T_i$ .

### 2.6.2 Power

Power costs are computed for the maximum average power draw, where the average is computed over a 15 minute sliding window. The average power can be computed as the energy in the window divided by the window length in hours. In this case, a 15 minute window equates to a quarter hour. Let  $\bar{p}_j$  be the average power from  $j - 15$  to  $j$ . Equation

(2.43) can be adapted to compute the average power as

$$\bar{p}_j - \left( \sum_{k \in T_j} \frac{1}{4} g_{i,k,l} \right) = \left( \sum_{i \in T_j} p_i \right) \cdot \frac{\Delta_t}{4}$$

$$\begin{bmatrix} 1_{\bar{p}_j} & -\frac{1_{g_1}}{4} & \dots & -\frac{1_{g_n}}{4} \end{bmatrix} \begin{bmatrix} e_j \\ g_1 \\ \vdots \\ g_n \end{bmatrix} = \frac{p_T \cdot \Delta_t}{4}. \quad (2.45)$$

Equation (2.45) can further be expanded and zero padded to compute the average power at each time,  $t_j$  by applying (2.45) to the corresponding window as

$$P\mathbf{y} = \mathbf{p}. \quad (2.46)$$

The maximum average power, denoted  $\hat{p}$ , is greater than or equal to each average power computed in (2.46). This yields an additional set of inequality constraints

$$\begin{bmatrix} -1_{\hat{p}} & 1_{\bar{p}_0} & 0 & \dots & 0 \\ -1_{\hat{p}} & 0 & 1_{\bar{p}_1} & \dots & 0 \\ -1_{\hat{p}} & 0 & 0 & \dots & 1_{\bar{p}_j} \end{bmatrix} \mathbf{y} \leq \mathbf{0} \quad (2.47)$$

$$P_{\max} \mathbf{y} \leq \mathbf{0}.$$

Because the max average power is minimized in the objective function, the value for  $\hat{p}_{\max}$  will be forced down to the value of the greatest average power computed in (2.46), and accurately reflect the maximum average power.

### 2.6.3 On/Off Peak Rates

Power providers divide each day into on and off-peak periods during which different rates are applied for both energy and power costs. Let  $H$  and  $L$  be the respective sets of all time indices in on and off peak periods respectively. The cost of energy during on-peak

hours can be expressed as

$$\begin{aligned}
c_{\text{energy}H} &= \left( \sum_{j \in H} e_j \right) r_{e_{\text{on}}} \\
&= \begin{bmatrix} r_{e_1} & 0 & \dots & 0 & r_{e_4} & \dots & 0 \end{bmatrix} \mathbf{y} \\
&= \mathbf{r}_{e_{\text{on}}}^T \mathbf{y},
\end{aligned} \tag{2.48}$$

where  $\mathbf{r}_e^{\text{on}}$  contains the value of  $r_e^{\text{on}}$  at the index corresponding to  $e_j$  in  $\mathbf{y} \forall j \in H$ . A similar formulation can be used to describe the cost of energy consumed during off-peak hours.

An on-peak rate also applies to charges for power. Equation (2.47) can be adapted to only include rows that correspond to average power values during on-peak hours such that

$$\begin{aligned}
\begin{bmatrix} -1_{\hat{p}_{\text{on}}} & 1_{\bar{p}_0} & 0 & \dots & 0 \\ -1_{\hat{p}_{\text{on}}} & 0 & 1_{\bar{p}_1} & \dots & 0 \\ -1_{\hat{p}_{\text{on}}} & 0 & 0 & \dots & 1_{\bar{p}_j} \end{bmatrix} \mathbf{y} \leq \mathbf{0} \\
P_{\text{on}} \mathbf{y} \leq \mathbf{0}.
\end{aligned} \tag{2.49}$$

Similarly, the off-peak max average power can be computed as

$$\begin{aligned}
\begin{bmatrix} -1_{\hat{p}_{\text{off}}} & 1_{\bar{p}_0} & 0 & \dots & 0 \\ -1_{\hat{p}_{\text{off}}} & 0 & 1_{\bar{p}_1} & \dots & 0 \\ -1_{\hat{p}_{\text{off}}} & 0 & 0 & \dots & 1_{\bar{p}_j} \end{bmatrix} \mathbf{y} \leq \mathbf{0} \\
P_{\text{off}} \mathbf{y} \leq \mathbf{0},
\end{aligned} \tag{2.50}$$

where each row corresponds to  $\bar{p}_j \forall j \in L$ .

Many power providers include a facilities charge. The facilities charge is assessed per kW of the maximum average power and ignores on and off-peak times. The total max average power is calculated using (2.47).

The total power cost can be computed as the sum of the on-peak, off-peak, and facilities charges as

$$\begin{aligned} c_{\text{power}} &= \begin{bmatrix} r_{\hat{p}_{\text{on}}} & 0 & \dots & 0 & r_{\hat{p}_{\text{off}}} & 0 & \dots & 0 & r_{\hat{p}_{\text{facilities}}} \end{bmatrix} \mathbf{y} \\ &= \mathbf{r}_{\hat{p}}^T \mathbf{y}. \end{aligned} \quad (2.51)$$

#### 2.6.4 Objective Function

The objective function combines the cost of energy and power, where the on-peak and off-peak energy is combined as

$$\begin{aligned} c_{\text{energy}} &= \mathbf{r}_{e_{\text{on}}}^T \mathbf{y} + \mathbf{r}_{e_{\text{off}}}^T \mathbf{y} \\ &= (\mathbf{r}_{e_{\text{on}}} + \mathbf{r}_{e_{\text{off}}})^T \mathbf{y} \\ &= \mathbf{r}_e^T \mathbf{y}. \end{aligned} \quad (2.52)$$

The combined expression is given as

$$\begin{aligned} c_{\text{total}} &= c_{\text{power}} + c_{\text{energy}} \\ &= \mathbf{r}_e^T \mathbf{y} + \mathbf{r}_{\hat{p}}^T \mathbf{y} \\ &= (\mathbf{r}_e + \mathbf{r}_{\hat{p}})^T \mathbf{y} \\ &= \mathbf{r}^T \mathbf{y}. \end{aligned} \quad (2.53)$$

Equation (2.53) is used as the objective function in a mixed integer linear program of the form

$$\begin{aligned} \min_{\mathbf{y}} \mathbf{r}^T \mathbf{y} \text{ subject to} \\ C_{\text{eq}} \mathbf{y} = \mathbf{c}_{\text{eq}}, \quad C_{\text{ineq}} \mathbf{y} \leq \mathbf{c}_{\text{ineq}}, \end{aligned} \quad (2.54)$$

where  $C_{\text{eq}}$ ,  $\mathbf{c}_{\text{eq}}$ ,  $C_{\text{ineq}}$ , and  $\mathbf{c}_{\text{ineq}}$  are formed by stacking the equality and inequality constraints from (2.6), (2.11), (2.35), (2.46), (2.47), (2.49), and (2.50),

$$\begin{aligned} & \min_{\mathbf{y}} \mathbf{r}^T \mathbf{y} \text{ subject to} \\ & \begin{bmatrix} \tilde{A} \\ D_{\text{eq}} \\ P \end{bmatrix} \mathbf{y} = \begin{bmatrix} \mathbf{c}_f \\ \mathbf{d}_{\text{eq}} \\ \mathbf{p} \end{bmatrix}, \quad \begin{bmatrix} \tilde{B} \\ D_{\text{ineq}} \\ P_{\text{max}} \\ P_{\text{on}} \\ P_{\text{off}} \end{bmatrix} \mathbf{y} \leq \begin{bmatrix} \mathbf{1} \\ \mathbf{d}_{\text{ineq}} \\ \mathbf{0} \\ \mathbf{0} \\ \mathbf{0} \end{bmatrix}. \end{aligned} \quad (2.55)$$

## 2.7 Results

This section contains results of the planning framework and is subdivided into three subsections: uncontested results, contested results, and multi-rate comparisons.

### 2.7.1 Baseline and Setup

The experiments in this section compare the results of the framework given in (2.55) with a baseline that models the general behavior of bus drivers at the Utah Transit Authority (UTA) in Salt Lake City, Utah and the planning framework from [20]. All methods use a MILP to find an optimal solution and are solved up to a 2% gap using Gurobi [39]. Model parameters such as  $\delta$ , arrival, and departure times were computed from historical data provided by UTA.

According to UTA, bus drivers generally charge whenever possible. Our baseline scenario reflects this default bus driver behavior using an objective function that maximizes the number of charging instances, which is computed as the sum of group flow values, resulting in the objective function

$$\max_{\mathbf{y}} \mathbf{1}^T B \mathbf{y}, \quad (2.56)$$

All other constraints are the same, which results in the baseline formulation

$$\begin{aligned} & \max_{\mathbf{y}} \mathbf{1}^T B \mathbf{y} \text{ subject to} \\ & \begin{bmatrix} \tilde{A} \\ D_{\text{eq}} \\ P \end{bmatrix} \mathbf{y} = \begin{bmatrix} \mathbf{c}_f \\ \mathbf{d}_{\text{eq}} \\ \mathbf{p} \end{bmatrix}, \quad \begin{bmatrix} \tilde{B} \\ D_{\text{ineq}} \\ P_{\text{max}} \\ P_{\text{on}} \\ P_{\text{off}} \end{bmatrix} \mathbf{y} \leq \begin{bmatrix} \mathbf{1} \\ \mathbf{d}_{\text{ineq}} \\ \mathbf{0} \\ \mathbf{0} \\ \mathbf{0} \end{bmatrix}. \end{aligned} \quad (2.57)$$

Each experiment is run using a five minute timestep such that the time difference between  $t_k$  and  $t_{k+1}$  is five minutes. Four charge rates are used during the following experiments:  $\bar{a}_1 = 0.9851$ ,  $\bar{a}_2 = 0.9418$ ,  $\bar{a}_3 = 0.9003$ , and  $\bar{a}_4 = 0.8607$ . Each value for  $\bar{a}$  represents a different charge rate and is referenced by how much time it would take a bus to charge from 0% to 99%. For the rates used in the following set of experiments, a bus would need 25.58 hours to charge from 0% to 99% with  $\bar{a}_1$ , 6.4 hours with  $\bar{a}_2$ , 3.65 with  $\bar{a}_3$ , and 2.56 with  $\bar{a}_4$ .

Night charging uses a single charge rate of  $\bar{a}_1$  for all experiments. Experiments with single rate day charging use  $\bar{a}_4$ , and multi-rate experiments incorporate four charge options:  $\bar{a}_1$ ,  $\bar{a}_2$ ,  $\bar{a}_3$ , and  $\bar{a}_4$ .

Uncontrolled loads are modeled with data from the TRAX Power Substation (TPSS) at the UTA Intermodel Hub site in Salt Lake City. It is also assumed that each bus starts and ends each day with an SOC of 80% and has a maximum charge capacity of 100 kWh.

### 2.7.2 Uncontested Results

This section explores performance in a scenario where there is one charger per bus during the day, making charge resources *uncontested*. The optimal charge schedule associated with equation (2.55) is compared with the schedule developed by the baseline in (2.57). The total monthly cost is computed using the rates given in Rocky Mountain Power Schedule 8

and is computed in equation (2.58).

$$\begin{aligned} \text{cost} = & \text{facilitiesPower} \cdot 4.81 + \text{onPeakPower} \cdot 15.73 + \\ & \text{onPeakEnergy} \cdot 0.058282 + \text{offPeakEnergy} \cdot 0.029624 \end{aligned} \quad (2.58)$$

There is also a customer service charge of 71.00 in the rate schedule, but because the service charge does not depend on a customer's behavior, it is ignored.

Because (2.58) is driven by facilities power, on-peak power, on-peak energy, and off-peak energy, these four criteria are used to evaluate the optimal and baseline charge plans. Furthermore, because the on and off-peak energy charges contribute little to the cost differences, they have been grouped together for comparison.

Fig. 3.8 compares the cost of energy, on-peak power, and facilities power for the baseline, [20], and this work's scheduling strategies. Note how the schedule given by Hu et al. is similar in both energy costs and on-peak power charges but is more expensive in the facilities charge. These differences are expected as Hu et al. minimizes cost of energy by charging during off-peak periods. Because there is minimal charging during on-peak times, the on-peak power charges reflect the uncontrolled loads and are therefore the same. The differences in facilities is present because He et al. does not include the overall maximum average power in their framework.

Additionally, the facilities and on-peak power costs for the baseline schedule are significantly larger than the optimized schedule. To better understand the cost disparity, we observe the load profiles to identify how the optimized schedule avoids the costs incurred by the baseline.

Fig. 2.18 shows the 15 minute average power for both the baseline and optimal schedules. Note how the optimal schedule incurs a lower average power for both on and off peak time intervals. The reduction in average power is what lead to the cost disparity between the on-peak and facilities power costs in Fig. 3.8.

The underlying behavior can be observed in Fig. 2.19, which separates the loads into their controlled and uncontrolled constituents. Because the uncontrolled loads are shared

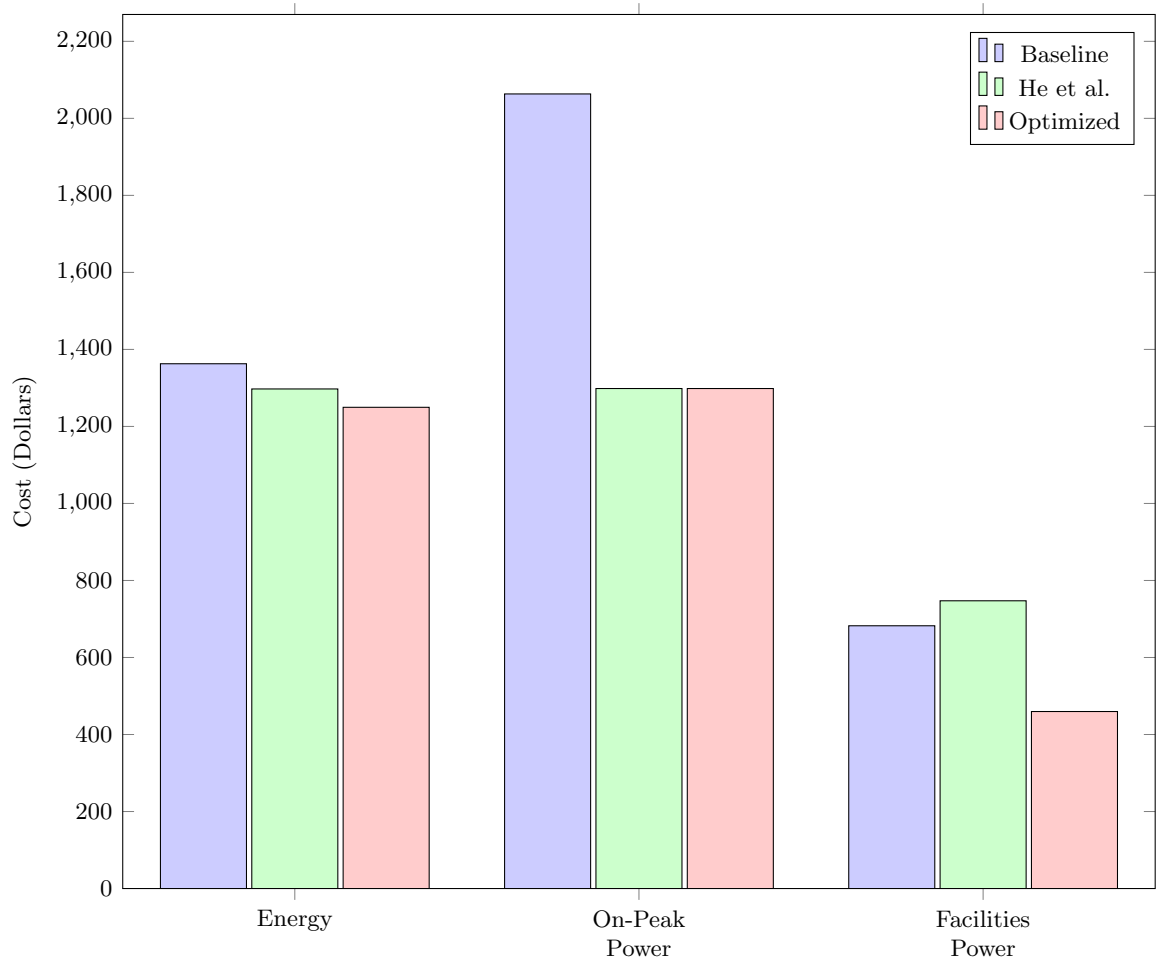


Fig. 2.17: Cost comparison between optimized and baseline algorithms.

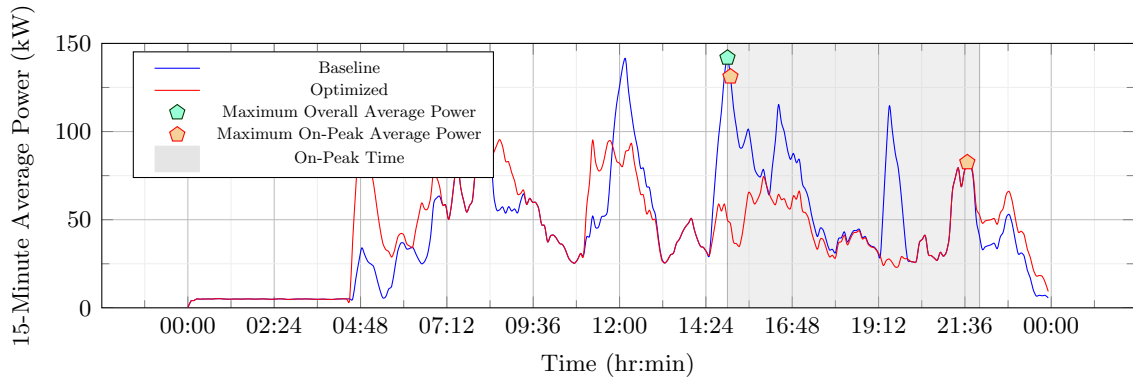


Fig. 2.18: 15-Minute average power for one day.

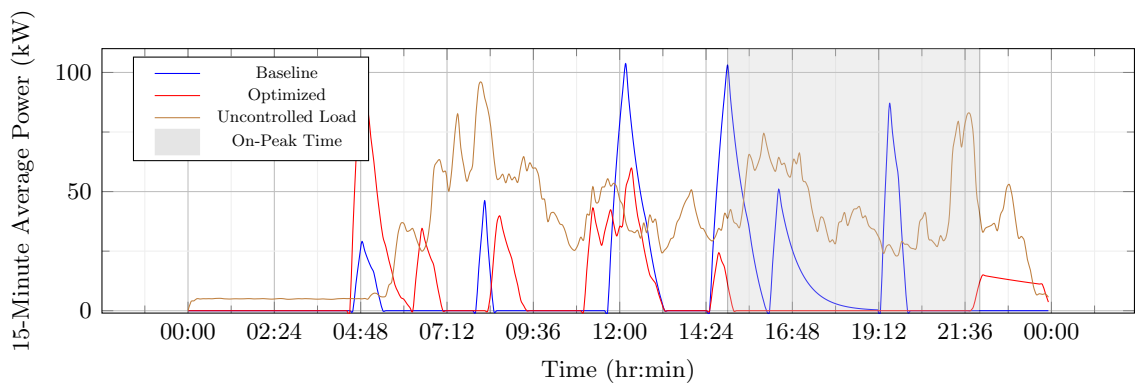


Fig. 2.19: Comparison between uncontrolled and bus loads.

between both scenarios, Fig. 2.19 shows the 15 minute average power for uncontrolled, optimal charging, and baseline charging loads.

Observe how the optimized schedule avoids charging during on-peak hours and regulates each charge event to spread the power draw over larger periods of time. Furthermore, bus charging is avoided when uncontrolled loads are high, resulting in a reduced 15 minute average power. Reducing the average power and not charging during on-peak periods results in the dramatic cost reduction shown in Fig. 3.8.

### 2.7.3 Contested Results

This section observes the performance of the optimal schedule as charge resources become scarce, creating a contested environment. Resource contention is most prevalent when

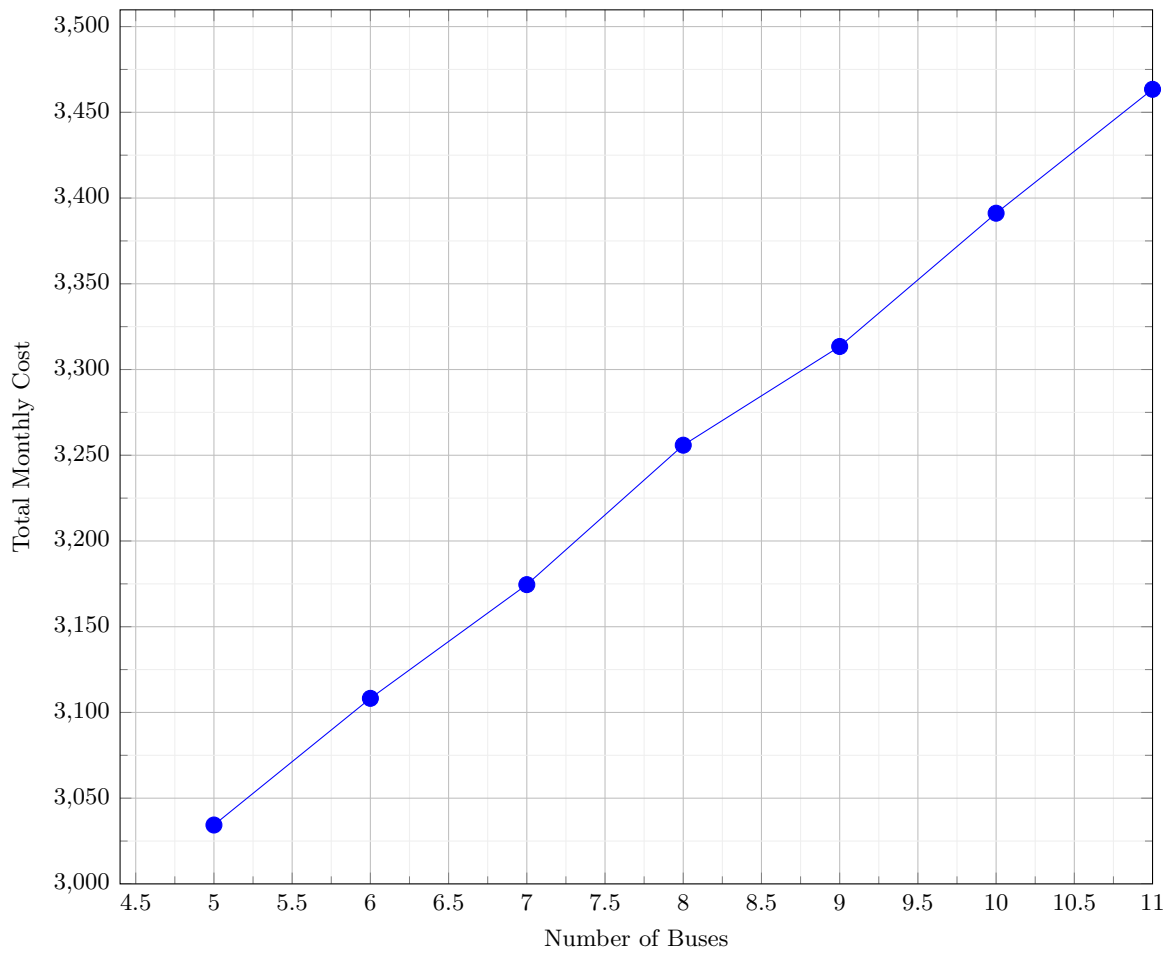


Fig. 2.20: Results for several single charger scenarios.

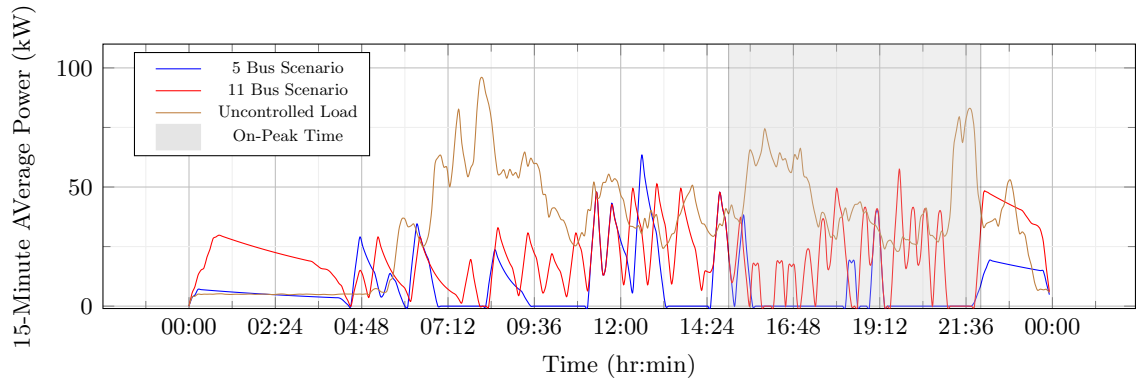


Fig. 2.21: Comparison of the loads for a 5 and 11 bus scenario with one overhead charger.

chargers are scarce and pushes buses to charge in non-ideal circumstances. For example, if charging resources are saturated during off-peak hours, other buses might be forced to charge in the on-peak window. The impact of contention is measured as the change in monthly cost when the number of chargers is held constant and the number of buses increases.

In this analysis, one charger is used and the number of buses is varied from five to eleven. Fig. 2.20 shows the monthly cost as a function of the number of buses. Note the minimal cost increase per bus, where each successive bus costs around \$75.00, which approaches the cost of energy that is required to provide transit services. Because the additional cost per bus is roughly the cost of energy, there are no additional facilities and on-peak power charges, showing that optimal charge plans also minimize cost in the presence of contention.

We desire to know how this is achieved. Fig. 2.21 shows the 15-minute average power for controlled and uncontrolled loads for a five bus and eleven bus scenario. In the 5 bus scenario, loads are easily distributed among off-peak hours, resulting in an optimized cost. The 11 bus scenario requires significantly more power and is forced to charge during on-peak hours. Note however that the average power is kept relatively low, and the additional charge sessions never cause the average power to supersede the maximum average power of the uncontrolled loads. Both scenarios also make ample use of night charging, where the number of chargers is the same as the number of buses.

#### 2.7.4 Multi-Rate Comparison

This subsection compares a multi-rate and single-rate charge schedule. The multi-rate schedule includes  $a_1$ ,  $a_2$ ,  $a_3$ , and  $a_4$  as defined in section 2.7.1. The single-rate schedule assumes the static charge rate associated with  $a_1$ . Two scenarios are considered. The first compares the cost of multi and single-rate plans for a 5 bus 1 charger scenario. The second compares performance for a 35 bus, 6 charger scenario.

The potential savings for using a variable charge rate in a 5 bus, 1 charge r scenario was found to be negligible. The cost of the multi-rate scenario is \$3006.94 and the cost of the single-rate scenario is \$3007.77 which gives a total savings of \$0.83. A 36 bus, 6 charger comparison also yielded minimal cost savings.

While examining the most commonly used edges, we observe that edges corresponding to a maximum charge rate are used most frequently as shown in Fig. 2.22 which explains the similarities in cost. If the highest rate is almost always selected, the resulting plan would resemble a single-rate schedule, resulting in a single-rate cost.

Another explanation for the cost similarity is found in how monthly cost is computed. Because the monthly cost is based on the average instantaneous power, both high and low charge rates can give the same results over a fixed time period. The charge schedules shown in both single and multi-rate plans charge buses in relatively small time periods. Fast charging over small periods of time is equivalent to slow charging over longer periods. In this way, the average power can be kept low even when using high charge rates (see Figs. 2.21 and 2.20).

## 2.8 Conclusions and Future Work

In conclusion, the charge schedules developed in equation (2.55) yield significant cost savings over both the baseline and the work by [20]. These savings come from minimizing the average power consumption, and charging during off-peak hours. Cost savings are maintained in both uncontested and resource constrained scenarios. There is also little to be gained by offering multiple charge rates because average power can be managed with high charge rates by reducing the charge duration. Furthermore, it was shown that when given

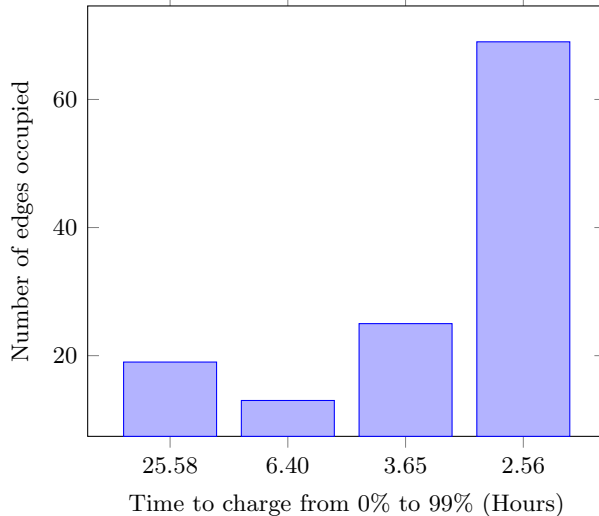


Fig. 2.22: Histogram of charge rates, where each rate is described by how much time it would take to charge a bus from 0% to 99%.

the choice, the optimizer primarily selected high charge rates, which reduces the problem complexity to the single-rate formulation.

Although multi-rate charging does not significantly reduce the monthly cost, it could be useful in prolonging battery life. The high power rates observed in this work can reduce the lifespan of the battery whereas lower charge rates can prolong battery life. Therefore, future work incorporating battery-health will be explored. We believe that multi-rate charging may offer some flexibility in this scenario. Future work will extend the discrete charge levels in this work to a continuous rate selection.

Because this work presents only a planning framework for a global solution over large stretches of time, it is computationally infeasible to recompute when unplanned events occur. Future work could move this framework toward real-time deployment using a hierarchical approach to control of charging. A precomputed global plan supports the real-time planner by providing top-level guidance. The lower-level real-time planner will adapt to unplanned events by controlling for a return from the current state to the global plan over a finite sliding horizon.

Finally, the computational complexity of our approach decreases as the number of chargers increase, but suffers when planning for large bus fleets as the number of constraints

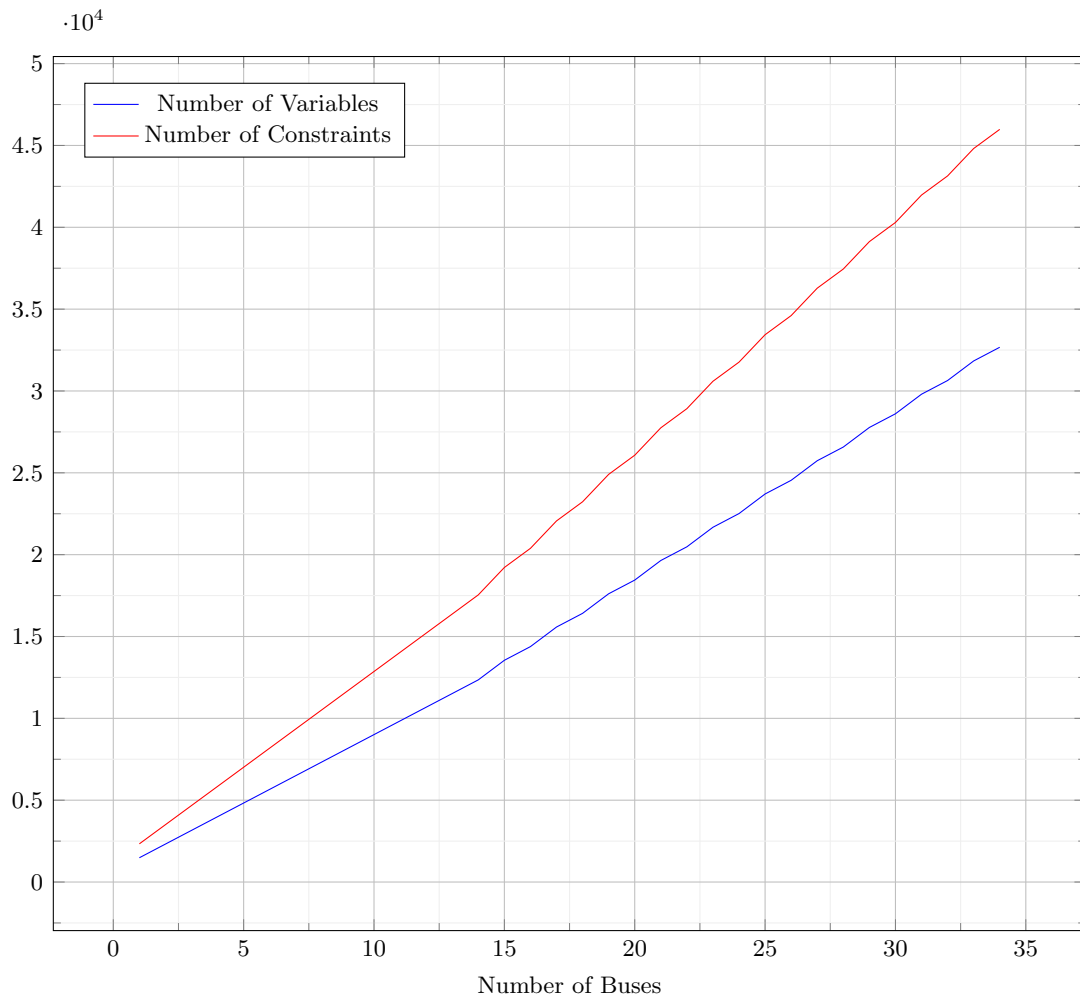


Fig. 2.23: Scalability Analysis.

and solution variables scales linearly with the number of buses as shown in Fig. 2.23. Future improvements might use a solution from a heuristic approach as a “warm start” for the optimizer which would reduce the computational complexity of finding a globally optimal solution.

## CHAPTER 3

### A Bin Packing Approach to Minimize Charging Cost for Electric Bus Fleets

#### 3.1 Introduction

Battery powered electric motors offer many benefits over the internal combustion engine [4] such as reduced maintenance [3], zero emissions [2], and access to renewable energy [5], which have caused many transit authorities to adopt battery powered electric buses (BEBs).

Despite their benefits, the transition to BEBS must address the challenge of extended refuel times. When a bus fueled by diesel or compressed natural gas (CNG) runs low on fuel, the bus may refuel in five to ten minutes, whereas an electric bus may require several hours, presenting logistical challenges for bus fleets. Therefore, maintaining a route schedule while staying charged is a primary concern that BEBs face, and requires careful planning that models how batteries discharge along routes, how long BEBs must charge, and limitations on the number of chargers.

One way in which charge times may be reduced is by charging a bus while it is in motion through dynamic charging. There are a number of ways to do this, including overhead [9] and inductive charging [10] [11]. An overhead charging scenario allows the bus to charge on overhead power lines while in motion. Inductive charging relies on specialized hardware in the roads that transfers energy to buses that pass overhead. Both methods remove the need to stop for service and allow an electric vehicle to stay in service indefinitely. Unfortunately, both methods require extensive infrastructure [12] that may not be available, or is cost prohibitive to install.

In the absence of infrastructure, [13] and [14] have proposed methods that exchange depleted batteries for fresh ones. Such a method would eliminate both the logistical challenges of planning and the infrastructure dependence of dynamic charging. The only drawback, is that BEBs are not built with battery exchanges in mind, therefore the task can require

specialized hardware, technical expertise, or automation, all of which add complexity and cost.

One charge option that avoids both the infrastructure demands of dynamic charging and the technical difficulties of battery swapping is stationary charging, which plans rest periods into a bus’s schedule during which that bus can charge. Stationary charging is the least invasive form of bus charging because it only requires charging hardware at specific locations and makes no exchanges to bus batteries. Prior work in this area addresses a number of problems, including distributed charging networks [29], bus availability, environmental impact [16], route scheduling [15], battery health [38], the cost of electricity [19], and the cost of charging infrastructure [31].

One drawback to using a stationary charging solution is that it does require significant rest periods for charging. One way to decrease the charge intervals is to use high power chargers, which deliver more energy in a smaller period of time. However doing so places large power demands on electrical infrastructure [6] which may result in problems with network reliability [7] and require additional maintenance and upgrades, which increase the cost of energy [8]. An effective charge plan must therefore balance the need to charge quickly with the desire to maintain a low power profile [22].

The authors of [23] and [24] propose simple, heuristic approaches to reduce power demands from BEB fleets. Work done by [25] uses a mixed integer linear program (MILP) to solve for a solution, which addresses both when buses should charge, and where they should deploy. Finally, a paper by [26] provides a MILP framework for minimizing the cost of demand power and both [20] and [21] minimize the cost from time of use tariffs. Each of the aforementioned methods focus on demand power in relation to electric bus fleets, but do not account for external activity on the grid, such as effects from electric trains, renewable energy devices, or other utilities which we refer to as “uncontrolled loads”.

In this paper, the uncontrolled load profile comes from historical data provided by the Utah Transit Authority in Salt Lake City which describes the power demands for an electric train as it passes through the station. In practice, buses would share a single meter with

the train. If buses were to charge at high rates while the train drew power from the grid to accelerate, the resulting 15-minute average power would become significant, increasing the monthly cost.

This paper considers a traditional scenario where each bus begins the day in the station and spends the day either on-route or in the station. Buses on route are considered unavailable and cannot charge until that bus returns to the station. For such a scenario, we develop a planning method to manage bus charging by viewing the charge problem in a bin packing context [40] in a way that minimizes the joint power use from the bus fleet and uncontrolled loads while yielding a precise time schedule for charging.

The rest of this paper is organized as follows: Section 3.2 discusses the basic problem formulation, Section 3.3 discusses linear constraints that govern the behavior and limitations of the rate of charge. Section 3.4 discusses how to incorporate uncontrolled loads into the optimization framework. Section 4.2.4 explains how the objective function is formed, and Section 3.6 discusses performance.

### 3.2 Bus Availability and Resource Contention

The charge scheduling framework described in this paper is formulated as a constrained optimization problem that can be solved as a Mixed Integer Linear Program (MILP) of the form

$$\begin{aligned} \min_{\mathbf{y}} \mathbf{y}^T \mathbf{v} \text{ subject to} \\ \tilde{A}\mathbf{y} = \tilde{\mathbf{b}}, A\mathbf{y} \leq \mathbf{b}, \end{aligned} \tag{3.1}$$

along with some integer constraints on elements of  $\mathbf{y}$ , where  $\mathbf{y}$ ,  $\tilde{A}$ ,  $A$ , and  $\mathbf{v}$  represent the solution vector, equality and inequality constraints, and cost vector respectively. In this

paper,  $\mathbf{y}$  is comprised of several variables, and is expressed as

$$\mathbf{y} = \begin{bmatrix} \boldsymbol{\sigma} \\ \mathbf{c} \\ \mathbf{s} \\ \mathbf{h} \\ \mathbf{k} \\ \mathbf{r} \\ \mathbf{g} \\ \mathbf{p} \\ \mathbf{l} \\ q_{\text{on}} \\ q_{\text{all}} \end{bmatrix}, \quad (3.2)$$

where  $\boldsymbol{\sigma}$  describes on which charger a bus will charge,  $\mathbf{c}$  and  $\mathbf{s}$  describe time intervals over which buses charge,  $\mathbf{h}$  gives the bus state of charge,  $\mathbf{k}$ ,  $\mathbf{r}$  and  $\mathbf{p}$  are used to discretize the effects from  $\mathbf{c}$  and  $\mathbf{s}$ ,  $\mathbf{g}$  is a slack variable for converting the effects of charging from continuous time to discrete intervals,  $\mathbf{l}$  is another slack variable that prevents two buses from simultaneously being assigned to the same charger, and  $q_{\text{on}}$  and  $q_{\text{all}}$  represent maximum average power values that are used to compute the monthly cost of power.

The cost function in (3.1) will be designed to model a realistic billing structure used by [18] and will minimize the cost in the presence of uncontrolled loads. Additionally, the constraints are designed to incorporate bus schedules, limit bus state of charges, and include a linear charge model calibrated on data from the Utah Transit Authority.

### 3.2.1 Setup

A solution to the bus charge problem includes both temporal and categorical information. The temporal aspect shows when and for how long a bus should charge, and is represented graphically as increasing from left to right. The vertical axis represents each

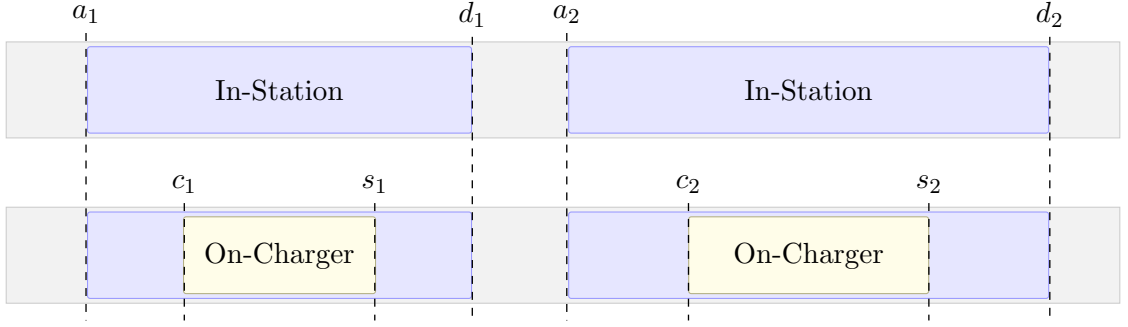


Fig. 3.1: Bus Charging

category as a bus and shows how each bus charges over time as shown in Fig. 3.2.

Each bus follows a schedule of arrival and departure times, where the  $i^{\text{th}}$  bus's  $j^{\text{th}}$  stop begins at arrival time  $a_{ij}$  and terminates at departure time  $d_{ij}$  (see Fig. 3.1). A bus can be assigned to charge anytime the bus is in the station, such that the charge start time,  $c_{ij}$ , is greater than or equal to  $a_{ij}$ , and the charge stop time,  $s_{ij}$ , is less than the departure time  $d_{ij}$ , as shown in Fig. 3.1. In the context of a MILP, the arrival and departure times  $a_{ij}$  and  $d_{ij}$  are known ahead of time and charge times  $c_{ij}$  and  $s_{ij}$  are optimization variables.

### 3.2.2 Constraints

The relationship between the arrival, departure, and charge intervals for the  $i^{\text{th}}$  bus at the  $j^{\text{th}}$  stop can be expressed as a set of inequality constraints such that

$$\begin{aligned}
 a_{ij} &\leq c_{ij} \\
 c_{ij} &\leq s_{ij} \\
 s_{ij} &\leq d_{ij}.
 \end{aligned}
 \tag{3.3}$$

These constraints can be rewritten such that the optimization variables are on the left, the known parameters are on the right, and the relationship is “less than” (or standard form)

such that

$$\begin{aligned}
 -c_{ij} &\leq -a_{ij} \\
 c_{ij} - s_{ij} &\leq 0 \\
 s_{ij} &\leq d_{ij}.
 \end{aligned} \tag{3.4}$$

Standard form is preferred because it is required by most solvers. Having the optimization variables on the left also allows the expression to be written using matrix notation as

$$\begin{bmatrix} -1 & 0 \\ 1 & -1 \\ 0 & 1 \end{bmatrix} \begin{bmatrix} c_{ij} \\ s_{ij} \end{bmatrix} \leq \begin{bmatrix} -a_{ij} \\ 0 \\ d_{ij} \end{bmatrix}. \tag{3.5}$$

However, because all constraints must follow the form  $A\mathbf{y} = \mathbf{b}$  as shown in (3.1), (3.5) is expressed in terms of  $\mathbf{y}$  such that

$$\begin{bmatrix} -1_{ij}^c & 0 & \dots & 0 \\ 1_{ij}^c & 0 & \dots & -1_{ij}^d \\ 0 & 0 & \dots & 1_{ij}^d \end{bmatrix} \mathbf{y} \leq \begin{bmatrix} -a_{ij} \\ 0 \\ d_{ij} \end{bmatrix} \quad \forall i, j \tag{3.6}$$

$$A_1 \mathbf{y} \leq \mathbf{b}_1,$$

where  $1_{ij}^c$  is 1 at the index that corresponds to  $c_{ij}$ ,  $1_{ij}^d$  is 1 at the index corresponding to  $s_{ij}$ , and  $A_1$  and  $\mathbf{b}_1$  stack the constraints given in (3.5) for all  $i, j$ .

The decision variables  $s_{ij}$  and  $c_{ij}$  from (3.5) show when a bus must start and finish charging, but do not indicate on which charger. The variable  $\boldsymbol{\sigma}$  from (3.2) is a vector of binary variables. Each element of  $\boldsymbol{\sigma}$  is denoted  $\sigma_{ijk}$  and is 1 when bus  $i$  charges during the  $j^{\text{th}}$  stop at charger  $k$ . Because a bus can only charge at one charger at a time, the values in  $\boldsymbol{\sigma}$  must be constrained such that

$$\sum_k \sigma_{ijk} \leq 1 \quad \forall i, j \tag{3.7}$$

or in standard form as

$$\begin{aligned} \begin{bmatrix} 1_{ij1} & 1_{ij2} & \dots & 1_{ijk} & 0 & \dots \end{bmatrix} \mathbf{y} \leq \mathbf{1} \quad \forall i, j \\ A_2 \mathbf{y} \leq \mathbf{b}_2, \end{aligned} \quad (3.8)$$

where  $1_{ijk}$  represents a 1 at the location corresponding to  $\sigma_{ijk}$ . The variable  $\sigma_{ijk}$  is used in several scenarios. The first is to ensure that buses without charge assignments have a charge time of zero by constraining  $s_{ij}$  and  $c_{ij}$  to be the same value. This is done by letting

$$\begin{aligned} s_{ij} - c_{ij} \leq M \sum_k \sigma_{ijk} \\ \begin{bmatrix} 1_s & -1_c & -M_{\sigma_1} & \dots & -M_{\sigma_k} \end{bmatrix} \begin{bmatrix} s_{ij} \\ c_{ij} \\ \sigma_{ij1} \\ \vdots \\ \sigma_{ijk} \end{bmatrix} \leq 0 \quad \forall i, j, \end{aligned} \quad (3.9)$$

where  $M$  is the maximum difference between  $s_{ij}$  and  $c_{ij}$ , or the number of seconds in a day, also referred to as nTime, and  $M_\sigma$  represents multiple values of  $M$  at locations corresponding to each  $\sigma_{ijk}$ . The constraints in (3.9) can be appropriately zero padded and stacked for all  $i, j$  to form the linear expression

$$A_3 \mathbf{y} \leq \mathbf{b}_3. \quad (3.10)$$

The values in  $\boldsymbol{\sigma}$ ,  $\mathbf{c}$ , and  $\mathbf{s}$  form a complete charge plan representation were  $c_{ij}$  and  $s_{ij}$  describe time periods when a bus will charge and  $\sigma_{ijk}$  gives which charger to use. (see Fig. 3.2). The variable  $\sigma_{ijk}$  is also necessary to prevent situations where more than one bus is assigned to the same charger at the same time. Note that two buses, bus  $i$  and bus  $i'$ , can only be assigned to the same charger at the same time when when  $a_{ij}$  for bus  $i$  is less than  $d_{i'j'}$  for bus  $i'$  as shown in Fig. 3.3. Let  $\mathcal{S}$  be the set of all bus-stop pairs such that  $((i, j), (i', j')) \in \mathcal{S}$  if overlap is possible between bus  $i$  and bus  $i'$  during the  $j$  and  $j'$  stops respectively. Charging overlap can be avoided by constraining  $c_{i'j'} > s_{ij}$  or  $c_{ij} > s_{i'j'}$  for

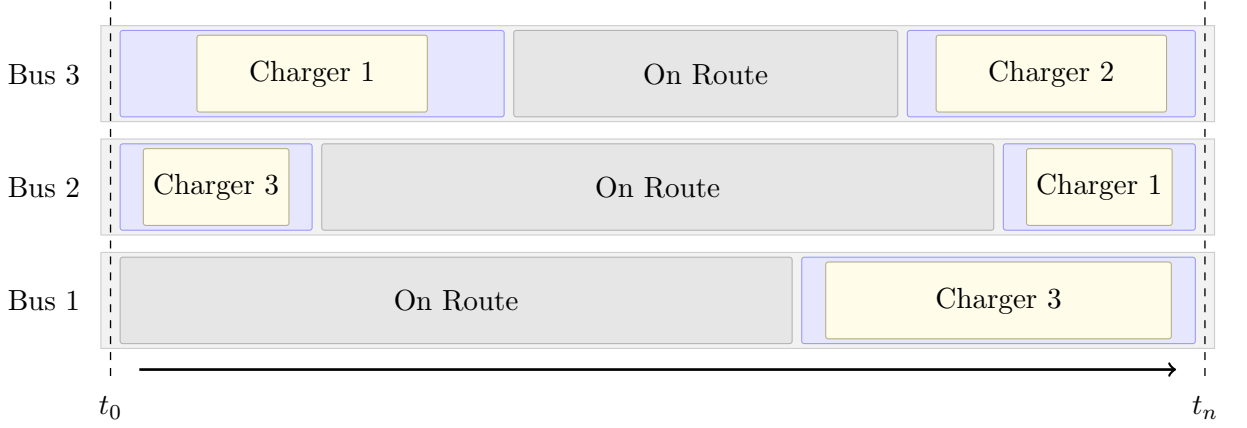


Fig. 3.2: Reserving time slots on chargers

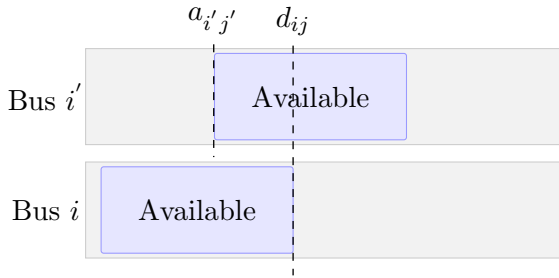


Fig. 3.3: Potential Overlap

all  $(ij, i'j') \in \mathcal{S}$ .

We desire to encode these constraints so that they may be included in our MILP. First, let  $l_{(ij, i'j')}$  be a binary decision variable that is 1 when  $c_{i'j'} > s_{ij}$ , and 0 when  $c_{ij} > s_{i'j'}$  so that the overlap constraints can be expressed as

$$\begin{aligned} c_{i'j'} - s_{ij} &> -Ml_{(ij, i'j')} \\ c_{ij} - s_{i'j'} &> -M(1 - l_{(ij, i'j')}). \end{aligned} \tag{3.11}$$

Note that this constraint is only necessary when buses  $i$  and  $i'$  are assigned to the same charger, so that both  $\sigma_{i'j'k}$  and  $\sigma_{ijk}$  are equal to 1 which can be done by modifying the switching technique from Eqn. (3.11) so that the overlap constraints are trivially satisfied

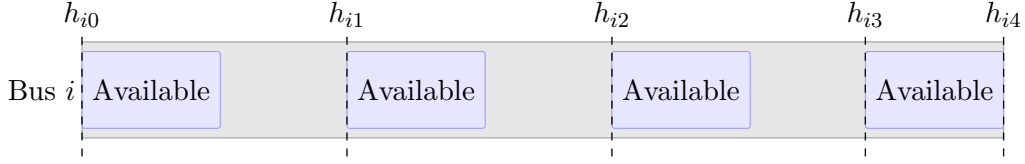


Fig. 3.4: State of Charge Variables

when either  $\sigma_{i'j'k}$  or  $\sigma_{ijk}$  is equal to zero. The expressions in (3.11) can be relaxed by letting

$$\begin{aligned} c_{i'j'} - s_{ij} &> M \left[ (\sigma_{i'j'k} + \sigma_{ijk}) - 2 \right] - M l_{(ij, i'j')} \quad \forall k \\ c_{ij} - s_{i'j'} &> M \left[ (\sigma_{i'j'k} + \sigma_{ijk}) - 2 \right] - M (1 - l_{(ij, i'j')}) \quad \forall k \end{aligned} \quad (3.12)$$

so that when  $(\sigma_{i'j'k} + \sigma_{ijk}) < 2$ , (3.12) is trivially satisfied for all values of  $c_{i'j'}$  and  $s_{ij}$  and when  $\sigma_{i'j'k} = \sigma_{ijk} = 1$ , (3.12) simplifies to (3.11). Equation (3.12) can be expressed in standard form using matrix notation as

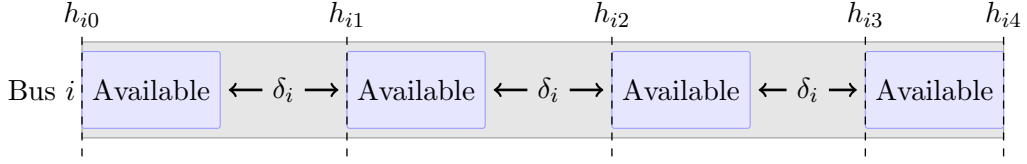
$$\begin{bmatrix} -1 & 0 & 0 & 1 & M & M & -M \\ 0 & 1 & -1 & 0 & M & M & M \end{bmatrix} \begin{bmatrix} c_{i'j'} \\ s_{i'j'} \\ c_{ij} \\ s_{ij} \\ \sigma_{i'j'k} \\ \sigma_{ijk} \\ l_{ij, i'j'} \end{bmatrix} \leq \begin{bmatrix} 2M \\ 3M \end{bmatrix} \quad \forall k. \quad (3.13)$$

The constraints in (3.13) can be repeated for all  $((i, j), (i', j')) \in \mathcal{S}$  and concatenated into a single matrix expression

$$A_4 \mathbf{y} \leq \mathbf{b}_4 \quad (3.14)$$

### 3.3 Battery State of Charge

BEBs must also maintain their state of charge above a minimum threshold, denoted  $h_{\min}$ . Let  $h_{ij}$  be the state of charge for bus  $i$  at the beginning of stop  $j$  as shown in Fig. 3.4. The initial value for bus  $i$ , denoted  $h_{i0}$ , is equal to some constant such that

Fig. 3.5: Placement for  $\delta_i$ 

$$\begin{aligned}
 h_{i0} &= \eta_i \quad \forall i \\
 \begin{bmatrix} 0 & 0 & \dots & 0 & 1_i & 0 \end{bmatrix} \mathbf{y} &= \eta_i \quad \forall i \\
 \tilde{A}_1 \mathbf{y} &= \tilde{\mathbf{b}}_1
 \end{aligned} \tag{3.15}$$

and is otherwise computed as the the sum of incoming and outgoing energy where incoming energy comes from charging, and outgoing energy comes from the battery discharge. The discharge from operating bus  $i$  over route  $j$  is denoted  $\delta_{ij}$  which is assumed to be know ahead of time either from historical data or from modeling such as [41]. The increase in battery state of charge follows a linear charge model such that the increase is equal to the energy rate, denoted  $p_i$ , times the time spent charging, denoted  $\Delta_{ij}$  [42]. The total change from  $h_{ij}$  to  $h_{ij+1}$  can be expressed as

$$h_{ij+1} = h_{ij} + \Delta_{ij} \cdot p_i - \delta_{ij}. \tag{3.16}$$

The value for  $\Delta_{ij}$  can also be expressed in terms of the difference between  $a_{ij}$  and  $d_{ij}$  such that

$$\begin{aligned}
 h_{ij} + p_i \cdot (s_{ij} - c_{ij}) - \delta_i &= h_{ij+1} \\
 h_{ij+1} - h_{ij} - p_i s_{ij} + p_i c_{ij} &= -\delta_i \\
 \begin{bmatrix} 1 & -1 & -p_i & p_i \end{bmatrix} \begin{bmatrix} h_{ij+1} \\ h_{ij} \\ s_{ij} \\ c_{ij} \end{bmatrix} &= -\delta_i \quad \forall i, j.
 \end{aligned} \tag{3.17}$$

The constraints for each  $i, j$  outlined in (3.17) can be vertically concatenated to form

$$\begin{aligned} A_{ij}\mathbf{y} &= \mathbf{b}_{ij} \quad \forall i, j \\ \tilde{A}_2\mathbf{y} &= \tilde{\mathbf{b}}_2. \end{aligned} \tag{3.18}$$

Now that the state of charge is defined, the next constraint ensures that the minimum battery state of charge remains both above the minimum threshold,  $h_{\min}$ , and below the battery capacity,  $h_{\max}$ . These constraints are given as

$$\begin{aligned} -h_{ij} &\leq -h_{\min} \quad \forall i, j \\ h_{ij} &\leq h_{\max} \end{aligned} \tag{3.19}$$

or

$$\begin{bmatrix} 0 & \dots & 0 & -1_h & 0 & \dots & 0 \\ 0 & \dots & 0 & 1_h & 0 & \dots & 0 \end{bmatrix} \mathbf{y} \leq \begin{bmatrix} h_{\min} \\ h_{\max} \end{bmatrix} \quad \forall i, j \tag{3.20}$$

$$A_5\mathbf{y} \leq \mathbf{b}_5.$$

The final constraint has to do with the assumption that we desire to use the model for one day to predict the expected cost over a month. To do this, the state of charge at the end of the day must equal the state of charge at the beginning. Let  $h_{i,\text{end}}$  be the final daily state of charge for bus  $i$ . This is constrained to be the same as the beginning state of charge as

$$\begin{aligned} h_{i0} &= h_{i,\text{end}} \quad \forall i \\ h_{i0} - h_{i,\text{end}} &= 0 \quad \forall i. \end{aligned} \tag{3.21}$$

However, because equality for two continuous variables is computationally demanding, the constraint in (3.21) can also be expressed as

$$h_{i0} - h_{i,\text{end}} \leq 0. \tag{3.22}$$

Because the final state of charge is dependent on the amount of power used to charge, and power/energy use is penalized (see section 4.2.4), the optimization process will drive the

final state of charge low until it approaches the initial value.

### 3.4 Integrating Uncontrolled Loads

A monthly power bill is made up of several costs, two of which depend on the maximum energy consumed over 15 minutes. This 15-minute average power includes energy that is consumed by loads other than bus chargers, or “uncontrolled loads”. In practice, data for uncontrolled loads is sampled and therefore discrete. The representations for how buses use power in Section 3.3 are continuous, making their effects difficult to integrate with a discrete uncontrolled load. This section integrates these uncontrolled loads into the planning framework by converting the continuous start and end points,  $c_{ij}$  and  $s_{ij}$  from Section 3.2, to a vector  $\mathbf{p}_{ij}$ , where the  $n^{\text{th}}$  element of the  $\mathbf{p}_{ij}$  vector represents the average power over the interval  $t_{i-1}$  to  $t_i$  from bus  $i$  during route  $j$ . The route power vectors,  $\mathbf{p}_{ij}$ , can be added together to form a discrete profile for the buses.

Let the day be divided into time segments, each of duration  $\Delta T$ . The first step is to determine the index of each segment that a bus begins charging, denoted  $k_{ij}^{\text{start}}$ , and the index of the segment that a bus finishes charging, denoted  $k_{ij}^{\text{end}}$ . Each index can be computed as an integer multiple of  $\Delta T$  that satisfies

$$\begin{aligned} (k_{ij}^{\text{start}} - 1) \cdot \Delta T + r_{ij}^{\text{start}} &= c_{ij} \\ (k_{ij}^{\text{end}} - 1) \cdot \Delta T + r_{ij}^{\text{end}} &= s_{ij} \\ k_{ij}^{\text{start}}, k_{ij}^{\text{end}} &\in \mathbb{Z} \\ 0 < r_{ij}^{\text{start}}, r_{ij}^{\text{end}} &< \Delta T. \end{aligned} \tag{3.23}$$

Equation (3.23) yields the discrete indices  $k_{ij}^{\text{start}}$  and  $k_{ij}^{\text{end}}$  along with corresponding remainder values  $r_{ij}^{\text{start}}$  and  $r_{ij}^{\text{end}}$ , which will be used later in this section to calculate the average power for time segments in which buses only charge part of the time. Equation (3.23) can

be rewritten in standard form and zero padded such that

$$\begin{bmatrix} \Delta T & 1 & -1 & 0 & 0 & 0 \\ 0 & 0 & 0 & \Delta T & 1 & -1 \end{bmatrix} \begin{bmatrix} k_{ij}^{\text{start}} \\ r_{ij}^{\text{start}} \\ c_{ij} \\ k_{ij}^{\text{end}} \\ r_{ij}^{\text{end}} \\ s_{ij} \end{bmatrix} = \begin{bmatrix} 0 \\ 0 \end{bmatrix} \quad \forall i, j \quad (3.24)$$

$$\tilde{A}_2 \mathbf{y} = \tilde{\mathbf{b}}_2$$

and

$$\begin{bmatrix} 0 & -1 & 0 & 0 & 0 & 0 \\ 0 & 1 & 0 & 0 & 0 & 0 \\ 0 & 0 & 0 & 0 & -1 & 0 \\ 0 & 0 & 0 & 0 & 1 & 0 \end{bmatrix} \begin{bmatrix} k_{ij}^{\text{start}} \\ r_{ij}^{\text{start}} \\ c_{ij} \\ k_{ij}^{\text{end}} \\ r_{ij}^{\text{end}} \\ s_{ij} \end{bmatrix} \leq \begin{bmatrix} 0 \\ \Delta T \\ 0 \\ \Delta T \end{bmatrix} \quad \forall i, j \quad (3.25)$$

$$A_6 \mathbf{y} \leq \mathbf{b}_6.$$

The next step is to use  $k_{ij}^{\text{start}}$  and  $k_{ij}^{\text{end}}$  to compute three sets of binary vectors, denoted  $\mathbf{g}_{ij}^{\text{start}}$ ,  $\mathbf{g}_{ij}^{\text{on}}$ , and  $\mathbf{g}_{ij}^{\text{end}}$ , which act as selectors for indices which correspond to charge times. The values in  $\mathbf{g}_{ij}^{\text{start}}$  and  $\mathbf{g}_{ij}^{\text{end}}$  are equal to 1 during intervals that contain energy from the remainders  $r_{ij}^{\text{start}}$  and  $r_{ij}^{\text{end}}$ . For example, the values for  $\mathbf{g}_{ij}^{\text{start}}$  and  $\mathbf{g}_{ij}^{\text{end}}$  from the scenario in Fig. 3.6b would be

$$\mathbf{g}_{ij}^{\text{start}} = \begin{bmatrix} 1 \\ 0 \\ 0 \\ 0 \end{bmatrix} \quad \text{and} \quad \mathbf{g}_{ij}^{\text{end}} = \begin{bmatrix} 0 \\ 0 \\ 1 \\ 0 \end{bmatrix}. \quad (3.26)$$

The values in  $\mathbf{g}_{ij}^{\text{on}}$  will be equal to 1 for all time indices where buses charges the entire time. For example, the values in  $g_{ij}^{\text{on}}$  that correspond to Fig. 3.6b would be

$$\mathbf{g}_{ij}^{\text{on}} = \begin{bmatrix} 0 \\ 1 \\ 0 \\ 0 \end{bmatrix}. \quad (3.27)$$

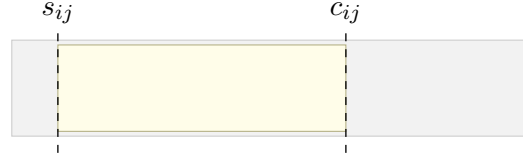
Let  $\mathbf{f}$  be a vector of one-based integer indices such that  $f_w = w \forall w \in (1, \text{nPoint})$ , where nPoint is the desired number of discrete samples. For example, if the day was discretized into 4 periods, then  $\mathbf{f}$  would be

$$\mathbf{f} = \begin{bmatrix} 1 & 2 & 3 & 4 \end{bmatrix}^T. \quad (3.28)$$

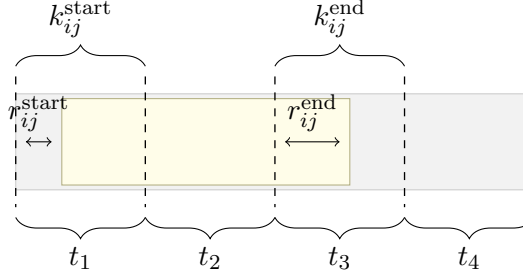
Defining the index as an element of  $\mathbf{f}$  allows us to convert from the single indices  $k_{ij}^{\text{start}}$  and  $k_{ij}^{\text{end}}$  to the binary vectors  $\mathbf{g}_{ij}^{\text{start}}$  and  $\mathbf{g}_{ij}^{\text{end}}$  by letting

$$\begin{aligned} k_{ij}^{\text{start}} &= \mathbf{f}^T \mathbf{g}_{ij}^{\text{start}} \\ k_{ij}^{\text{end}} &= \mathbf{f}^T \mathbf{g}_{ij}^{\text{end}} \\ 1 &= \mathbf{1}^T \mathbf{g}_{ij}^{\text{start}} \\ 1 &= \mathbf{1}^T \mathbf{g}_{ij}^{\text{end}} \end{aligned} \quad (3.29)$$

$$\begin{aligned} \mathbf{g}_{ij}^{\text{start}} &\in \{0, 1\}^{\text{nPoint}} \\ \mathbf{g}_{ij}^{\text{end}} &\in \{0, 1\}^{\text{nPoint}}, \end{aligned}$$



(a) Continuous Charging Segment



(b) Discrete Charging Segments

Fig. 3.6: Discretization of continuous charging intervals

which can be expressed in standard form and zero padded to form a set of linear constraints.

$$\begin{bmatrix} 0 & \mathbf{0}^T & -1 & \mathbf{f}^T \\ 0 & \mathbf{1}^T & 0 & 0 \\ -1 & \mathbf{f}^T & 0 & \mathbf{0}^T \\ 0 & 0 & 0 & \mathbf{1}^T \end{bmatrix} \begin{bmatrix} k_{ij}^{\text{start}} \\ \mathbf{g}_{ij}^{\text{start}} \\ k_{ij}^{\text{end}} \\ \mathbf{g}_{ij}^{\text{end}} \end{bmatrix} = \begin{bmatrix} 0 \\ 1 \\ 0 \\ 1 \end{bmatrix} \quad \forall i, j \quad (3.30)$$

$$\tilde{A}_3 \mathbf{y} = \tilde{\mathbf{b}}_3.$$

The values of  $\mathbf{g}_{ij}^{\text{on}}$  can be computed by first noticing that indices that correspond to complete charge intervals must remain between  $k_{ij}^{\text{start}}$  and  $k_{ij}^{\text{end}}$ , implying that

$$\begin{cases} g_w f_w \leq k_{ij}^{\text{end}} - 1 \\ g_w f_w \geq k_{ij}^{\text{start}} + 1 \end{cases} \quad g_w = 1, \quad (3.31)$$

which can be expressed as a set of linear constraints such that

$$\begin{aligned} g_w \cdot f_w &\leq k_{ij}^{\text{end}} + M(1 - g_w) - 1 \\ g_w \cdot f_w &\geq k_{ij}^{\text{start}} - M(1 - g_w) + 1, \end{aligned} \quad (3.32)$$

where  $M$  is  $2 \cdot \text{nPoint}$ . The constraints in (3.32) do not require that all values between  $k_{ij}^{\text{start}}$  and  $k_{ij}^{\text{end}}$  be set to one, rather that them being equal to one implies that they are between  $k_{ij}^{\text{start}}$  and  $k_{ij}^{\text{end}}$ . For all values between  $k_{ij}^{\text{start}}$  and  $k_{ij}^{\text{end}}$  to be 1, the sum of  $\mathbf{g}_{ij}^{\text{on}}$  must be equal to the difference between  $k_{ij}^{\text{end}}$  and  $k_{ij}^{\text{start}}$  such that

$$\begin{aligned} g_w \cdot f_w &\leq k_{ij}^{\text{end}} + M(1 - g_w) - 1 \\ g_w \cdot f_w &\geq k_{ij}^{\text{start}} - M(1 - g_w) + 1 \\ \mathbf{1}^T \mathbf{g}_{ij}^{\text{on}} &= k_{ij}^{\text{end}} - k_{ij}^{\text{start}} - 1. \end{aligned} \tag{3.33}$$

The constraints in (3.33) work well for a general use case, however when  $k_{ij}^{\text{end}}$  is equal to  $k_{ij}^{\text{start}}$ , the last constraint in (3.33) becomes

$$\mathbf{1}^T \mathbf{g}_{ij}^{\text{on}} = -1, \tag{3.34}$$

which leads to an empty feasible set because the elements of  $\mathbf{g}_{ij}^{\text{on}}$  are all binary. Let  $k_{ij}^{\text{eq}}$  be a binary variable which is equal to 0 when  $k_{ij}^{\text{end}}$  is not equal to  $k_{ij}^{\text{start}}$ . Equation (3.33) can be modified to incorporate  $k_{ij}^{\text{eq}}$  to switch between the cases where  $k_{ij}^{\text{end}}$  is equal, and not equal to  $k_{ij}^{\text{start}}$  by letting

$$\begin{aligned} g_w \cdot f_w &\leq k_{ij}^{\text{end}} + M(1 - g_w) - 1 \\ g_w \cdot f_w &\geq k_{ij}^{\text{start}} - M(1 - g_w) + 1 \\ \mathbf{1}^T \mathbf{g}_{ij}^{\text{on}} &= k_{ij}^{\text{end}} - k_{ij}^{\text{start}} - k_{ij}^{\text{eq}} \end{aligned} \tag{3.35}$$

and constraining  $k_{ij}^{\text{eq}}$  such that

$$\begin{aligned} k_{ij}^{\text{end}} - k_{ij}^{\text{start}} - M k_{ij}^{\text{eq}} &\leq 0 \\ -k_{ij}^{\text{end}} + k_{ij}^{\text{start}} + M k_{ij}^{\text{eq}} &\leq M. \end{aligned} \tag{3.36}$$

The constraints from (3.35) and (3.36) can be expressed in standard form as

$$\begin{aligned}
\mathbf{1}^T \mathbf{g}_{ij}^{\text{on}} - k_{ij}^{\text{end}} + k_{ij}^{\text{start}} + k_{ij}^{\text{eq}} &= 0 \\
k_{ij}^{\text{end}} - k_{ij}^{\text{start}} - M k_{ij}^{\text{eq}} &\leq 0 \\
-k_{ij}^{\text{end}} + k_{ij}^{\text{start}} + M k_{ij}^{\text{eq}} &\leq M \\
g_w (f_w + M) - k_{ij}^{\text{end}} &\leq M - 1 \\
g_w (M - f_w) + k_{ij}^{\text{start}} &\leq M - 1.
\end{aligned} \tag{3.37}$$

The inequality constraints from equation (3.37) imply that

$$\begin{bmatrix} f_w + M & -1 & 0 \\ M - f_w & 0 & 1 \end{bmatrix} \begin{bmatrix} g_w \\ k_{ij}^{\text{end}} \\ k_{ij}^{\text{start}} \end{bmatrix} \leq \begin{bmatrix} M - 1 \\ M - 1 \end{bmatrix} \forall g_w \in \mathbf{g}_{ij}^{\text{on}} \tag{3.38}$$

and that

$$\begin{bmatrix} 1 & -1 & -M \\ -1 & 1 & M \end{bmatrix} \begin{bmatrix} k_{ij}^{\text{end}} \\ k_{ij}^{\text{start}} \\ k_{ij}^{\text{eq}} \end{bmatrix} \leq \begin{bmatrix} 0 \\ M \end{bmatrix} \forall i, j, \tag{3.39}$$

which can be concatenated for all  $i, j$ , and zero padded to form a joint matrix, satisfying

$$A_7 \mathbf{y} \leq \mathbf{b}_7. \tag{3.40}$$

Similarly, the equality constraint from (3.37) can also be concatenated and zero padded such that

$$\begin{aligned}
\mathbf{1}^T \mathbf{g}_{ij}^{\text{on}} - k_{ij}^{\text{end}} + k_{ij}^{\text{start}} + k_{ij}^{\text{eq}} &= 0 \quad \forall i, j \\
\begin{bmatrix} \mathbf{1}^T & -1 & 1 & -1 \end{bmatrix} \begin{bmatrix} \mathbf{g}_{ij}^{\text{on}} \\ k_{ij}^{\text{end}} \\ k_{ij}^{\text{start}} \\ k_{ij}^{\text{eq}} \end{bmatrix} &= 0 \\
\tilde{A}_4 \mathbf{y} &= \tilde{\mathbf{b}}_4.
\end{aligned} \tag{3.41}$$

The next step is to define the average power during intervals that only charge for part of the time. These intervals correspond to the remainder values  $r_{ij}^{\text{start}}$  and  $r_{ij}^{\text{end}}$  and, as with previous constraints, maintain different behavior when  $k_{ij}^{\text{eq}} = 0$  and  $k_{ij}^{\text{eq}} = 1$ . The average power that corresponds to  $r_{ij}^{\text{start}}$  and  $r_{ij}^{\text{end}}$  can be computed as

$$\begin{cases} p_{ij}^{\text{start}} = \frac{p \cdot (\Delta T - r_{ij}^{\text{start}})}{\Delta T} \\ p_{ij}^{\text{end}} = \frac{p \cdot r_{ij}^{\text{end}}}{\Delta T} \end{cases} \quad k_{ij}^{\text{eq}} = 1$$

$$\begin{cases} p_{ij}^{\text{start}} = \frac{p \cdot (r_{ij}^{\text{end}} - r_{ij}^{\text{start}})}{\Delta T} \\ p_{ij}^{\text{end}} = 0 \end{cases} \quad k_{ij}^{\text{eq}} = 0, \quad (3.42)$$

where  $p$  is the charge rate. Equation (3.42) can also be expressed as a set of linear inequality constraints such that

$$\begin{aligned} p_{ij}^{\text{start}} &\leq p - \frac{p}{\Delta T} r_{ij}^{\text{start}} + M(1 - k_{ij}^{\text{eq}}) \\ p_{ij}^{\text{start}} &\geq p - \frac{p}{\Delta T} r_{ij}^{\text{start}} - M(1 - k_{ij}^{\text{eq}}) \\ p_{ij}^{\text{start}} &\leq \frac{p}{\Delta T} r_{ij}^{\text{end}} - \frac{p}{\Delta T} r_{ij}^{\text{start}} + M k_{ij}^{\text{eq}} \\ p_{ij}^{\text{start}} &\geq \frac{p}{\Delta T} r_{ij}^{\text{end}} - \frac{p}{\Delta T} r_{ij}^{\text{start}} - M k_{ij}^{\text{eq}} \\ p_{ij}^{\text{end}} &\leq \frac{p}{\Delta T} r_{ij}^{\text{end}} + M(1 - k_{ij}^{\text{eq}}) \\ p_{ij}^{\text{end}} &\geq \frac{p}{\Delta T} r_{ij}^{\text{end}} - M(1 - k_{ij}^{\text{eq}}) \\ p_{ij}^{\text{end}} &\leq M k_{ij}^{\text{eq}} \\ p_{ij}^{\text{end}} &\geq -M k_{ij}^{\text{eq}}, \end{aligned} \quad (3.43)$$

where  $M$  is the battery capacity, and can be expressed in standard form as

$$\begin{aligned}
p_{ij}^{\text{start}} + \frac{p}{\Delta T} r_{ij}^{\text{start}} + M k_{ij}^{\text{eq}} &\leq M + p \\
-p_{ij}^{\text{start}} - \frac{p}{\Delta T} r_{ij}^{\text{start}} + M k_{ij}^{\text{eq}} &\leq M - p \\
p_{ij}^{\text{start}} - \frac{p}{\Delta T} r_{ij}^{\text{end}} + \frac{p}{\Delta T} r_{ij}^{\text{start}} - M k_{ij}^{\text{eq}} &\leq 0 \\
-p_{ij}^{\text{start}} + \frac{p}{\Delta T} r_{ij}^{\text{end}} - \frac{p}{\Delta T} r_{ij}^{\text{start}} - M k_{ij}^{\text{eq}} &\leq 0 \\
p_{ij}^{\text{end}} - \frac{p}{\Delta T} r_{ij}^{\text{end}} + M k_{ij}^{\text{eq}} &\leq M \\
-p_{ij}^{\text{end}} + \frac{p}{\Delta T} r_{ij}^{\text{end}} + M k_{ij}^{\text{eq}} &\leq M \\
p_{ij}^{\text{end}} - M k_{ij}^{\text{eq}} &\leq 0 \\
-p_{ij}^{\text{end}} - M k_{ij}^{\text{eq}} &\leq 0
\end{aligned} \tag{3.44}$$

and by using matrix multiplication such that

$$\begin{bmatrix}
1 & 0 & \frac{p}{\Delta T} & 0 & M \\
-1 & 0 & -\frac{p}{\Delta T} & 0 & M \\
1 & 0 & \frac{p}{\Delta T} & -\frac{p}{\Delta T} & -M \\
-1 & 0 & -\frac{p}{\Delta T} & \frac{p}{\Delta T} & -M \\
0 & 1 & 0 & -\frac{p}{\Delta T} & M \\
0 & -1 & 0 & \frac{p}{\Delta T} & M \\
0 & 1 & 0 & 0 & -M \\
0 & -1 & 0 & 0 & -M
\end{bmatrix}
\begin{bmatrix}
p_{ij}^{\text{start}} \\
p_{ij}^{\text{end}} \\
r_{ij}^{\text{start}} \\
r_{ij}^{\text{end}} \\
k_{ij}^{\text{eq}}
\end{bmatrix}
\leq
\begin{bmatrix}
M + p \\
M - p \\
0 \\
0 \\
M \\
M \\
0 \\
0
\end{bmatrix}
\forall i, j \tag{3.45}$$

$$A_8 \leq \mathbf{b}_8,$$

where  $p_{ij}^{\text{start}}$ ,  $p_{ij}^{\text{end}}$ , and  $p$  represent the average power that corresponds to  $r_{ij}^{\text{start}}$ ,  $r_{ij}^{\text{end}}$ , and full charging intervals respectively. The total average power use is calculated as

$$\mathbf{p}_{\text{total}} = \bar{\mathbf{p}}_{\text{load}} + \sum_{ij} \mathbf{g}_{ij}^{\text{start}} \cdot p_{ij}^{\text{start}} + \mathbf{g}_{ij}^{\text{on}} \cdot p + \mathbf{g}_{ij}^{\text{end}} \cdot p_{ij}^{\text{end}}, \tag{3.46}$$

where  $\bar{\mathbf{p}}_{\text{load}}$  is the average power of the uncontrolled loads.

Note, however that (3.46) contains the bilinear terms  $\mathbf{g}_{ij}^{\text{start}} \cdot p_{ij}^{\text{start}}$  and  $\mathbf{g}_{ij}^{\text{end}} \cdot p_{ij}^{\text{end}}$ . The expression  $\mathbf{g}_{ij}^{\text{start}} \cdot p_{ij}^{\text{start}}$  from (3.46) can be thought of as a vector,  $\mathbf{p}_{ij}^{\text{start}}$  which contains values for  $p_{ij}^{\text{start}}$  whenever  $g_{ij}^{\text{start}}$  is not equal to 0 such that

$$\left. \begin{array}{l} p_w = p_{ij}^{\text{start}} \quad g_w = 1 \\ p_w = 0 \quad g_w = 0 \end{array} \right\} \forall p_w \in \mathbf{p}_{ij}^{\text{start}}, \quad (3.47)$$

which can be rewritten as a set of linear inequality constraints such that

$$\begin{aligned} p_w &\geq p_{ij}^{\text{start}} - M(1 - g_w) \forall p_w \in \mathbf{p}_{ij}^{\text{start}} \\ p_w &\leq p_{ij}^{\text{start}} + M(1 - g_w) \forall p_w \in \mathbf{p}_{ij}^{\text{start}} \\ p_w &\geq -Mg_w \forall p_w \in \mathbf{p}_{ij}^{\text{start}} \\ p_w &\leq Mg_w \forall p_w \in \mathbf{p}_{ij}^{\text{start}}. \end{aligned} \quad (3.48)$$

The same approach can be taken to replace  $\mathbf{g}_{ij}^{\text{end}} \cdot p_{ij}^{\text{end}}$  with the vector  $\mathbf{p}_{ij}^{\text{end}}$  by letting

$$\begin{aligned} p_w &\geq p_{ij}^{\text{end}} - M(1 - g_w) \forall p_w \in \mathbf{p}_{ij}^{\text{end}} \\ p_w &\leq p_{ij}^{\text{end}} + M(1 - g_w) \forall p_w \in \mathbf{p}_{ij}^{\text{end}} \\ p_w &\geq -Mg_w \forall p_w \in \mathbf{p}_{ij}^{\text{end}} \\ p_w &\leq Mg_w \forall p_w \in \mathbf{p}_{ij}^{\text{end}}, \end{aligned} \quad (3.49)$$

which can be written in standard form, stacked to accommodate the constraints for all  $i, j$ , and zero padded in the usual fashion as

$$\begin{bmatrix} -1 & 1 & M \\ 1 & -1 & M \\ -1 & 0 & -M \\ 1 & 0 & -M \end{bmatrix} \begin{bmatrix} p_w \\ p_{ij}^{\text{start}} \\ g_w \end{bmatrix} \leq \begin{bmatrix} M \\ M \\ 0 \\ 0 \end{bmatrix} \forall p_w \in \mathbf{p}_{ij}^{\text{start}} \quad (3.50)$$

$$A_9 \leq \mathbf{b}_9.$$

Equation (3.49) can be expressed in standard form, stacked for all  $i, j$ , and zero padded in a similar fashion such that

$$\begin{bmatrix} -1 & 1 & M \\ 1 & -1 & M \\ -1 & 0 & -M \\ 1 & 0 & -M \end{bmatrix} \begin{bmatrix} p_w \\ p_{ij}^{\text{end}} \\ g_w \end{bmatrix} \leq \begin{bmatrix} M \\ M \\ 0 \\ 0 \end{bmatrix} \quad \forall p_w \in \mathbf{p}_{ij}^{\text{end}} \quad (3.51)$$

$$A_{10}\mathbf{y} \leq \mathbf{b}_{10}.$$

An expression for the total power used can then be expressed as

$$\mathbf{p}^{\text{total}} = \mathbf{p}^{\text{load}} + \sum_{ij} \mathbf{p}_{ij}^{\text{start}} + \mathbf{p}_{ij}^{\text{end}} + \mathbf{g}_{ij}^{\text{on}} \cdot p \quad (3.52)$$

and in standard form as

$$\begin{bmatrix} 1 & -1^{\text{start}} & -1^{\text{end}} & -1^{\text{on}} \cdot p \end{bmatrix} \begin{bmatrix} \mathbf{p}_w^{\text{total}} \\ \mathbf{p}_w^{\text{start}} \\ \mathbf{p}_w^{\text{end}} \\ \mathbf{g}_w^{\text{on}} \end{bmatrix} = \mathbf{p}_w^{\text{load}} \quad (3.53)$$

$$\tilde{A}_4\mathbf{y} = \tilde{\mathbf{b}}_4.$$

### 3.5 Objective Function

This work adopts uses an objective function which implements the rate schedule from [18]. The rate schedule in [18] is based on of two primary components: power and energy.

Power is billed per kW for the highest 15 minute average power over a fixed period of time. It is common practice for power providers to use a higher rate during “on-peak” periods when power is in higher demand and use a lower rate during “off-peak” hours, which account for all other time periods.

The rate schedule given in [18] assesses a fee for a user’s maximum average power during on-peak hours, called the On-Peak Power charge, and a user’s overall maximum average

	On-Peak	Off-Peak	Both
Energy	On-Peak Energy Charge	Off-Peak Energy Charge	None
Energy Rate	$u_{e-on}$	$u_{e-off}$	None
Power	Demand Charge	None	Facilities Charge
Power Rate	$u_{p-on}$	None	$u_{p-all}$

Fig. 3.7: Description of the assumed billing structure

power, called a facilities charge as shown in Fig. 3.7.

Energy fees are also assessed per kWh of energy consumed with a higher rate for energy consumed during on-peak hours and a lower rate for energy consumed during off-peak hours.

### 3.5.1 Power Charges

It is necessary to compute the maximum power both overall and for on-peak periods. Section 3.4 adopted the convention that  $\Delta T$  denotes the time offset between power samples and that each power reading would reflect the average power used in the previous interval. Now let us set  $\Delta T$  to 15 minutes, making  $\mathbf{p}_{total}$  an expression of the 15 minute average power. Next, let  $\mathcal{S}_{on}$  be the set of all indices belonging to on-peak time periods such that  $j \in \mathcal{S}_{on}$  implies that the  $j^{\text{th}}$  element of  $\mathbf{p}^{total}$ ,  $p_j^{total}$ , represents a 15 minute average during an on-peak interval and let  $q_{on}$  be the maximum on-peak average power. With these definitions, constraints for determining the maximum on-peak average are defined as

$$\begin{aligned}
 p_j^{total} &\leq q_{on} \quad \forall j \in \mathcal{S}_{on} \\
 \begin{bmatrix} 1 & -1 \end{bmatrix} \begin{bmatrix} p_j^{total} \\ q_{on} \end{bmatrix} &\leq 0 \quad \forall j \in \mathcal{S}_{on} \\
 A_{11}\mathbf{y} &\leq \mathbf{0} \\
 A_{11}\mathbf{y} &\leq \mathbf{b}_{11}.
 \end{aligned} \tag{3.54}$$

Because an increased value in  $q_{on}$  is directly related to an increase in cost, the optimizer will minimize  $q_{on}$  until it is equal to the maximum value in  $\{p_j^{total} \mid j \in \mathcal{S}_{on}\}$ . A similar procedure can be used to derive a set of constraints for the overall maximum average power,

denoted  $q_{\text{all}}$ , and is represented as

$$\begin{aligned} A_{12}\mathbf{y} &\leq \mathbf{0} \\ A_{12}\mathbf{y} &\leq \mathbf{b}_{12}. \end{aligned} \tag{3.55}$$

The charges for power are then expressed as

$$\begin{aligned} \text{power cost} &= q_{\text{on}} \cdot u_{\text{p-on}} + q_{\text{all}} \cdot u_{\text{p-all}} \\ &= \begin{bmatrix} u_{\text{p-on}} & u_{\text{p-all}} \end{bmatrix} \begin{bmatrix} q_{\text{on}} \\ q_{\text{all}} \end{bmatrix} \\ &= \mathbf{u}_{\text{p}}^T \mathbf{y}, \end{aligned} \tag{3.56}$$

where  $u_{\text{p-on}}$  is the rate per kW for on-peak power use, or the demand charge and  $u_{\text{p-all}}$  is the rate per kW for the overall maximum 15 minute average.

### 3.5.2 Energy Charges

Energy is defined as the integral of power over a length of time. Because the values for power given in this work reflect an average power, the energy over a given period can be computed by multiplying the average power by the change in time, or  $\Delta T$  such that

$$\text{Total Energy} = \mathbf{1}^T \mathbf{p}_{\text{total}} \cdot \Delta T. \tag{3.57}$$

However, because the energy is billed for on-peak and off-peak time periods, we define two binary vectors  $\mathbf{1}_{\text{on}}$  and  $\mathbf{1}_{\text{off}}$  such that  $1_j^{\text{on}} = 1 \forall j \in S_{\text{on}}$  and zero otherwise. Similarly,  $\mathbf{1}_{\text{off}} = \mathbf{1} - \mathbf{1}_{\text{on}}$ . The on-peak and off-peak energy can then be computed as

$$\begin{aligned} \text{On-Peak Energy} &= \mathbf{1}_{\text{on}}^T \mathbf{p}_{\text{total}} \cdot \Delta T \\ \text{Off-Peak Energy} &= \mathbf{1}_{\text{off}}^T \mathbf{p}_{\text{total}} \cdot \Delta T. \end{aligned} \tag{3.58}$$

Let  $u_{e\text{-on}}$  and  $u_{e\text{-off}}$  represent the on-peak and off-peak energy rates respectively. The total cost for energy is computed as

$$\begin{aligned}
\text{Energy Cost} &= (\mathbf{1}_{\text{on}} \cdot u_{e\text{-on}} \cdot \Delta T)^T \mathbf{p}_{\text{total}} + (\mathbf{1}_{\text{off}} \cdot u_{e\text{-off}} \cdot \Delta T)^T \mathbf{p}_{\text{total}} \\
&= (\mathbf{u}_{e\text{-on}} + \mathbf{u}_{e\text{-off}})^T \mathbf{p}_{\text{total}} \\
&= \mathbf{u}_e^T \mathbf{y}.
\end{aligned} \tag{3.59}$$

### 3.5.3 Cost Function and Final Problem

The entire cost function is given as the sum of the energy and power costs such that

$$\begin{aligned}
\text{Cost} &= \mathbf{u}_p^T \mathbf{y} + \mathbf{u}_e^T \mathbf{y} \\
&= (\mathbf{u}_p + \mathbf{u}_e)^T \mathbf{y} \\
&= \mathbf{v}^T \mathbf{y}.
\end{aligned} \tag{3.60}$$

The complete problem can now be formulated as

$$\begin{aligned}
&\min_{\mathbf{y}} \mathbf{y}^T \mathbf{v} \text{ subject to} \\
&\tilde{A}_{1:3} \mathbf{y} = \tilde{\mathbf{b}}_{1:3} \quad A_{1:12} \mathbf{y} \leq \mathbf{b}_{1:12}
\end{aligned} \tag{3.61}$$

or

$$\begin{aligned}
&\min_{\mathbf{y}} \mathbf{y}^T \mathbf{g} \text{ subject to} \\
&\tilde{A} \mathbf{y} = \tilde{\mathbf{b}}, \quad A \mathbf{y} \leq \mathbf{b}.
\end{aligned} \tag{3.62}$$

## 3.6 Results

This section shows performance for the proposed bus charging algorithm and contains three subsections. Section 3.6.1 compares the proposed method with a previously published algorithm [20].

The comparisons in this section consider a 5 bus, 5 charger scenario with a charge rate of 300 kW. Each solution is expressed in terms of a MILP and solved up to a 2% gap using Gurobi [39], unless otherwise specified. The uncontrolled loads from Section 3.4 are represented with a scaled version of historical data from the Trax Power Substation at UTA.

The scaling served to increase the difficulty of the charging problem and better illustrates the capabilities of the proposed algorithm.

### 3.6.1 Cost Comparison with Prior Work

This section compares the monthly cost of energy for the proposed method with three other methods in equivalent 5 bus 5 charger scenarios. The first method is a baseline algorithm that simulates how bus drivers at the Utah Transit Authority (UTA) in Salt Lake City (SLC) charge by default. The second method comes from [26], which was selected because it is very similar to the proposed algorithm, and the third compares with [22] because of how [22] focuses on reducing the instantaneous load from charging. The charge plan for each method is computed using mixed integer linear programs as described below.

Conversations with bus drivers at the UTA in SLC have shown that bus drivers generally top off their batteries whenever a charger is available. In essence, the bus drivers are solving a maximization problem by default as they maximize the number of charge sessions in a day. Hence, the baseline algorithm follows the constraints in (3.61) but incentivizes buses to charge as frequently as possible. Let  $v_{\sigma}^{ijk}$  be the value of the objective function  $v$  at the index corresponding to  $\sigma_{ijk}$  from Section 3.2.2. By letting  $v_{\sigma}^{ijk} = -1$ ,  $\forall i, j, k$  and zero otherwise, the baseline method effectively maximizes the number of times a bus can charge. All methods are evaluated according to the rate schedule in [18].

A comparison for each method is given in Fig. 3.8. Note how the cost of energy is generally the same for each algorithm and that the primary differences in cost come from the on-peak and facilities power charges, illustrating the need to minimize peak average power. To understand the difference in power management between the baseline and the proposed method, refer to Fig. 3.9. Note how the power for the proposed method (blue line) is almost completely flat, indicating a steady power use. In comparison, the baseline algorithm (red line) is less steady and includes periods of high power use, which leads to the increased power charges in Fig. 3.8.

A similar phenomena is observed when comparing the proposed method to [26]. Fig. 3.10 compares the average power for the proposed algorithm and [26]. Note how the pro-

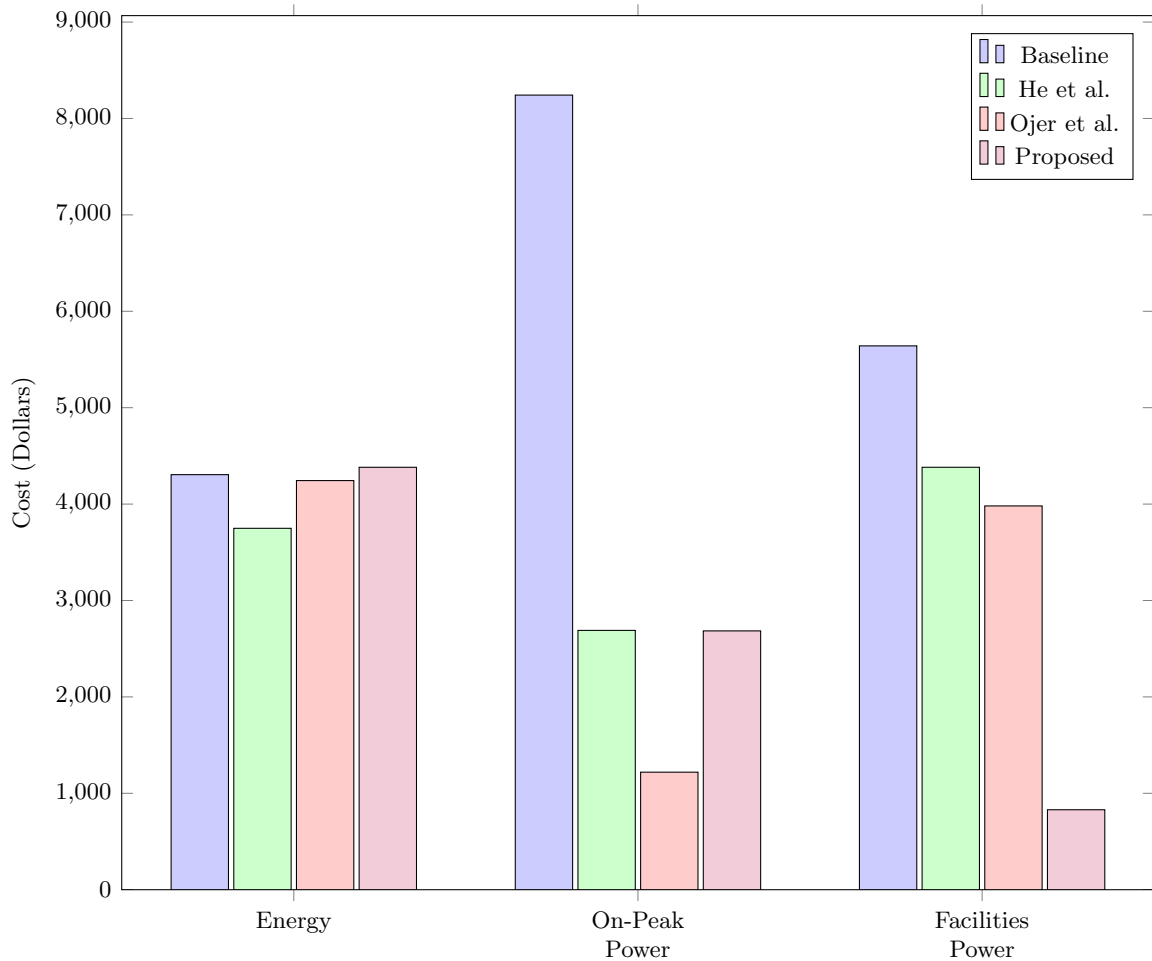


Fig. 3.8: Cost comparison with prior work

posed algorithm shifts the timing of charging events to produce a charge profile (blue line) that is complementary to the uncontrolled load (tan line). When the uncontrolled load increases the bus load decreases, yielding a flat overall load profile (not shown), whereas the load profile from [26] (red line) shifts charging events to minimize charging during on-peak periods only, but ignores uncontrolled loads. The ability of the proposed method to produce a consistent load profile improves upon [26] because it accounts for the effects of uncontrolled loads and the costs of average power.

### 3.6.2 Scalability

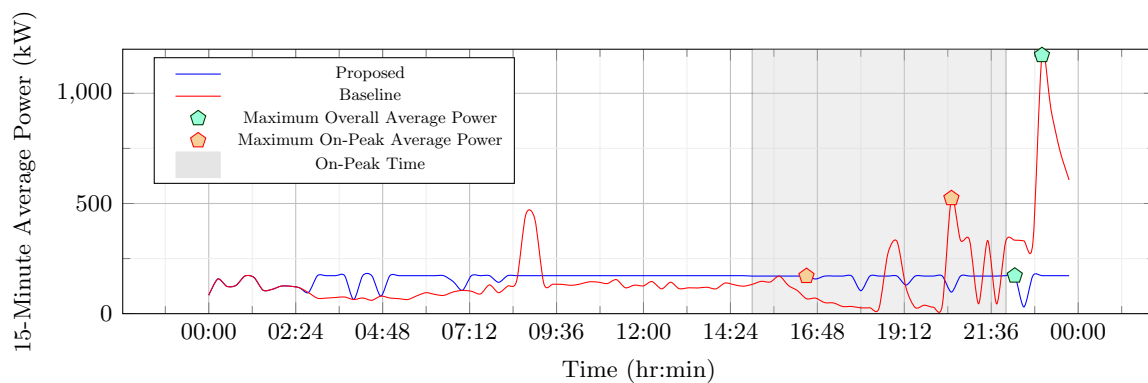


Fig. 3.9: 15-Minute average power for one day

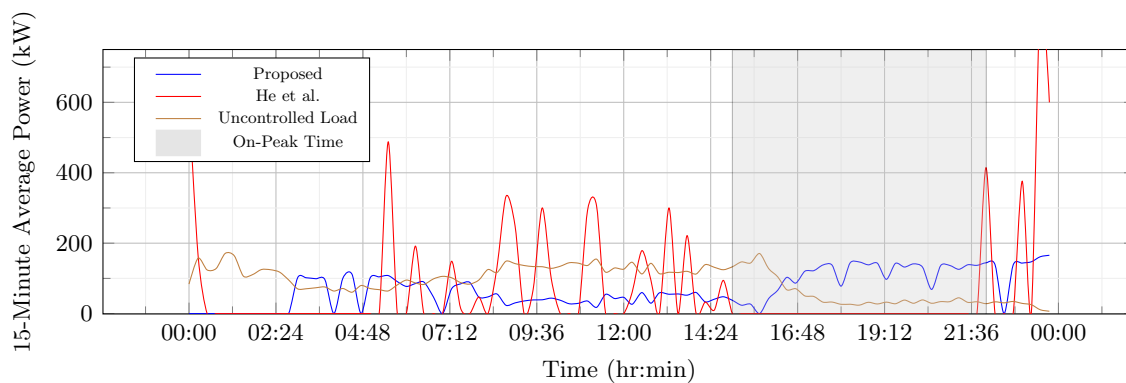


Fig. 3.10: Comparison between uncontrolled and bus loads

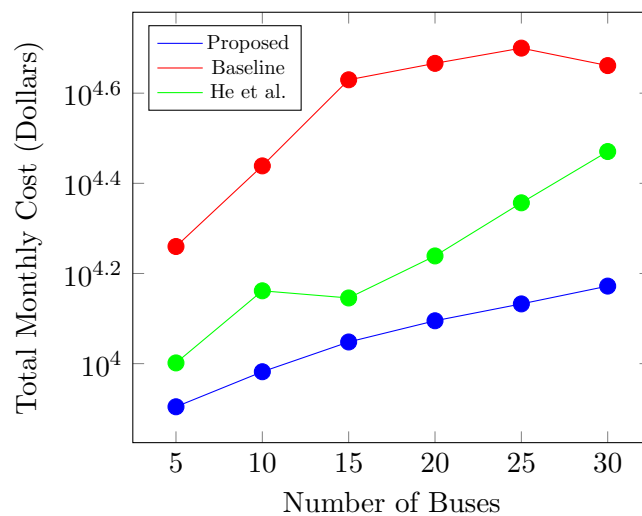


Fig. 3.11: Monthly Cost with 5 Chargers

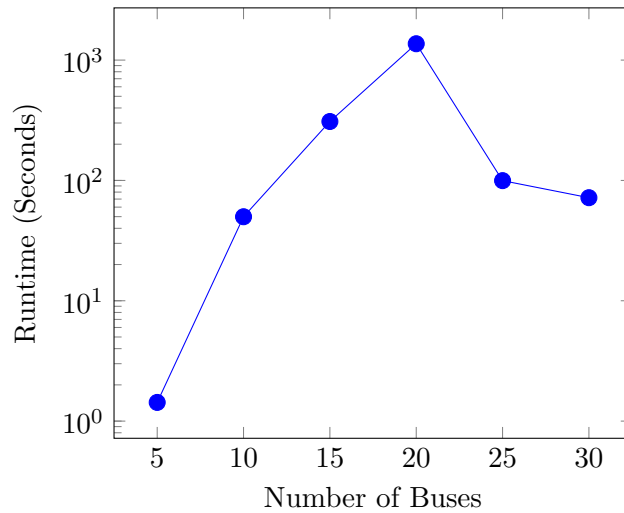


Fig. 3.12: Runtime with 5 Chargers at a 7% Gap

In this section we discuss the limitations for scaling the proposed method with respect to the number of buses. Specifically, we desire to show that the proposed method both performs well with large numbers for buses and can be computed in a reasonable period of time. In Fig. 3.11, we show how the cost increases with additional buses. Note how the monthly cost of power generally increases by approximately \$780 per bus, and that the relationship between cost and bus is linear. This indicates that for each additional bus in the fleet, the added expense comes from energy because the peak loads are intelligently managed. Additionally, the baseline algorithm which refuels buses whenever there is an opportunity reports significant cost increases as the number of buses increase. It is interesting to note how the cost does taper as the bus-to-charger ratio increases, which is not unreasonable as the baseline method does not optimize with respect to cost. The differences between the proposed method and [26] continued to scale as well so the proposed outperformed both the baseline and the method given in [26] in scenarios where there were more buses.

The results for Fig. 3.12 were obtained by optimizing the monthly cost of 5 to 30 buses up to a 7% gap. Note how the runtime increases significantly as the fleet size increases from 5 to 20 buses and then begins to decrease as the fleet size grows to 30 buses. To understand this behavior, recall that the optimizer is essentially addressing two problems. The first problem is how to schedule charging sessions so that each bus leaves on time and

carries sufficient charge. The second problem is to minimize the monthly cost of charging. When the fleet size is small, there are many different charging schedules that meet time and charge constraints and the optimizer has flexibility to select the schedule that minimizes cost. As fleet size increases, the complexity of the scheduling problem increases and this is manifest in increasing runtimes. Past a certain point (above 20 buses in the given scenario) contention for time on the chargers increases and there are fewer charging schedules that meet time and charge constraints. The optimizer has fewer options from which to choose (smaller feasible set) and the optimizer converges more quickly, reducing runtimes.

Variable	Description	Range	Variable	Description	Range
Indices					
$i$	Bus index	$\mathbb{N}$	$j$	Route index	$\mathbb{N}$
$k$	Charger index	$\mathbb{N}$			
Route Variables					
$a_{ij}$	The $j^{\text{th}}$ anticipated arrival time of bus $i$	$\mathbb{R}$	$c_{ij}$	The start time of the commanded charge window if bus $i$ charges during stop $j$ .	$\mathbb{R}$
$s_{ij}$	The stop time of the commanded charge window if bus $i$ charges during stop $j$ .	$\mathbb{R}$	$d_{ij}$	The $j^{\text{th}}$ anticipated departure time of bus $i$ .	$\mathbb{R}$
$\sigma_{ijk}$	A binary decision variable that is one when bus $i$ charges during stop $j$ at charger $k$ .	$\{0, 1\}$	$l_{(ij, i'j')}$	A slack variable that is 1 when bus $i$ uses a charger before bus $i'$ and 0 otherwise.	$\{0, 1\}$
$\mathcal{S}$	The set of all pairs $((i, j), (i', j'))$ where bus $i$ and bus $j$ may use the same charger during the $j$ and $j'$ stops respectively.	$(i, j) \times (i', j')$			
State of Charge					
$h_{\min}$	The minimum allowable state of charge	$(0, h_{\max})$	$h_{\max}$	The maximum state of charge	$\mathbb{R}$
$\eta_i$	The beginning state of charge for bus $i$	$(h_{\min}, h_{\max})$	$h_{ij}$	The state of charge for bus $i$ at the beginning of the $j^{\text{th}}$ stop.	$(h_{\min}, h_{\max})$
$\Delta_{ij}$	The time bus $i$ spent charging during the $j^{\text{th}}$ stop.	$(h_{\min}, h_{\max})$	$p_i$	The power at which bus $i$ is charged.	$\mathbb{R}_+$

$\delta_{ij}$	The battery discharge for bus $i$ over route $j$ .	$\mathbb{R}_+$	$h_{i,\text{end}}$	Bus $i$ 's final state of charge.	$(h_{\min}, h_{\max})$
<hr/>					
Uncontrolled Loads					
$k_{ij}^{\text{start}}$	The time index for the start of bus $i$ 's $j^{\text{th}}$ stop	$\mathbb{Z}$	$k_{ij}^{\text{end}}$	The time index for when bus $i$ disconnects from a charger during its $j^{\text{th}}$ stop.	$\mathbb{Z}$
$\Delta T$	The time difference between each time index.	$\mathbb{R}$	$r_{ij}^{\text{start}}$	The remaining time after $c_{ij}$ has been descritized.	$[0, \Delta T)$
$r_{ij}^{\text{end}}$	The remaining time after $s_{ij}$ has been descritized.	$[0, \Delta T)$	nPoint	the number of desired discrete indices	$\mathbb{Z}$
$\mathbf{g}_{ij}^{\text{start}}$	A binary indicator variable which is one at the $k_{ij}^{\text{start}}$ index.	$\{0, 1\}^{\text{nPoint}}$	$\mathbf{g}_{ij}^{\text{end}}$	A binary indicator variable which is one at the $k_{ij}^{\text{end}}$ index.	$\{0, 1\}^{\text{nPoint}}$
$\mathbf{g}_{ij}^{\text{on}}$	A binary indicator variable which is one at each index between $k_{ij}^{\text{start}}$ and $k_{ij}^{\text{end}}$ .	$\{0, 1\}^{\text{nPoint}}$	$\mathbf{f}$	A index vector so that $\mathbf{f}_i = i$ for all integer $i$ between 1 and nPoint.	$\mathbb{Z}^{\text{nPoint}}$
$k_{\text{eq}}$	a binary indicator variable which is one when $k_{ij}^{\text{start}} = k_{ij}^{\text{end}}$ .	$\{0, 1\}$	$p_{ij}^{\text{start}}$	The average power corresponding to the $k_{ij}^{\text{start}}$ time index for bus $i$ 's $j^{\text{th}}$ stop.	$\mathbb{R}_+$
$p_{ij}^{\text{end}}$	The average power corresponding to the $k_{ij}^{\text{end}}$ time index for bus $i$ 's $j^{\text{th}}$ stop.	$\mathbb{R}_+$	$\mathbf{p}_{ij}^{\text{start}}$	$\mathbf{g}_{ij}^{\text{start}} \cdot p_{ij}^{\text{start}}$	$\mathbb{R}_+^{\text{nPoint}}$
$\mathbf{p}_{ij}^{\text{end}}$	$\mathbf{g}_{ij}^{\text{end}} \cdot p_{ij}^{\text{end}}$	$\mathbb{R}_+^{\text{nPoint}}$	$\mathbf{p}^{\text{load}}$	A vector containing the 15-minute averages for the uncontrolled loads	$\mathbb{R}_+^{\text{nPoint}}$

$\mathbf{p}^{\text{total}}$	The total 15-minute average power for both the uncontrolled loads and bus chargers.	$\mathbb{R}^{\text{nPoint}}$			
Objective Function					
$\mu_{e\text{-on}}$	On-Peak Energy Rate	$\mathbb{R}$	$\mu_{e\text{-off}}$	Off-Peak Energy Rate	$\mathbb{R}$
$\mu_{p\text{-on}}$	On-Peak Demand Power Rate	$\mathbb{R}$	$\mu_{p\text{-all}}$	Facilities Power Rate	$\mathbb{R}$
$\mathcal{S}_{\text{on}}$	The set of on-peak time indices	$\{1, \dots, \text{nPoint}\}_{\text{on}}$		Maximum average power during on-peak periods	$\mathbb{R}$
$q_{\text{all}}$	Maximum average power for all time.	$\mathbb{R}$	$\mathbf{1}_{\text{on}}$	a binary vector which is 1 at the on-peak time indices	$\{0, 1\}^{\text{nPoint}}$
$\mathbf{1}_{\text{off}}$	a binary vector which is 1 at the off-peak time indices	$\{0, 1\}^{\text{nPoint}}$	$\mathbf{u}_{e\text{-on}}$	a vector of conversion factors from average on-peak power to consumption cost.	$\mathbb{R}^{\text{nPoint}}$
$\mathbf{u}_{e\text{-off}}$	a vector of conversion factors from off-peak average power to consumption cost.	$\mathbb{R}^{\text{nPoint}}$	$\mathbf{u}_e$	a vector of conversion factors from on and off-peak power to consumption cost.	$\mathbb{R}^{\text{nPoint}}$
$\mathbf{u}_p$	A vector of conversion factors from on and off-peak max power to demand cost.	$\mathbb{R}^{\text{nPoint}}$	$\mathbf{v}$	a vector of conversion factors such that $\mathbf{v}^T \mathbf{y}$ yields the total montly cost of power.	$\mathbb{R}^{\text{nPoint}}$

## CHAPTER 4

## A Scalable Approach for Computing Charge Plans for Large Bus Fleets

**4.1 Introduction**

Battery electric buses (BEBs) are replacing diesel and natural gas buses in public transportation because BEBs offer many benefits [4] including reduced maintenance [3], zero emissions [2], and access to renewable energy [5]. The challenge of prolonged charging times has been addressed in prior research including distributed charging networks [29], bus availability, environmental impact [16], route scheduling [15], battery health [38], the cost of electricity [19], and the cost of charging infrastructure [31].

Because charge times can be lengthy, some prefer to use high power chargers, which deliver more energy in a smaller period of time. However doing so places large power demands on electrical infrastructure [6] so that power networks becomes unreliable [7] and expensive because high power requires additional maintenance and upgrades [8]. An effective charge plan must therefore balance the need to charge quickly with the desire to maintain a low power profile [22].

Methods for developing a charge plan range from heuristic approaches [23], to network flow on a graph [17], to reinforcement learning [24], to mixed integer linear programs (MILP) [25]. Generally, each method minimizes cost by either decreasing the instantaneous power needs for the fleet, or optimizing over time of use tariffs [26].

Scaling these methods to large bus fleets (>100 BEBs) and numerous chargers is a challenge due to the size of the problem that must be solved. For small fleets (<50 BEBs) and less than 10 chargers, the optimization problems in [17, 25, 26] have over  $10^5$  variables (including binary or integer variables) and over  $10^5$  constraints. Scaling to larger fleets and more chargers leads can stress computational resources and require lengthy solve times.

This paper continues the main theme of prior work which is to develop charging schedules for electric buses that minimize the monthly electricity bill (energy consumption plus power demand) while satisfying route constraints that demand buses be in specific locations at specific times. One novelty is that our formulation considers the aggregated effects of loading across multiple meters. While meter aggregation is not widespread today, distribution networks must be built to supply worst case loads to each metered circuit. Therefore, our approach begins to explore how optimization of loads across multiple meters can reduce the overall impact of BEB charging on the grid. In this work, meter aggregation is modeled through the inclusion of uncontrolled (i.e. non-BEB charging) loads. Specifically, we incorporate historical load data from an electric train (UTA TRAX) that visits a central intermodal hub site in Salt Lake City, Utah which is also a charging stop for BEBs.

The main contribution of the present paper is addressing the matter of scale. Rather than posing a single large MILP that incorporates every aspect of the charging problem, we solve a series of small subproblems in which the solution to the charging problem becomes successively more refined and moves closer to the optimal schedule. Our results show that the intermediate subproblems can be solved with a dramatic reduction in runtimes allowing our method to be applied to significantly larger bus fleets. In a sense, this work explores what is gained in runtime by sacrificing optimality in the schedule. The subproblems fall into three groups as shown in Fig. 4.1. Each sub-problem is solved using a linear, quadratic, or integer program and when used together the series of programs provides a near optimal charge plan. Each sub-problem addresses elements from one of three areas: energy allocation and bus grouping, session length and bus-to-charger assignments, and second-by-second optimization.

#### 4.1.1 Energy Allocation and Group Assignment

The first set of problems answers two primary questions: At which time should energy be delivered to each bus and which buses are most able to share chargers, and contains three sub-problems: Unconstrained charge schedule, Smooth charge schedule, and group separation.

The unconstrained schedule problem from Section 4.2 is denoted  $p_1$  and computes an optimal charge schedule which minimizes the monthly cost of power in the presence of uncontrolled loads under the assumption that each bus maintains a dedicated charger.

The smooth schedule problem from Section 4.3 is denoted  $p_2$  and has the same form as the unconstrained scheduling problem with two differences: The monthly cost is required to match the optimal cost from the solution to the unconstrained scheduling problem and the objective for the smooth schedule problem penalizes change in the scheduled charge rates.

The group assignment problem from Section 4.4 is denoted  $p_3$  and uses the resulting charge schedules from the solution to the smooth schedule problem to separate buses into groups where each bus's schedule overlaps as little as possible with the other schedules for buses in the same group so that each group can be addressed separately to manage the number of computations in succeeding problems.

#### 4.1.2 Session Time and Charger Assignment

The problems in the session time and charger assignment section are computed on a per-group basis to reduce the number of computations, address when charge sessions must start and stop, assign sessions to chargers and are comprised of three sub-problems: defragmentation ( $p_4$ ), charger assignment ( $p_5$ ), and session refinement ( $p_6$ ).

The defragmentation problem from Section 4.5 is denoted  $p_4$  and attempts to consolidate charge sessions with small amounts of energy to reduce the number of charge sessions and serves to both decrease the computational complexity of the charger assignment problem by reducing the number of charge sessions and simplify the charge schedule to make it more operationally feasible.

After consolidation, each charge session is defined by a minimum/maximum start/stop time as given by the bus's arrival and departure times and an energy requirement in kW. The charger assignment problem from Section 4.6 is denoted  $p_5$  and uses the availability and energy constraints to assign chargers to charge sessions.

Once charge sessions are placed, the final step is to ensure each session makes the most of each charger's availability. Many times, especially when using non-optimal gaps in



Fig. 4.1: Overall Processing Chain

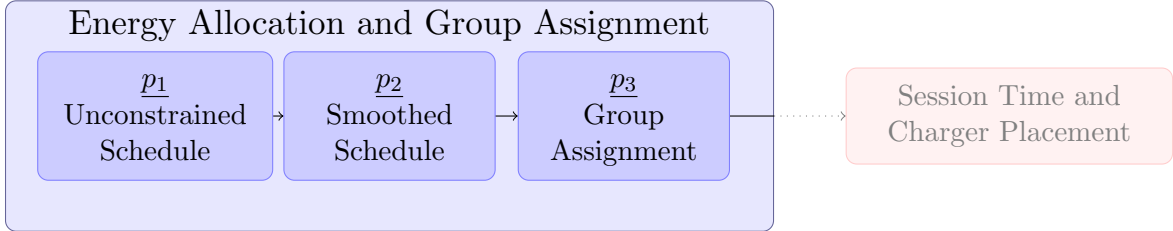


Fig. 4.2: Processing chain for the energy allocation and group assignment problems

the charger assignment problem, the charge schedules may not use all available time on a charger. The charger refinement problem is denoted  $p_6$  and expands each charge session to fill unused time on either side and prioritizes sessions with higher energy demands for adjacent sessions.

### 4.1.3 Final Optimization

Solutions to the previous problems provide us with a set of charge sessions, energy requirements, and time schedules for specific chargers. The final question to be answered is how should the energy for each session will be delivered. The two sub-problems in the final optimization section,  $p_7$  and  $p_8$ , mirror the first two problems from the Energy Allocation and Group Assignment section. The first is denoted  $p_7$ , uses the energy and time constraints from previous solutions to compute an optimal charge schedule in Section 4.8 and is analogous to the unconstrained charge problem. The second is denoted  $p_8$  and computes a smoothed charge schedule with the same cost as the constrained schedule solution in Section 4.9 and is analogous to the Smooth charge schedule problem in Section 4.3. The table given in Fig. 4.5 lists each problem and which features each problem incorporates.

## 4.2 $p_1$ : Unconstrained Schedule

This section describes a program that solves  $p_1$  by finding an optimal charge schedule

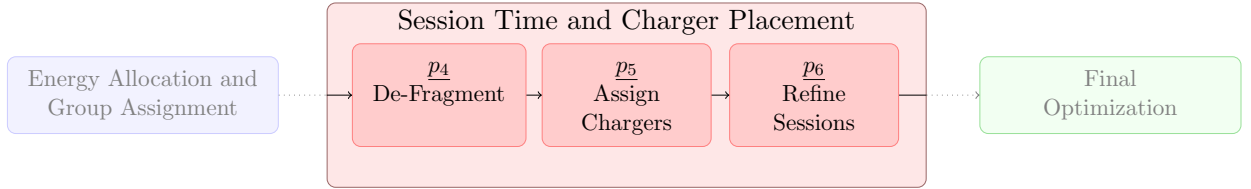


Fig. 4.3: Processing chain for each group

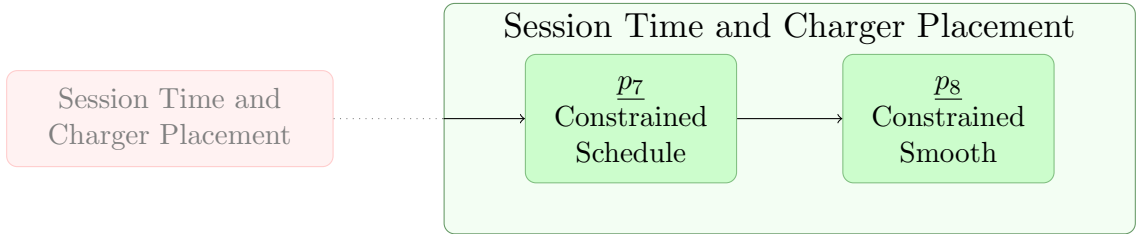


Fig. 4.4: Processing chain for the Final Optimization set

Feature	$p_1$	$p_2$	$p_3$	$p_4$	$p_5$	$p_6$	$p_7$	$p_8$
Battery State of Charge	x	x		x			x	x
Minimize Cost	x	x		x			x	x
Charger Capacity	x	x	x	x	x		x	x
Energy Placement	x	x		x			x	x
Smooth Charge Plan		x						x
Computationally Scalable			x				x	x
Small Number of Charge Sessions				x			x	x
Number of Chargers					x		x	x
Efficient Charger Use						x	x	x
Precise Charge Plan							x	x

Fig. 4.5: Descriptions of in which problems features are addressed

Table 4.1: Description of the billing structure

	On-Peak	Off-Peak	Facilities (Both)
Energy Rate	\$ 0.058282 /kWh	\$ 0.029624 /kWh	None
Energy Rate Symbol	$\mu_{e-on}$	$\mu_{e-off}$	None
Power Rate	\$ 15.73 /kW	None	\$ 4.81 /kW
Power Rate Symbol	$\mu_{p-on}$	None	$\mu_{p-all}$

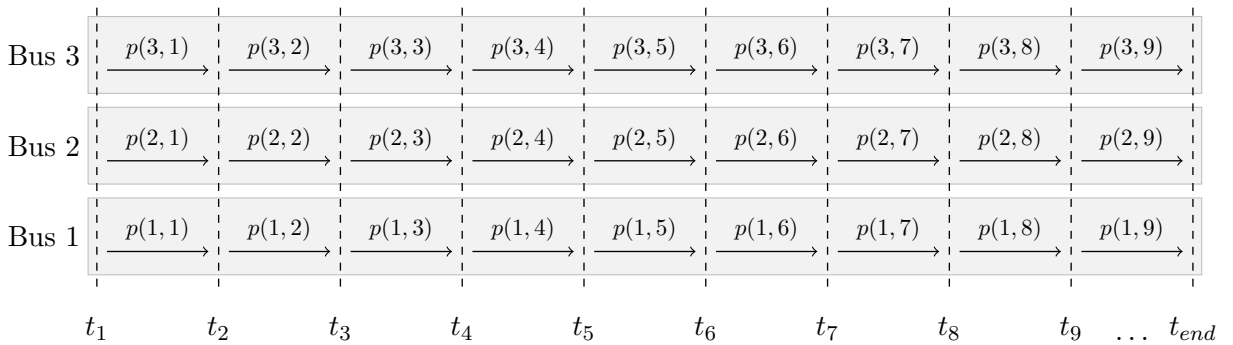


Fig. 4.6: Demonstrates how bus power use is conceptualized

where buses are allowed to charge without regard to the number of available chargers. This solution is considered “optimal” and will be used in later sections to formulate a feasible solution that accounts for the number of chargers.

#### 4.2.1 Formulation

The cost objective we minimize is based on the rate schedule from [18], which contains two primary elements: the cost of energy, and power demand. Energy is billed per kWh for on-peak and off-peak hours. The on-peak rate is more expensive because there is generally more demand for power during this time, whereas off-peak hours tend to be less expensive. The demand is covered in two separate chargers. The first is a facilities charge which is billed per kW for the highest 15-minute average power use over the course of the month.

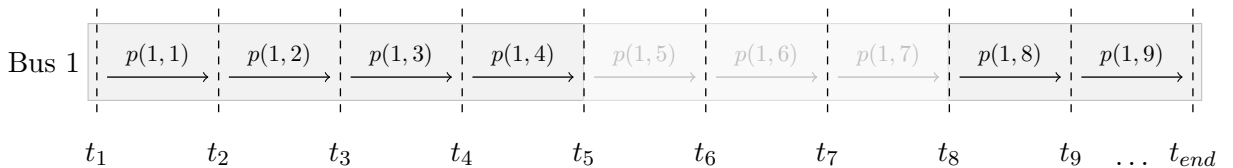


Fig. 4.7: Bus schedule with availability

The second is a demand charge, which is also billed per kW, but is only billed for the highest 15-minute average power used during on-peak hours. The rates for each component are given in Table 4.1.

Before we may compute the total monthly cost of electricity, we must define expressions for the average power and energy over time. Let each day be divided into time intervals of length  $\Delta T$  for each bus where the average power expended for bus  $i$  during time  $j$  is denoted  $p(i, j)$  as shown in Fig. 4.6 (Note that  $\Delta T$  may not be 15 minutes, and expressions for the 15-minute average will be computed later). The resulting solution of  $p_1$  will yield the average power expended by each bus during each period of time.

One constraint for which the solution must account is bus availability. When a bus is out of the station, the maximum average power for that time must be zero. For example, if bus 1 were out on route for  $t_5, t_6$ , and  $t_7$ , then the average power for those periods would be equal to zero as shown in Fig. 4.7. Let  $b_{p(i,j)}$  be the average power used by bus  $i$  at time index  $j$ , and  $\mathbf{b}$  be a vector which contains  $b_{p(i,j)}$  for each bus and time index. Also let  $\mathcal{A} \subset i \times j$  be the set of all indices where bus  $i$  is in the station during time  $t_j$  and  $\tilde{\mathcal{A}}$  be its complement. Furthermore, let  $p_{\max}$  be the maximum power that a charger can deliver.

We define a set of constraints so that buses do not use power when not in the station by letting

$$\begin{aligned} b_{p(i,j)} &= 0 \quad \forall i, j \in \tilde{\mathcal{A}} \\ b_{p(i,j)} &\leq p_{\max} \quad \forall i, j \in \mathcal{A} \\ -b_{p(i,j)} &\leq 0 \quad \forall i, j \in \mathcal{A}. \end{aligned} \tag{4.1}$$

### 4.2.2 Battery

Each bus must also maintain its state of charge above acceptable levels throughout the day. When buses leave the station, each bus discharges some quantity of energy throughout the course of the route. Let  $\delta(i, j)$  be the amount of charge lost by bus  $i$  at time  $j$  and let  $h(i, j)$  be the state of charge of bus  $i$  at time  $j$ . The state of charge for each bus can be

defined as

$$\begin{aligned} h(i, j) &= h(i, j - 1) + b_p(i, j - 1) \cdot \Delta T - \delta(i, j) \quad \forall i, j > 1 \\ h(i, 1) &= \eta_i \quad \forall i, \end{aligned} \tag{4.2}$$

where  $\eta_i$  is the initial state of charge for bus  $i$  and  $\Delta T$  is the difference in time between  $t_{i,j}$  and  $t_{i,j+1}$ . Now that each value for the state of charge is defined, each value for  $h$  must be constrained so that it is greater than a given threshold,  $h_{\min}$  but does not exceed the maximum battery capacity  $h_{\max}$ . This yields

$$\begin{aligned} -h(i, j) &\leq -h_{\min} \quad \forall i, j \\ h(i, j) &\leq h_{\max} \quad \forall i, j. \end{aligned} \tag{4.3}$$

The final battery related constraint has to do with how we are planning for the bus. The expenses that come from power are computed monthly, but we desire to simulate the movements of the bus for only a day, and use this to extrapolate what the monthly cost may be. Therefore, the state of charge for a bus at the end of the day must reflect its starting value. This yields the following constraint:

$$h_{i,\text{end}} = h(i, 1) \quad \forall i. \tag{4.4}$$

### 4.2.3 Cumulative Load Management

While this formulation does not directly account for the number of available chargers, we do account for the cumulative load capacities of all chargers. Let the number of chargers be denoted  $n_{\text{charger}}$ . We desire to maintain the average cumulative power for each time step at a level that is serviceable given  $n_{\text{charger}}$ . We define a slack variable  $p_c(j)$  which represents the total average power consumed by all buses at time  $j$ . The variable  $p_c(j)$  is computed as the sum of average bus powers so that

$$p_c(j) = \sum_i b_p(i, j). \tag{4.5}$$

#### 4.2.4 Objective

Now that the relevant constraints have been addressed, we must work towards computing the total objective function. We do so by first computing the total average power for the complete system. This total power is comprised of power used by the buses, and power used by external sources such as lights, ice melt, electric trains, etc which we refer to as “uncontrolled loads”, where the average power for the uncontrolled loads at time step  $j$  is denoted  $u(j)$ . We compute the total power as the sum of power used by the buses,  $p_c(j)$  and the power consumed by uncontrolled loads  $u(j)$  so that the total power, denoted  $p_t(j)$  is computed as

$$p_t(j) = p_c(j) + u(j). \quad (4.6)$$

The next step is to compute the fifteen minute average power use for each time step, denoted  $p_{15}$ . We do this by letting

$$p_{15}(j) = \frac{1}{n} \sum_{l \in \{j_{15}\}} p_t(l), \quad (4.7)$$

where  $\{j_{15}\}$  is the set of all indices 15 minutes prior to  $j$  and  $n$  is the cardinality of  $\{j_{15}\}$ . Next, note that the rate schedule requires both the maximum overall average power, denoted  $p_{\text{facilities}}$ , and the maximum average power during on-peak hours, or  $p_{\text{demand}}$ . Let  $\mathcal{S}_{\text{on}}$  be the set of time indices belonging to on-peak hours, and recall that the max over all average power values is greater than or equal to  $p_{15}(j)$  for all  $j$ . We can express this constraint is

$$p_{\text{facilities}} \geq p_{15}(j) \quad \forall j. \quad (4.8)$$

Because  $p_{\text{facilities}}$  will be used in the objective function, the value for  $p_{\text{facilities}}$  will be minimized until it is equal to the largest value in  $p_{15}$ . Following a similar logic, we also define a set of constraints for the maximum average on-peak power,  $p_{\text{demand}}$  so that

$$p_{15}(i) - p_{\text{demand}} \leq 0 \quad \forall i \in \mathcal{S}_{\text{on}}. \quad (4.9)$$

The next step in computing the objective function is to compute the total *energy* consumed during on and off-peak hours respectively. Let  $e_{\text{on}}$  be the total energy consumed during on-peak hours and  $e_{\text{off}}$  be the energy consumed during off-peak hours. We can compute energy as the product of average power and time. In our case, we compute this as

$$\begin{aligned} e_{\text{on}} &= \Delta T \cdot \sum_{i \in \mathcal{S}_{\text{on}}} p_t(i) \\ e_{\text{off}} &= \Delta T \cdot \sum_{i \notin \mathcal{S}_{\text{on}}} p_t(i). \end{aligned} \tag{4.10}$$

We can now compute the total monthly cost in dollars as

$$J_{\text{cost}} = \begin{bmatrix} e_{\text{on}} \\ e_{\text{off}} \\ p_{\text{facilities}} \\ p_{\text{demand}} \end{bmatrix}^T \begin{bmatrix} \mu_{\text{e-on}} \\ \mu_{\text{e-off}} \\ \mu_{\text{p-all}} \\ \mu_{\text{p-on}} \end{bmatrix}, \tag{4.11}$$

where  $\mu_{\text{e-on}}$ ,  $\mu_{\text{e-off}}$ ,  $\mu_{\text{p-all}}$ , and  $\mu_{\text{p-on}}$  represent the cost for on-peak energy, the cost of off-peak energy, the facilities rate, and demand charge respectively.

In summary, the problem  $p_1$  described in Section 4.2 computes a charge schedule without constraints on the number of chargers. We have also observed that the resulting charge commands tend to be either 0 or  $p_{\text{max}}$  which is difficult to implement and imparts additional stress on charging hardware. Before additional steps can be taken, a smoothed version of the solution for  $p_1$  must be computed.

Summary for  $p_1$

$$\text{Min}_{\mathbf{y}} \text{ (4.11) subject to (4.1) - (4.10).}$$

where  $\mathbf{y}$  represents the variables of optimization for  $p_1$ .

### 4.3 $p_2$ : Unconstrained Smooth Schedule

This section implements a smoothing criteria so that the “on-off” patterns from the

first solution are softened. This is done by first solving the un-constrained charge problem as given. Next, the same problem is solved again but with two primary differences. The first is that the demand, facilities, on-peak energy, and off-peak energy are constrained so that they are equal to the values obtained in  $p_1$  so that

$$\begin{aligned}
 e_{\text{on}} &= \tilde{e}_{\text{on}} \\
 e_{\text{off}} &= \tilde{e}_{\text{off}} \\
 p_{\text{facilities}} &= \tilde{p}_{\text{facilities}} \\
 p_{\text{demand}} &= \tilde{p}_{\text{demand}}.
 \end{aligned} \tag{4.12}$$

Next, we define an alternative objective which incentivizes “smooth” transitions between time steps.

This objective is defined as

$$J_{\text{thrash}} = \frac{1}{n} \sum_{i,j \in \mathcal{K}} \|b(i, j) - b(i, j - 1)\|_2^2, \tag{4.13}$$

where  $\mathcal{K}$  is the set of all  $i, j$  where bus  $i$  may charge during time  $j$  and  $j - 1$ .

The smoothed schedule computed in  $p_2$  minimizes the cost of charging in a way that maintains smooth charge schedules but is undesirable because the charge sessions tend to be small so that many are required. Additionally, the current schedule does not account for the number of chargers and contention. Unfortunately, resolving these issues requires the use of binary variables and becomes intractable for large numbers of buses. Before the fragmentation and charger assignment problems can be addressed, we must first segment the buses into groups so that they can be processed separately which will better manage the computations for binary-centric problems.

Summary for  $p_2$

$$\text{Min}_{\mathbf{y}} \text{ (4.13) Subject to (4.1) – (4.10), (4.12)}$$

#### 4.4 $p_3$ : Group Assignment

Before the bus charge problem can be solved, we need to address how the problem will scale. In previous attempts to solve the charge problem, routing buses to chargers requires a program which selects an optimal, contention-free schedule by evaluating all possible combinations.

Because contention increases on the order of  $O(n^2)$  with the number of charge sessions and requires that each combination be evaluated to find an optimal solution, the placement problem is NP-hard [43]. Before we can formulate a scalable solution to the bus problem, we need a method to separate buses into groups to reduce the coupling between charge sessions.

The group assignment problem separates buses into  $n_{\text{group}}$  groups, where group  $m$  is allocated  $n_{\text{charger}}^m$  chargers and  $n_{\text{bus}}^m$  buses. Each group must have sufficient chargers to fill it's needs and prefer buses with dissimilar schedules to better avoid contention.

We know that the number of cross-terms in future problems will be reduced when each group has the same number of buses. Therefore, let  $n_{\text{bus}}^m$  be described as

$$\begin{aligned} n_{\text{bus}}^m &\geq \left\lfloor \frac{n_{\text{bus}}}{n_{\text{group}}} \right\rfloor \\ n_{\text{bus}}^m &\leq \left\lceil \frac{n_{\text{bus}}}{n_{\text{group}}} \right\rceil. \end{aligned} \tag{4.14}$$

We must also ensure that the number of chargers assigned to each group is exactly equal to the number of available chargers so that

$$n_{\text{charger}} = \sum_m n_{\text{charger}}^m, \tag{4.15}$$

where  $n_{\text{charger}}^m$  is the number of chargers assigned to group  $m$ .

The next set of constraints ensures that each bus is part of a group exactly once. Let  $\beta(i, m)$  be a binary variable which is one when bus  $i$  is in group  $m$ . We constrain each

bus to be a member of exactly one group by letting

$$\sum_m \beta(i, m) = 1 \quad \forall i. \quad (4.16)$$

We must also ensure that buses are assigned to groups where the power delivered to each bus can be achieved with the number of chargers assigned to that group. First, we define a slack variable which gives the total power used in group  $m$  at time step  $j$  as  $p(m, j)$ . Recall, we also know the expected power use for each bus as this is a result of  $p_1$  as  $b_{p(i,j)}$ , which allows us to describe the total power for any one group as

$$p(m, j) = \sum_i \beta(i, m) b_{p(i,j)}. \quad (4.17)$$

Next, we know that the total load of each group must be less than or equal to the collective capability of that group's chargers, which can be expressed as

$$n_{\text{charger}}^m \cdot p_{\text{max}} \geq p(m, j) \quad \forall m, j \quad (4.18)$$

so that the number of chargers is sufficient to charge the collective load of the group.

We also desire to group buses together who's routes have the least overlap. If two buses contain no overlap, they will be easiest to schedule and the inner product of their schedules from  $p_1$  will be equal to zero. Let

$$\phi(i, i') = \mathbf{b}(i, :)^T \mathbf{b}(i', :),$$

where  $\mathbf{b}(i, :)$  is the charge schedule for bus  $i$  as computed in the  $p_1$ . We desire to minimize the total cross terms  $\phi(i, i')$  for all buses in the same group. Define a slack variable  $v(i, i', m)$  which is equal to  $\phi(i, i')$  if buses  $i$  and  $i'$  are both in group  $m$  and zero otherwise so that

$$\begin{cases} v(i, i', m) = \phi(i, i') & \beta(i, m) = 1, \beta(i', m) = 1 \\ v(i, i', m) = 0 & \text{otherwise,} \end{cases}$$

which can also be expressed by letting

$$\begin{aligned}
v(i, i', m) &\leq \phi(i, i') \\
v(i, i', m) &\geq \phi(i, i') - M(2 - \beta(i, m) - \beta(i', m)) \\
v(i, i', m) &\leq 0 + M\beta(i, m) \\
v(i, i', m) &\leq 0 + M\beta(i', m) \\
v(i, i', m) &\geq 0.
\end{aligned} \tag{4.19}$$

The final objective can then be expressed as

$$J_{\text{select}} = \sum_{i, i', m} v(i, i', m). \tag{4.20}$$

Problems  $p_1$  through  $p_3$  have yielded preliminary estimates for charge schedules as well as groups into which the buses can be subdivided but have not addressed the problem of fragmentation, where each bus's schedule contains many small charge events where fewer are desired. Before we can address where buses should charge, we must first finalize each bus's charge schedule by decreasing the number of charge events.

Summary for  $p_3$

$$\text{Min}_{\mathbf{y}} \text{ (4.20) subject to (4.14) - (4.19)}$$

#### 4.5 $p_4$ : Defragmentation

A minimum charge session length is another operational constraint that must be considered. We also consider constraints on minimum energy delivered per session. The intent of these constraints is to avoid charging for small durations or for small amounts of energy so that charge sessions are consolidated for convenience.

To solve this program, assume there exists a “smoothed” solution from  $p_2$  which has been appropriately placed in a group from  $p_3$ . Next, let the preliminary solution be subdivided into charge sessions, each with a specific amount of energy, a minimum start time,

and a maximum stop time. If the energy for any charge session is less than the allowed, then this session is marked as “fragmented”. The remaining sessions are either marked as “used” or “unused”, where a used session delivers more power than specified in the “fragmentation-threshold”, and an unused session delivers zero power.

The purpose of  $p_4$  is to determine which sessions will be “active” in deployment while adhering to minimum charge thresholds. The sessions in question are the “fragmented” sessions. Let  $\theta(i, r)$  be a binary variable which indicates if session  $r$  from bus  $i$  will be active. Because the only sessions in question are fragmented, we only need to define  $\theta(i, r)$  for fragmented sessions. Limiting the binary variables in this fashion significantly reduces the computational complexity of this step. The charge problem will be resolved using the same constraints and objective as  $p_1$ , but with two primary changes.

The first change constrains the minimum power delivery for each “active” charge session to be *at least* as large as the original power delivery. Let  $\rho(i, r)$  be a vector which is  $\Delta T$ , in hours, during the times bus  $i$  charges during session  $r$  and zero otherwise so that

$$\mathbf{b}(i, :)\rho(i, r) \geq \psi(i, j), \quad (4.21)$$

where  $\psi(i, j)$  is the minimum energy for session  $i, r$  and session  $i, r$  is considered “active”. For inactive sessions, the energy is constrained so that it is equal to zero. Finally, for fragmented sessions, the session energy must be greater than the minimum threshold,  $\omega$  when active and zero otherwise which can be expressed as

$$\begin{aligned} \mathbf{b}(i, :)\rho(i, r) &\geq \omega - \omega(1 - \theta(i, r)) \\ \mathbf{b}(i, :)\rho(i, r) &\leq 0 + \theta(i, r)e_{\max}, \end{aligned} \quad (4.22)$$

where  $e_{\max}$  is the maximum energy delivered in a session.

The solution to the defragmentation problem,  $p_4$  provides a charge plan that optimizes the cost of power while requiring that each charge session meets a minimum energy criteria. Up to this point however, we still have not addressed constraints related to the number of chargers which is the focus of  $p_5$  in the next section.

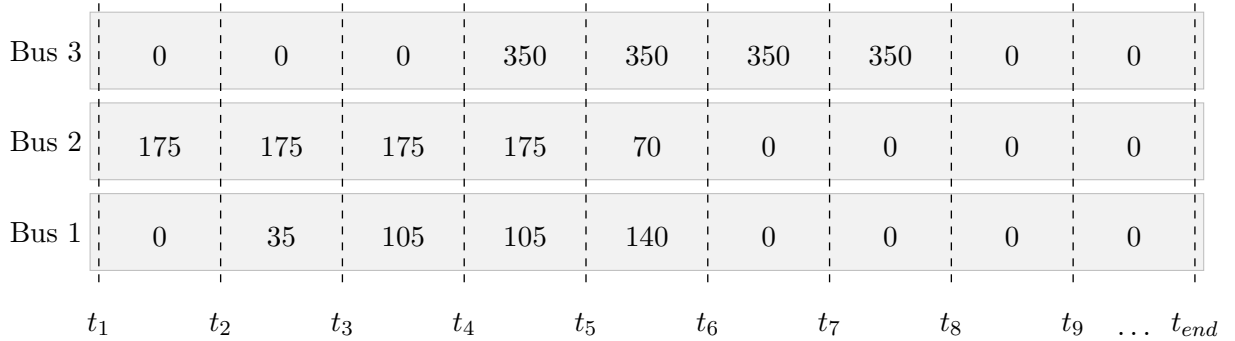


Fig. 4.8: An example solution to a 3-bus, 2-charger scenario from  $p_4$

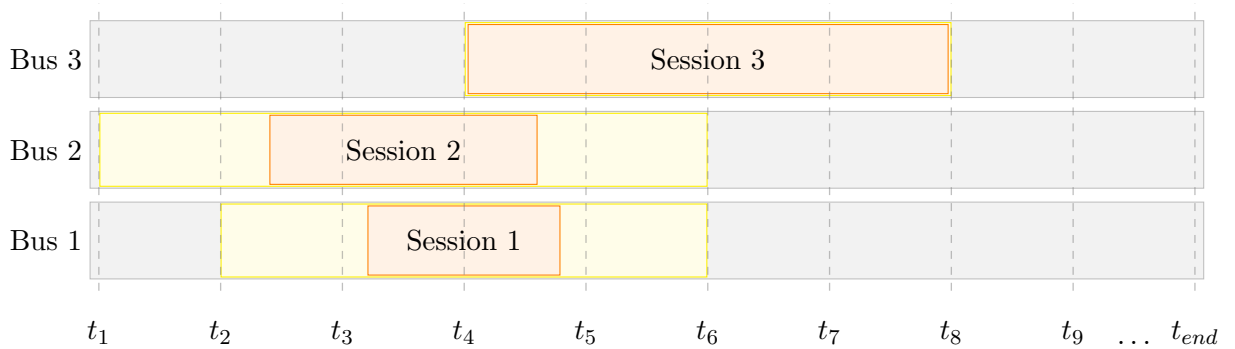


Fig. 4.9: Demonstrates how results from  $p_4$  can be reexpressed in terms of continuous variables

Summary for  $p_4$

Min<sub>y</sub> (4.11) subject to (4.1) – (4.10), (4.21), (4.22).

#### 4.6 $p_5$ : Charger Assignment

The results from  $p_4$  give a general estimate of how much and when buses should charge,

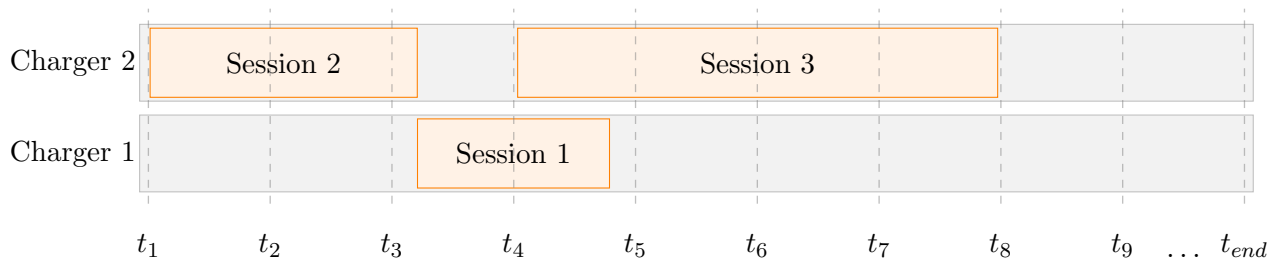


Fig. 4.10: Demonstrates the solution to  $p_5$

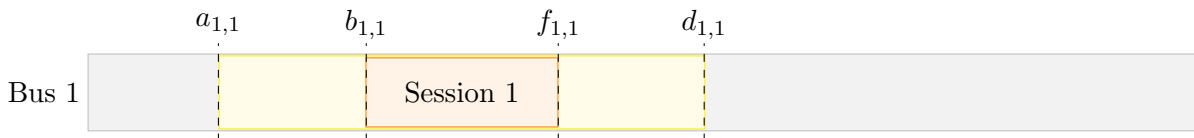


Fig. 4.11: Gives variables of optimization for  $p_5$

however we must still address two primary issues. The first is defining concrete start and stop times for each charge session. The second is limiting the charge sessions to a finite number of chargers.

Consider a solution to a three bus, two charger scenario given in Fig. 4.8. Note that there appears to be three buses charging at the same time from  $t_5$  to  $t_6$  even though there are only two chargers. We can reformulate this solution in terms of continuous start and stop variables and a variable charge rate so that the *duration* of each charge session may be relaxed. The objective is to store the given energy in the corresponding bus within the given charge interval.

Note how few of the charge sessions utilize the chargers to full capacity. This implies that there exists a smaller charge window in which equivalent power can be delivered. This allow us to use the charge durations from the solution from Fig. 4.8 as bounds on *allowable* charge windows instead of absolute truth.

An example of how Fig. 4.8 may be reformulated is given in Fig. 4.9. Note how the actual charge sessions don't necessarily need to take up all the time they were initially allocated in the first solution and that these times can fluctuate if the average charge rate is less than the maximum charger capacity. In this example, we assume a maximum charge capacity of 350kW.

Note how the third charge session does have to be exactly where it was scheduled because the average is equal to the maximum charge rate. If we examine just the schedule for Bus 1, we note that there are four essential variables for the corresponding charge session:  $a(i, r)$ ,  $b(i, r)$ ,  $f(i, r)$  and  $d(i, r)$  which represent the minimum start time, actual start time, actual end time, and maximum end time respectively.

The problem we must now solve is one of arranging these “rectangles” such that each

one is larger than its minimum width (or charge time). We must also account for the number of chargers. It can be helpful to view the problem as a bin packing problem, where each session must fit within the “swim lane” of a charger. For example, taking the charge sessions given in Fig. 4.9 and arranging them so that there is no overlap between sessions will yield a valid solution as shown in Fig. 4.10.

From Fig. 4.11, we know that  $a(i, r)$ ,  $b(i, r)$ ,  $f(i, r)$  and  $d(i, r)$  must be such that

$$\begin{aligned} a(i, r) &\leq b(i, r) \\ b(i, r) &\leq f(i, r) \\ f(i, r) &\leq d(i, r), \end{aligned} \tag{4.23}$$

where  $a(i, r)$  and  $d(i, r)$  are known from the previous optimization problem, and  $b(i, r)$  and  $f(i, r)$  are optimization variables.

We must differentiate between chargers and so, define  $\sigma(i, r, k)$  as a binary selector variable which is one if charger  $k$  services bus  $i$  for session  $r$  and zero otherwise. We know that only one charger can charge each bus at a time. We also know that each charge session *must* be serviced, which implies that

$$\sum_k \sigma(i, r, k) = 1 \quad \forall i, r. \tag{4.24}$$

Next, we also know that during each session a certain amount of energy must be transferred from the charger to the battery. The amount of energy that must be transferred to bus  $i$  during session  $r$  are given in the solution to  $p_4$  and are denoted  $e(i, r)$ . We can compute a minimum time window from these values by letting

$$w(i, r)_{\min} = \frac{e(i, r)}{p_{\max}}. \tag{4.25}$$

If we include constraints for a minimum time per session, then the previous expression becomes

$$w(i, r)_{\min} = \max \left( w_{\min}, \frac{e(i, r)}{p_{\max}} \right).$$

Because this is the minimum time window, we must ensure that the difference between the start and stop times is at least this large so that

$$f(i, r) - b(i, r) \geq w(i, r) \quad \forall i, r. \quad (4.26)$$

The final set of constraints deals with contention so that no charger can be scheduled for two sessions that overlap. let  $\mathcal{L} = \{(i, r) \times (i', r')\}$  where charge sessions  $i, r$  and  $i', r'$  have the potential to overlap. Before we can prevent overlap, we must define a binary variable  $l(i, r, i', r')$  which is equal to one when session  $i, r$  is scheduled before session  $i', r'$  and zero otherwise so that

$$\begin{cases} f(i, r) \leq b(i', r') & l(i, r, i', r') = 1 \\ f(i', r') \leq b(i, r) & l(i, r, i', r') = 0. \end{cases} \quad (4.27)$$

Here we can expand this thought through use of the “big-M” technique. Let  $M$  be large. In this case, we can set it equal to the number of seconds in a day. We know what the top constraint must be trivially satisfied when  $l(i, r, i', r') = 0$  and the bottom must also when  $l(i, r, i', r') = 1$ . This leads to a reformulation so that

$$\begin{aligned} f(i, r) - b(i', r') &\leq M(1 - l(i, r, i', r')) \\ f(i', r') - b(i, r) &\leq l(i, r, i', r')M. \end{aligned}$$

However, this constraint *only* needs to hold when sessions  $i, r$  and  $i', r'$  are scheduled to charge on the same charger or that  $\sigma(i, r, k) = \sigma(i', r', k) = 1$ . We can reformulate the

above constraint to satisfy this condition by letting

$$\begin{aligned} f(i, r) - b(i', r') &\leq M(3 - \sigma(i, r, k) - \sigma(i', r', k) - l(i, r, i', r')) \\ f(i', r') - b(i, r) &\leq M(2 - \sigma(i, r, k) - \sigma(i', r', k) + l(i, r, i', r')). \end{aligned} \quad (4.28)$$

Finally, we desire the schedule to closely match the charge plan from  $p_4$ , which occurs when each charge session matches the durations given in  $p_4$  and so we formulated an objective function which minimizes the differences in the given plan and the results from  $p_4$  by letting the objective be

$$\min_{f,b} \sum_{i,r} \|b(i, r) - a(i, r)\|_2^2 + \|f(i, r) - d(i, r)\|_2^2, \quad (4.29)$$

which has the effect of driving each variable to the desired value and more heavily penalizing values that are further from their optimal.

Ideally, when  $p_5$  is solved to optimality, the chargers are fully utilized. However, optimality for  $p_5$  is computationally demanding and scalable solutions may require relaxations in the optimality gap so that time on the chargers is not fully utilized. The next section uses the ordering from  $p_5$ , but recomputes session start/stop times to better utilize the charger availability even when sub-optimal gaps are given for  $p_5$ .

#### Summary for $p_5$

Min  $\mathbf{y}$  (4.29) subject to (4.23) – (4.28).

## 4.7 $p_6$ : Optimizing Charge Schedules

Many times it is not feasible to compute the optimal set of charge schedules given in the previous sections. As the number of buses and charge sessions becomes large, computing a small-MIPGap solution becomes intractable. Using a large MIPGap resolves issues related to computational complexity, but results in sub-optimal charge-time windows.

We compute a more optimal set of charge windows by using the results from  $p_5$  to infer charger assignment, and ordering for each charge session. We also know that the optimal

solution will expand the charge windows to use any available time where a charger is unused, implying that the “stop” time for each session will either be equal to it’s buse’s departure time, or the start time of the next window which can be expressed as

$$\begin{cases} c(s, i, r + 1) = c(f, i, r) & c(d, i, r) > c(a, i, r + 1) \\ c(s, i, r + 1) = c(a, i, r + 1) & c(d, i, r) \leq c(a, i, r + 1), \\ c(f, i, r) = c(d, i, r) \end{cases} \quad (4.30)$$

where  $c(s, i, r)$  is the start time for charger  $i$ ’s  $r^{\text{th}}$  charge session,  $c(f, i, r)$  is the stop time for charger  $i$ ’s  $r^{\text{th}}$  charge session,  $c(d, i, r)$  is the departure time for the bus scheduled for charger  $i$ ’s  $r^{\text{th}}$  charge session, and  $c(a, i, r)$  is the arrival time for the bus scheduled for charger  $i$ ’s  $r^{\text{th}}$  charge session. The minimum charge length must also be used so that energy can be properly delivered, so that

$$c(f, i, r) - c(s, i, r) \geq w(i, r), \quad (4.31)$$

where  $w(i, r)$  is the corresponding minimum charge time corresponding the session.

The final step to optimizing the charge windows is to give preference to windows with larger power deliveries. Let the objective for the optimization program be

$$J_{\text{window}} = \frac{1}{n} \sum_{i,r} \left\| \frac{c(f, i, r) - c(s, i, r)}{e(i, r)} \right\|_2^2. \quad (4.32)$$

When the function  $J$  contains windows with equal amounts of energy, the minimum will be found where each charge interval is the same width. As the amount of energy increases, the objective penalizes less for larger window sizes and thus gives preference to high energy sessions.

Now each charge session is assigned to a charger so that contention for limited chargers has been managed for each group. Furthermore, each session also specifies target energy requirements which manage the risks of depleting batteries but does not give instructions

on how the energy is to be delivered. The energy delivery problem is addressed in  $p_7$  and combined results for all groups so that the charge schedule begins to approach a more global solution.

Summary for  $p_5$

$$\text{Min}_{\mathbf{y}} \text{ (4.32) subject to (4.30), (4.31)}$$

#### 4.8 $p_7$ : Constrained Schedule

Up to this point, we have computed the “optimal” schedule which assumes any bus can charge without regard to the number of chargers. We then separate buses into groups to reduce the scope of the problem and treat each sub-problem separately while we defragment and assign each charge session to specific chargers before determining the final start and stop times for each bus’s charge session.

The final step in this process is to determine how the energy will be delivered so that cost is minimised. Begin with constraints for bus power, energy, and cost from Section 4.2 that are given in (4.1), (4.4), (4.6), (4.7), (4.8), (4.9) and (4.10). Next, include constraints for energy so that the energy for each charge session is properly delivered using a modified version of Eqn. (4.21) so that

$$\mathbf{b}(i, :) \rho(i, r) = \psi(i, r), \quad (4.33)$$

where  $\psi(i, r)$  is the required energy for bus  $i$  during rest period  $r$  as computed from the solution of the defragmentation problem.

Summary for  $p_7$

$$\text{Min}_{\mathbf{y}} \text{ (4.11) subject to (4.1), (4.4), (4.6) – (4.10), (4.33)}$$

#### 4.9 $p_8$ : Constrained Smooth Schedule

The charge schedule from  $p_7$  will contain the same on-off defects as the solution to  $p_1$  which can be managed as before by executing  $p_7$  once again with two changes: The first constrains the objective so that it achieves the optimal cost. The second reduces the

difference of adjacent charge rates with the smoothing objective from (4.13).

Summary for  $p_8$

Min  $\mathbf{y}$  (4.13) subject to (4.1), (4.4), (4.6) – (4.10), (4.12), (4.33)

## 4.10 Results

The results given in this section aim to demonstrate how the proposed method can be used to find a scalable solution to the bus charge problem. Because the proposed solution contains various sub-problems, optimization parameters for each sub-problem may be tuned to best meet the demands of a given scenario, allowing for a wide degree of flexibility that is not present in prior works which formulate solutions to the bus charge problem as a single program.

### 4.10.1 Overall Performance

In this section, we compare the proposed method with a baseline algorithm and a method developed by [44]. The baseline method models how bus drivers charge their electric vehicles at the Utah Transit Authority in Salt Lake City, Utah. At UTA, when bus drivers arrive at the station, they refuel their electric buses whenever a charger is available so that the number of charge sessions is maximized. The method from [44] works somewhat differently by minimizing the cost of energy with respect to the time of use tariffs  $\mu_{e-on}$  and  $\mu_{e-off}$ .

The comparison we observe is given for a 10-bus, 10-charger scenario and a single group. Each method was used to compute a charge schedule and the costs from demand, facilities, and energy charges are given in Fig. 4.12. Note how the baseline algorithm suffers significantly from the demand charges associated with On-Peak Power, and [44] incurs additional cost from the facilities charges, indicating that an emphasis on energy charges and habitual charging patterns can be improved.

We observe where the differences in cost originate in Fig. 4.14. Observe how the baseline charge profile achieved the largest 15-minute average power between 19:12 and 21:36

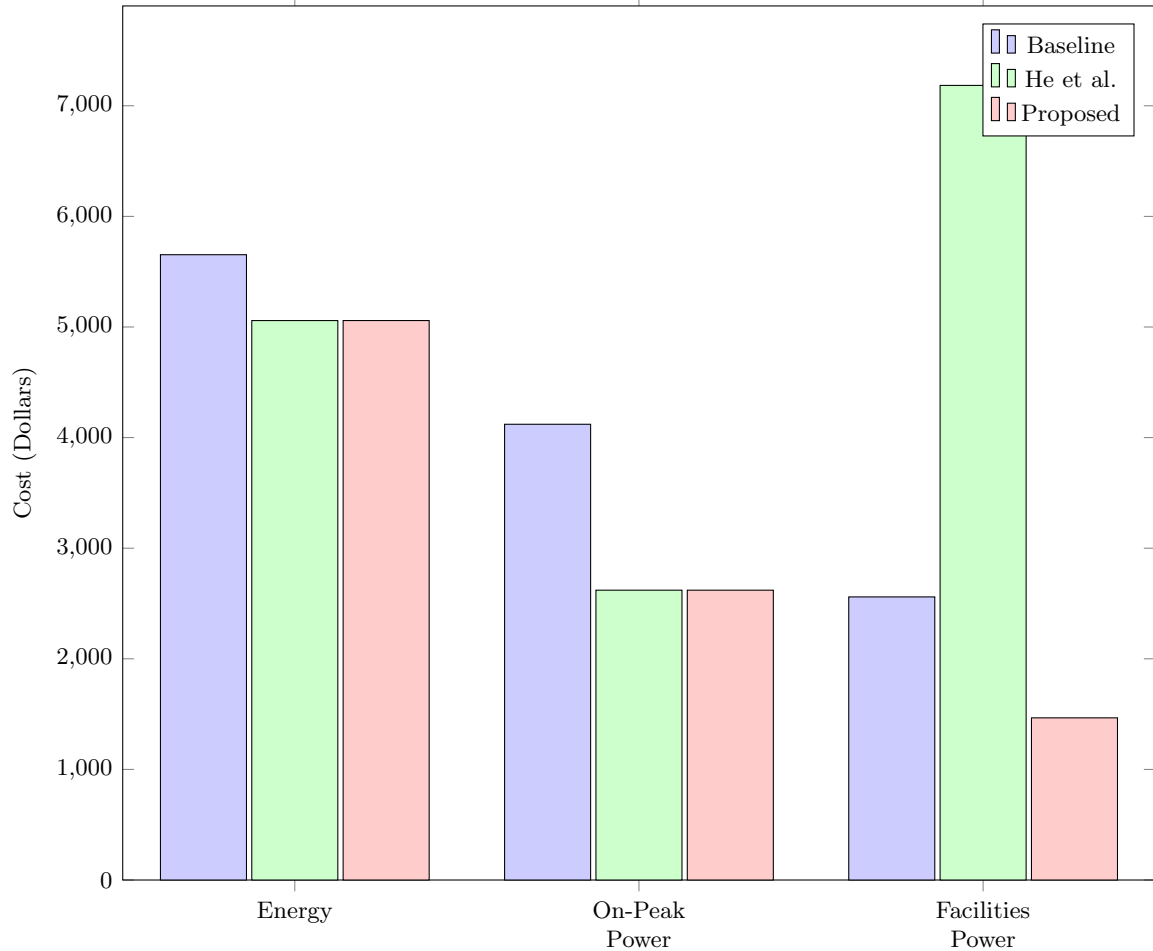


Fig. 4.12: Cost comparison with prior work

which is during on-peak hours and consequently yielded the large On-Peak Power charges given in Fig. 4.12. Additionally, note how the proposed method maintains a relatively flat power profile so that the load is balanced throughout the day which we investigate in Fig. 4.13.

In Fig. 4.13, note how the proposed method produces a bus load that mirrors the uncontrolled load, yielding the flat load profile from Fig. 4.14 which is especially prevalent from 7:12 to 14:24. The results show that the proposed method works well, outperforming both historical patterns at UTA as well and improves upon prior academic techniques.

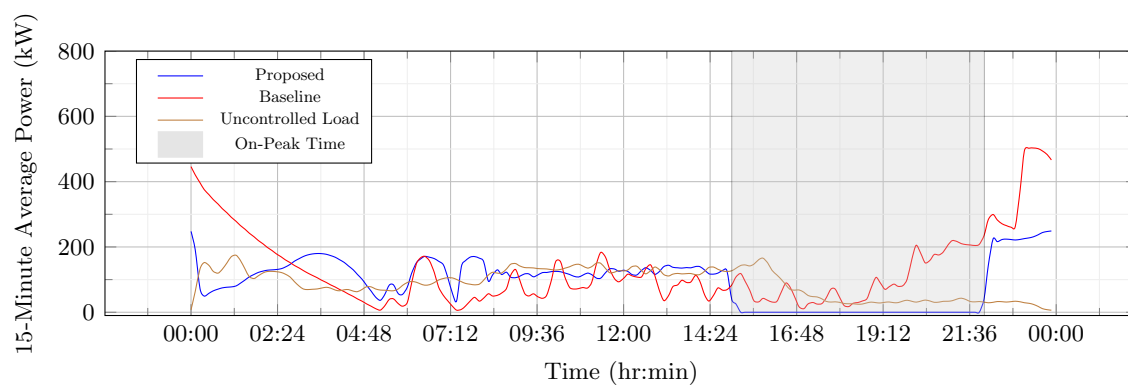


Fig. 4.13: Comparison between uncontrolled and bus loads

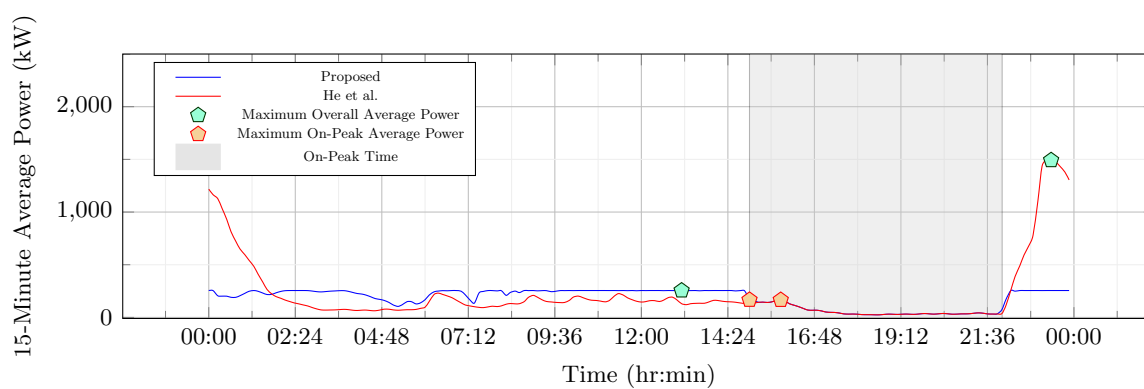


Fig. 4.14: 15-Minute average power for one day

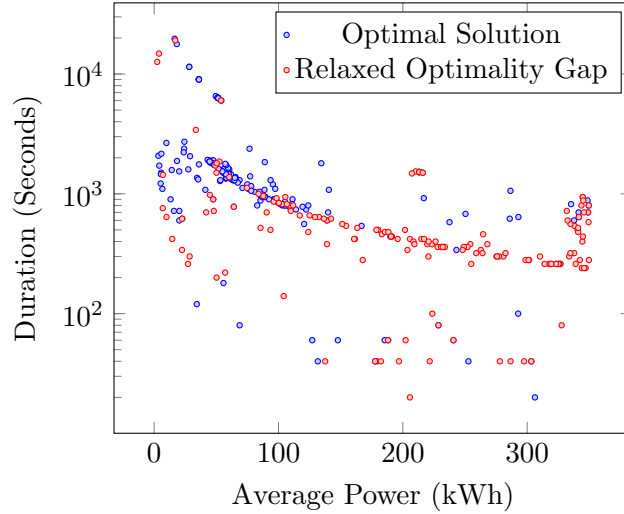


Fig. 4.15: Comparison of charge session duration vs average charge rate

#### 4.10.2 Optimality Gaps and Contention

In the previous section, we discussed performance of the proposed method when each program is solved to an optimal solution. In general, the most computationally demanding solution addressed bus-to-charger placement and generally requires a gap of  $1 \times 10^{-5}$  for optimality. This work also seeks to address how to compute a solution in a scalable manner and so this section reviews computational time as the number of buses increases.

This section considers a 7-charger scenario and compares runtime results for 8, 9, and 10 buses to illustrate how runtimes for set optimality gaps change as contention increases. Fig. 4.16 shows how the computational time increases as the optimality gap decreases. Note how the computational time suddenly increases as the gap decreases, a phenomena which is exacerbated as contention increases. Additionally, note that the optimality gaps are small even before the sudden increase in runtime indicating that it may not be necessary to solve past the turning point where the runtime suddenly increases.

#### 4.10.3 Contention: Sub-Optimal Schedules

In the previous section we observed that the proposed method cannot scale with contention if the optimality gap dips below the turning point where runtime suddenly increases. In this section, we show that a relaxed optimality gap in the charger placement problem

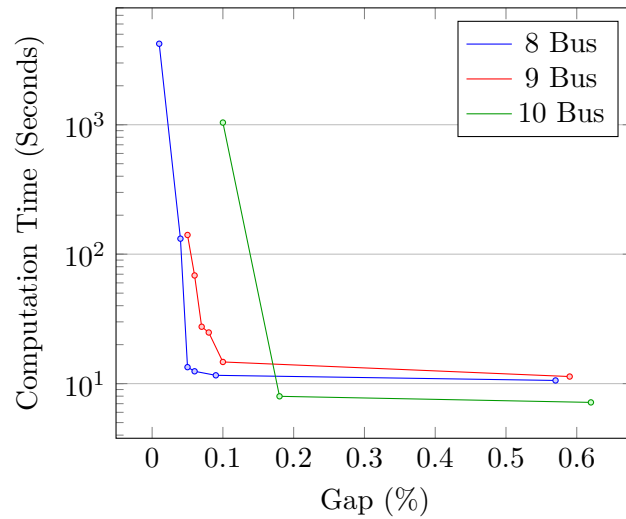


Fig. 4.16: Comparison of Runtime for a 7-Charger Scenario

may result in an undesirable solution and consequently that there exist scenarios that require small optimality gaps which normally lie beyond the turning point shown in Fig. 4.16, indicating the need to reduce the charger assignment problem’s computational complexity.

Fig. 4.15 displays the charge session durations as a function of average charge rate for two 18 bus 6 charger scenarios where the first was computed using a small optimality gap and the second resulted when the gap was relaxed. Note how the charge sessions from the optimal solution tend to have larger session durations and lower charge rates than the relaxed solution which is desired because sessions with low charge rates and long durations are simpler to carry out in practice.

Figures 4.17 and 4.18 show the corresponding optimal and relaxed charge plans by letting the color at the  $i, j$  location represent the charge rate for bus  $i$  at time  $j$  and show why an optimal solution to the charger assignment problem yields better charge sessions. Observe how the first sessions for buses 1 – 4 and 6 – 13 are assigned to a single charger in the relaxed solution, which compresses the charge sessions to accommodate the large number of buses while the remaining chargers appear to have one session at most. In comparison, the optimal solution in Fig. 4.18 has a more evenly distributed session load for each charger so that each session is lengthened, leading to lower charge rates.

It is also interesting to note that the monthly costs of each solution may or may not

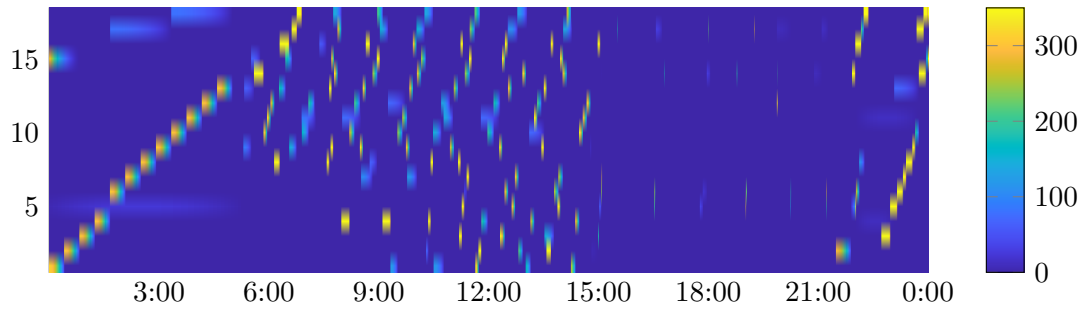


Fig. 4.17: Routes with a large gap in the route placement problem

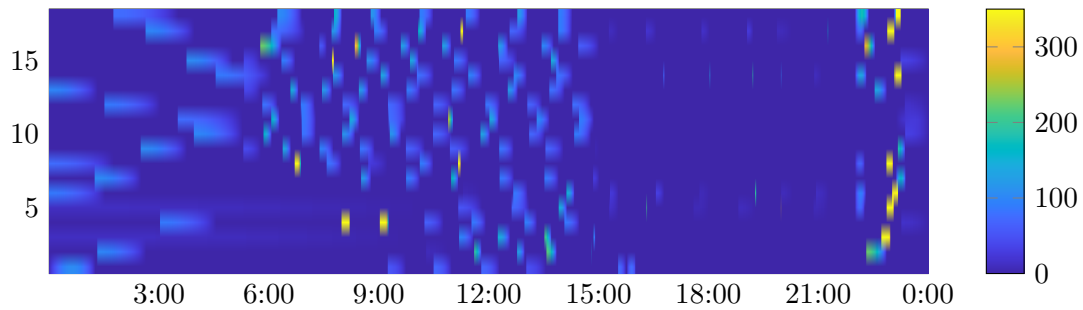


Fig. 4.18: Routes with a small gap in the route placement problem

be equivalent even though an optimal solution is clearly superior. Therefore, a small gap is required to consistently achieve optimal session placement. We also know from Fig. 4.16 that small optimality gaps may increase the number of computations so that the charger assignment problem becomes intractable for large numbers of buses.

#### 4.10.4 The Importance of Groups

One contribution this work provides is a *scalable* way to compute cost-oriented charge schedules. We know from the previous section that the charger assignment problem will not scale for small optimality gaps. This section describes how the computational complexity of the charger assignment problem can be managed by separating the buses into groups so that the charger assignment problem can be solved for each group independently.

In this section, we consider a 18 bus, 12 charger scenario with a 0.13% gap in the charger assignment problem. Fig. 4.19, shows the respective runtimes for a one and two group scenario as computed in Section 4.4. Note how the runtime for the two group scenario is several orders of magnitude less than the runtime for the single group case which

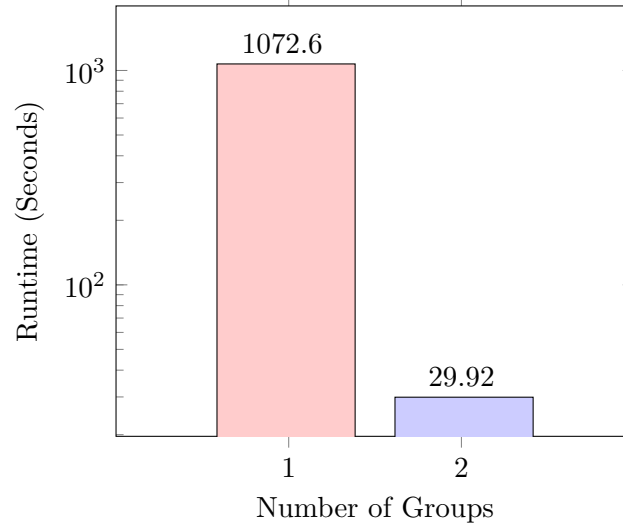


Fig. 4.19: Runtimes for a 18 bus 12 charger scenario at a 0.13% gap

demonstrates how a small number of groups can manage the runtime for optimal charger assignment solutions.

#### 4.10.5 Effects of defragmentation

This paper also addresses the operational preference to consolidate charge sessions when possible. This section demonstrates the effectiveness of the defragmentation method given in Section 4.5 and how consolidation affects the monthly cost. In Section 4.5, the threshold for defragmentation is given by the minimum allowable energy per charge session. In this section we compare two 40 bus 7 charger scenarios where the first contains results without defragmentation and the second consolidates charge sessions so that each session delivers at least 30 kWh. The results for each session are presented in Figs. 4.21 and 4.20 where the color of  $i, j$  element of a figure represents the charge rate for bus  $i$  during time  $j$ . Note how Fig. 4.21 contains *many* small and inconsequential charge sessions and requires each bus to charge each time it enters the station. In comparison, Fig. 4.20 contains only a handful of charge sessions so that each bus only need charge 4 – 5 times throughout the day.

Furthermore, Fig. 4.22 demonstrates that despite the additional constraints associated

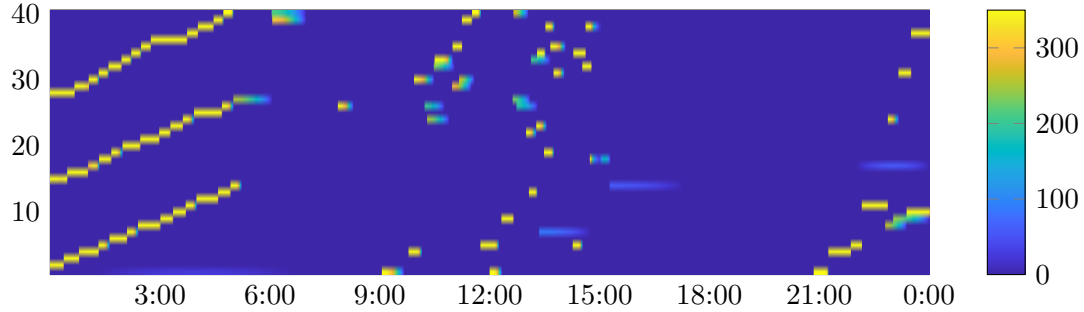


Fig. 4.20: Routes with De-Fragmentation

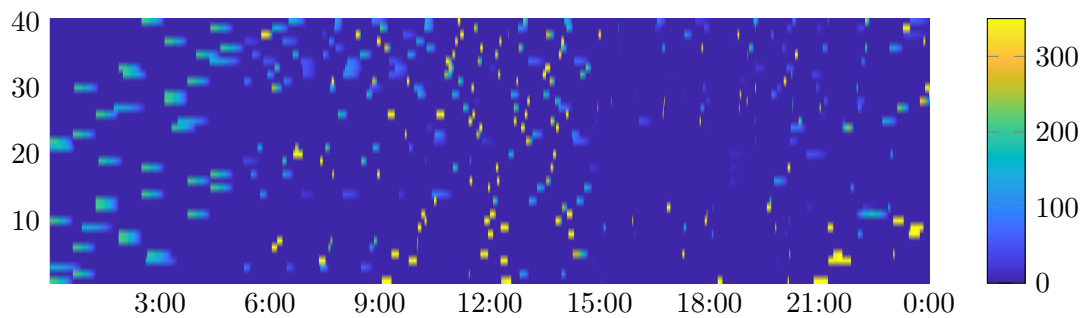


Fig. 4.21: Routes without De-Fragmentation

with consolidation, the monthly cost remains consistent over a large window of thresholds. As the minimum allowable energy per session increases, the number of binary variables in the defragmentation problem increases, resulting in significant runtimes for the defragmentation problem as shown in Fig. 4.23. However, because buses are divided into groups prior to defragmentation, the smaller groups decrease the computational complexity for defragmentation so that larger consolidation thresholds can be applied in a scalable manner.

#### 4.10.6 Scalability

In this section, we consolidate what we have learned in the previous sections to demonstrate how the proposed framework can be used to compute a scalable and cost effective solution for large numbers of buses. This section focuses on a scenario with a minimum energy per session of 20 kWh, a relaxed gap for the charger assignment solution, and a single group.

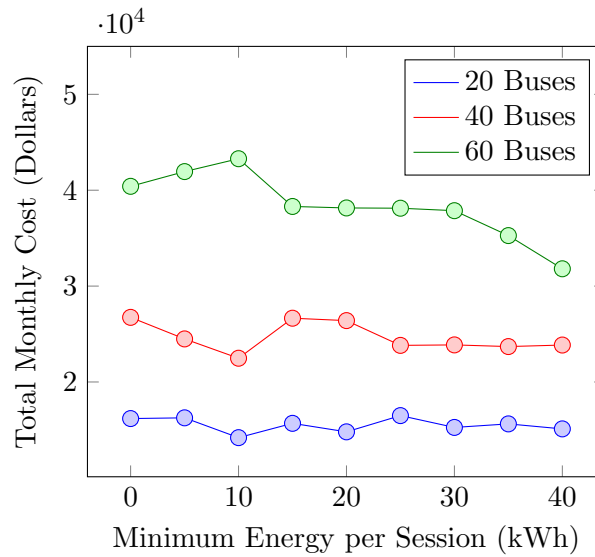


Fig. 4.22: Cost comparison of different defragmentation thresholds in a pro-time optimization scheme.

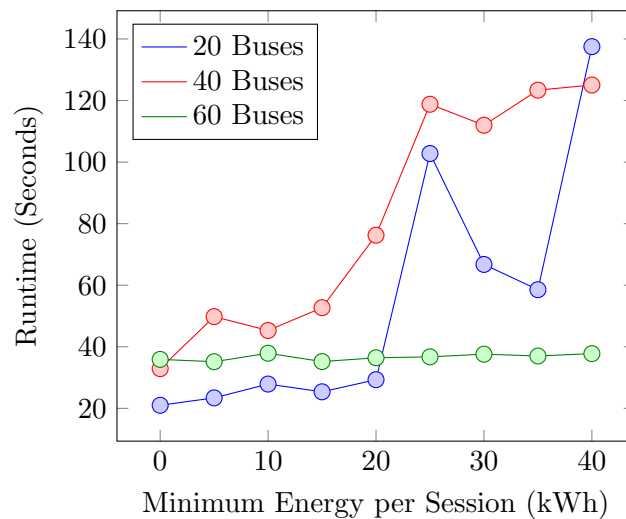


Fig. 4.23: Comparison of runtime for the uncontested and contested scenarios over different de-fragmentation criteria

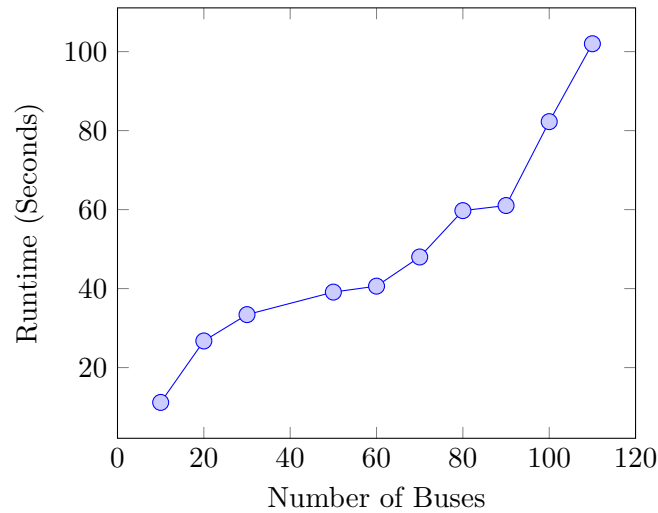


Fig. 4.24: Runtime comparison for different numbers of buses

The results given in Fig. 4.24 show a runtime that generally increases by one second per bus from 10 to 110 buses. One would expect the runtime to increase at least on the order of  $O(n^2)$  for a globally optimal solution because of the coupling between bus variables. The fact that the proposed method appears linear on the given range indicates a scalable solution.

Generally, one would also expect such savings to come with significant increases to the monthly cost. The results in Fig. 4.25 however demonstrate how the proposed solution yields a quasi-linear increase of approximately \$404.10 dollars per bus per month.

#### 4.11 Conclusions

In summary, this paper proposes a method to compute cost-oriented charge schedules for large numbers of battery electric buses by dividing the charge problem into several sub-problems which focus on energy placement and group separation, charge session length and assignment, and cost optimization. The proposed method has been shown to scale as both the runtime and monthly cost increase linearly with the number of buses.

Furthermore, because the proposed method contains a number of sub-problems, setting the optimization criteria for each sub-problem gives the user flexibility so that the proposed method can be adapted to solve a variety of scenarios and optimization preferences.

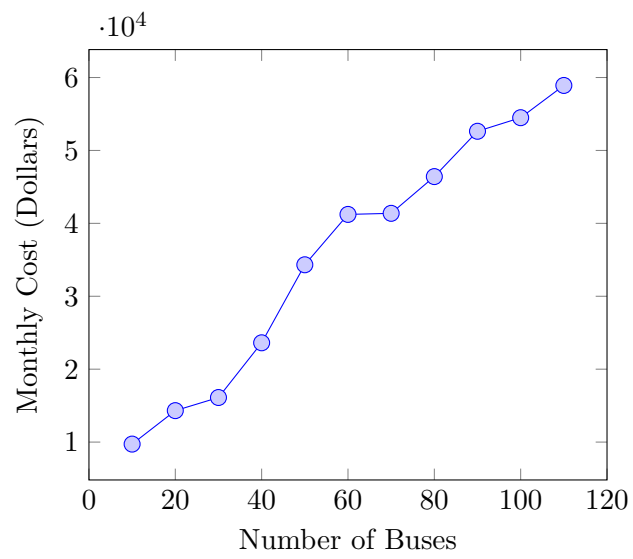


Fig. 4.25: Cost comparison for different numbers of buses

Variable	Description	Range	Variable	Description	Range
Indices					
$i$	Bus index	$\mathbb{N}$	$j$	Time Index	$\mathbb{N}$
$k$	Charger index	$\mathbb{N}$	$r$	Route Index	
$m$	group index	$\mathbb{N}$			
Optimal Solution — Formulation					
$n_{\text{bus}}$	The number of buses in the optimization framework.	$\mathbb{Z}$	$n_{\text{time}}$	The number of time indices in a day.	$\mathbb{Z}^+$
$b_{p(i,j)}$	The average power consumed by bus $i$ during time period $j$ .	$\mathbb{R}$	$t_j$	The time at time index $j$ . This paper also refers to the period of time from $t_j$ to $t_{j+1}$ as “period $t_j$ ”.	$\mathbb{R}$
$\mathbf{b}$	A vector containing each value for $b_{p(i,j)}$ .	$\mathbb{R}^{n_{\text{bus}} \cdot n_{\text{time}}}$	$\tilde{\mathcal{A}}$	The complement of $\mathcal{A}$ .	$i \times j$
$\mathcal{A}$	The set of all $i \times j$ elements where bus $i$ can charge at time index $j$	$i \times j$	$p_{\text{max}}$	The maximum power a bus charger can deliver to a bus in kW. This paper assumes a value of 350 for most examples and results.	$\mathbb{R}^+$
Optimal Solution — Battery					
$h_{\text{min}}$	The minimum allowable state of charge	$(0, h_{\text{max}})$	$h_{\text{max}}$	The maximum state of charge	$\mathbb{R}^+$
$\eta_i$	The beginning state of charge for bus $i$	$(h_{\text{min}}, h_{\text{max}})$	$h(ij)$	The state of charge for bus $i$ at time $t_j$ .	$(h_{\text{min}}, h_{\text{max}})$

$\Delta T$	The change in time from $t_j$ to $t_{j+1}$	$\mathbb{R}_+$	$\mathbf{h}$	A vector containing all state of charge values.	$\mathbb{R}_+^{n_{\text{bus}} \cdot n_{\text{time}}}$
$\delta(i, j)$	The battery discharge for bus $i$ during time period $j$ .	$\mathbb{R}_+$	$h(i, \text{end})$	Bus $i$ 's final state of charge.	$(h_{\min}, h_{\max})$

---

### Optimal Solution — Cumulative Load Management

---

$n_{\text{charger}}$	The time index for the start of bus $i$ 's $j^{\text{th}}$ stop	$\mathbb{Z}_+$	$p_c(j)$	The average power consumed by all buses during time period $j$ .	$\mathbb{R}$
$\mathbf{p}_c$	A vector containing all values of $p_c(j)$ .	$\mathbb{R}_+^{n_{\text{time}}}$	$J_{\text{thrash}}$	A secondary objective function which penalizes multiple plug-in instances per charge session.	$\mathbb{R}_+$
$g(i, j)$	A slack variable used to compute the absolute value of $ b_{p(i, j)} - b_{p(i, j-1)} $	$\mathbb{R}_+$			

---

### Optimal Solution — Objective

---

$\mu_{\text{e-on}}$	On-Peak Energy Rate	$\mathbb{R}_+$	$\mu_{\text{e-off}}$	Off-Peak Energy Rate	$\mathbb{R}_+$
$\mu_{\text{p-on}}$	On-Peak Demand Power Rate	$\mathbb{R}_+$	$\mu_{\text{p-all}}$	Facilities Power Rate	$\mathbb{R}_+$
$\mathcal{S}_{\text{on}}$	The set of on-peak time indices	$\{1, \dots, n_{\text{time}}\}$	$p_{\text{demand}}$	Maximum average power during on-peak periods	$\mathbb{R}$
$p_{\text{facilities}}$	Maximum average power over all time instances.	$\mathbb{R}_+$	$p_t(j)$	The total average power consumed by both the bus chargers and the uncontrolled loads.	$\mathbb{R}_+^{n_{\text{time}}}$

$u(j)$	The average power over time $j$ consumed by the uncontrolled loads	$\mathbb{R}_+^{n_{\text{time}}}$	$\mathbf{p}_t$	a vector containing $p_t(i)$ for all $i$ .	$\mathbb{R}_+^{n_{\text{time}}}$
$e_{\text{on}}$	The total amount of energy consumed by the bus chargers and uncontrolled loads during off-peak hours.	$\mathbb{R}_+$	$e_{\text{off}}$	The total energy consumed by the bus chargers and uncontrolled loads during on-peak hours.	$\mathbb{R}_+$
$J_{\text{cost}}$	The section of the objective function pertaining to the fiscal expense of charging buses.	$\mathbb{R}$	$J_{\text{all}}$	The expression for the complete objective function.	$\mathbb{R}$
Scalability					
$n_{\text{group}}$	The number of groups in which to divide the buses and available chargers in preparation for the $p_4$ , $p_5$ , and $p_6$ .	$\mathbb{Z}_+$	$n_{\text{charger}}^m$	The number of chargers assigned to group $m$ .	$\mathbb{Z}_+$
$n_{\text{bus}}^m$	The number of buses in group $m$ .	$\mathbb{Z}_+$	$p(j, m)$	The total power used during time index $j$ by all buses in group $m$ .	$\mathbb{R}_+$
$\beta(i, m)$	A binary selector variable which is one when bus $i$ is in group $m$ and zero otherwise.	$\{0, 1\}$	$n_{\text{charger}}^m$	The number of chargers assigned to group $m$	$\mathbb{Z}_+$
$\phi(i, i')$	The inner product of the optimal charge schedules for buses $i$ and $i'$ respectively.	$\mathbb{R}_+$	$v(i, i', g)$	A variable that is $w(i, i')$ when buses $i$ and $i'$ are in group $g$ and zero otherwise.	$\mathbb{Z}_+$
$M_s$	The maximum value for $\phi(i, i')$ .	$\mathbb{R}_+$	$J_{\text{select}}$	The objective function for the group-selection problem	$\mathbb{R}_+$
Defragmentation					

$\theta(i, r)$	A binary variable which is one when charge session $r$ from bus $i$ will be used in a defragmented solution.	$\{0, 1\}$	$\rho(i, r)$	A vector whose elements are equal to $\Delta T$ during time indices when bus $i$ is charging during charge session $r$ and zero otherwise.	$\mathbb{R}^{n_{\text{time}}}$
----------------	--	------------	--------------	--	--------------------------------

$\psi(i, j)$	The minimum allowable energy delivered to bus $i$ during charge session $r$ where the session in question is considered “active”.	$\mathbb{R}$	$\omega$	The minimum allowable energy for any charge session.	$\mathbb{R}$
--------------	---	--------------	----------	--	--------------

$e_{\max}$	The maximum allowable energy delivered in any session.	$\mathbb{R}$
------------	--	--------------

---

### Charge Schedules

$a(i, r)$	The beginning of the allowable charge interval for bus $i$ 's $r^{\text{th}}$ charge session.	$\mathbb{R}_+$	$b(i, r)$	The commanded start time for bus $i$ 's $r^{\text{th}}$ charge session	$\mathbb{N}$
-----------	---	----------------	-----------	--	--------------

$f(i, r)$	The commanded end time for bus $i$ 's $r^{\text{th}}$ charge session.	$\mathbb{R}_+$	$d(i, r)$	The end time of the allowable charge interval for bus $i$ 's $r^{\text{th}}$ charge session.	$\mathbb{R}_+$
-----------	---	----------------	-----------	--	----------------

$\sigma(i, r, k)$	A selector variable which is one when bus $i$ charges at charger $k$ for session $r$ .	$\{0, 1\}$	$M$	The number of seconds in a day	$\mathbb{Z}_+$
-------------------	--	------------	-----	--------------------------------	----------------

$l(i, r, i', r')$	A selector variable which is one when bus $i$ charges before bus $i'$ during the $r$ and $r'$ sessions respectively.	$\{0, 1\}$
-------------------	--	------------

---

### Optimizing Charge Schedules

$c(s, i, r)$	The start time for bus $i$ 's $r^{\text{th}}$ charge session.	$\mathbb{R}$	$c(f, i, r)$	The stop time for bus $i$ 's $r^{\text{th}}$ charge session.	$\mathbb{R}$
--------------	---	--------------	--------------	--	--------------

---

$c(a, i, r)$	The arrival time of bus $i$ for charge session $r$ .	$\mathbb{R}$	$c(d, i, r)$	The departure time for bus $i$ after having completed the $r^{\text{th}}$ charge session	$\mathbb{R}$
--------------	--	--------------	--------------	--	--------------

---

$J_{\text{window}}$	The loss function which drives charge windows to the desired length.	$\mathbb{R}$			
---------------------	--	--------------	--	--	--

---

Multi-Rate Charging

---

$x(i, j)$	The final charge schedule for bus $i$ at time $j$ , yielding the power at which bus $i$ will charge.	$\mathbb{R}_+$	$z(j)$	The total power used by all buses at time $j$ .	$\mathbb{R}_+$
-----------	--	----------------	--------	---	----------------

---

$\gamma(i, d)$	A binary vector which is one at all time steps where bus $i$ charges during charge session $d$ .	$\{0, 1\}^{n_{\text{time}}}$	$e(i, r)$	The amount of energy to be delivered to bus $i$ during charge session $r$ .	$\mathbb{R}_+$
----------------	--	------------------------------	-----------	---	----------------

---

$J_{\text{multi-rate}}$	The objective function over which we minimize to solve the multi-rate section of the bus charge problem.	$\mathbb{R}_+$			
-------------------------	--	----------------	--	--	--

---

## CHAPTER 5

### Conclusions

The research objective for this dissertation was to find a cost effective way to charge large BEB fleets with a solution which addressed the following considerations: battery capacity, BEB state of charge and energy demands, bus availability, contention for chargers, charger power capacity, smooth charge schedules, meaningful charge sessions, precise charge plans, and manageable compute times.

Because this dissertation follows a multi-paper format, we begin exploring solutions to the charge problem in Chapter 2 which formulates the charge problem discretely as a graph search problem. We found that solutions to this problem addressed a number of the aforementioned constraints including battery capacity, route energy demands, meter aggregation and arrival and departure times so that the plan did not impact bus schedules but fell short in two ways. First, the schedule was only as precise as the granularity of the temporal discretization. More precision required many additional variables, making the problem intractable for precise solutions. Second, more buses introduced more variables making this method computationally expensive for fleets of size 20 and computationally infeasible after 40 on a desktop computer.

Chapter 3 focuses on a method which computes precise charge schedules by starting with a bin packing approach to charge scheduling so that the charge plan variables are continuous instead of discrete which demonstrated significant improvements in compute time as a function of accuracy. However, Chapter 3 does not allow for multi-rate charging and continues to fail with fleet sizes surpassing 40 BEBs because the compute time quickly increases with the number of buses.

Finally, Chapter 4 organizes the desired solution features in the charge problem into sub-problems which make up an eight-part solution where each succeeding problem uses information in the solutions from previous problems to simplify their formulation. Addi-

tionally, the multi-problem framework allows the user to specify different optimality criteria for each sub-problem which makes the approach in Chapter 4 flexible and able to scale both computationally and cost-wise with different environments and scenarios. Results for Chapter 4 show how the method from Chapter 4 can compute cost-oriented charge plans for 110 buses in under two minutes which is significant.

## CHAPTER 6

### Future Work

Findings from this dissertation have demonstrated that not only can we find charge plans that minimize cost for BEB fleets, but we can also find these plans with manageable compute time. Future work might extend the results from this dissertation in a number of ways.

A likely extension of this work might discuss how to optimally charge BEB fleets when the charging infrastructure is decentralized so that there are more than one charge station. Up to this point, we have only considered availability in terms of binary parameters, 0 if a bus is not available, and 1 if the bus is in the station. Adding more than one charge station changes that underlying assumption so that availability depends on which station a bus enters.

Electric vehicles may also be desired for a police force because they accelerate quickly and would do well to support law enforcement. Planning for patrol routes would be difficult as each patrol vehicle would need to account for state of charge, availability, power, etc. but must also be ready for the unexpected car chase. The methods in this dissertation could also be used to plan for Electric postal or UPS vehicles for similar reasons.

Much of this work may also transfer to USU's recent "connected communities" program which looks at methods for allocating power for buildings and apartment complexes. In fact,  $p_1$  from Chapter 4 may be sufficient because buildings are always connected to the grid, making them perpetually available to "charge" or draw power.

## REFERENCES

- [1] D. Zhou, Z. Ren, K. Sun, and H. Dai, "Optimization method of fast charging buses charging strategy for complex operating environment," in *2nd IEEE Conf. on Energy Internet and Energy System Integration (EI2)*, 2018.
- [2] H. Kato, R. Ando, Y. Kondo, T. Suzuki, K. Matsushashi, and S. Kobayashi, "Comparative measurements of the eco-driving effect between electric and internal combustion engine vehicles," in *2013 World Electric Vehicle Symposium and Exhibition (EVS27)*, 2013, pp. 1–5.
- [3] K. Poornesh, K. P. Nivya, and K. Sireesha, "A comparative study on electric vehicle and internal combustion engine vehicles," in *2020 International Conference on Smart Electronics and Communication (ICOSEC)*, 2020, pp. 1179–1183.
- [4] M. Mahmoud, R. Garnett, M. Ferguson, and P. Kanaroglou, "Electric buses: A review of alternative powertrains," *Renewable and Sustainable Energy Reviews*, vol. 62, pp. 673–684, 2016.
- [5] Q. Cheng, L. Chen, Q. Sun, R. Wang, and D. Ma, "A smart charging algorithm-based fast charging station with energy storage system-free," *CSEE JPES*, vol. 7, no. 4, pp. 850–861, 2020.
- [6] D. Stahleder, D. Reihs, S. Ledinger, and F. Lehfuss, "Impact assessment of high power electric bus charging on urban distribution grids," in *IEEE Industrial Electronics Society*, vol. 1, 2019, pp. 4304–4309.
- [7] S. Deb, K. Kalita, and P. Mahanta, "Impact of electric vehicle charging stations on reliability of distribution network," in *IEEE Internat. Conf. on Tech. Adv. in Power and Energy*, 2017, pp. 1–6.
- [8] T. Boonraksa, A. Paudel, P. Dawan, and B. Marungsri, "Impact of electric bus charging on the power distribution system a case study IEEE 33 bus test system," in *IEEE Grand Internat. Conf. and Exposition Asia*, 2019, pp. 819–823.
- [9] B. Csonka, "Optimization of static and dynamic charging infrastructure for electric buses," *Energies*, vol. 14, no. 12, p. 3516, 2021.
- [10] S. Y. Jeong, J. H. Park, G. P. Hong, and C. T. Rim, "Automatic current control by self-inductance variation for dynamic wireless EV charging," in *IEEE Workshop on Emerg. Tech.: Wireless Power Transfer*, 2018, pp. 1–5.
- [11] B. J. Balde and A. Sardar, "Electric road system with dynamic wireless charging of electric buses," in *IEEE Trans. Electrification Conf.*, 2019, pp. 1–4.
- [12] Y. Alwesabi, F. Avishan, I. Yanikoglu, Z. Yiu, and Y. Wang, "Robust strategic planning of dynamic wireless charging infrastructure for electric buses," *Applied Energy*, vol. 230, p. 120806, 2022.

- [13] S. Jain, Z. Ahmad, M. S. Alam, and Y. Rafat, "Battery swapping technology," in *IEEE Internat. Conf. on Recent Advances and Innovations in Engineering*, 2020, pp. 1–4.
- [14] X. Zhang and G. Wang, "Optimal dispatch of electric vehicle batteries between battery swapping stations and charging stations," in *IEEE Power and Energy Society General Meeting*, 2016, pp. 1–5.
- [15] M. Rinalde, E. Picarelli, A. D'Ariano, and F. Viti, "Mixed-fleet single-terminal bus scheduling problem: Modeling, solution scheme and potential applications," *Omega*, vol. 96, p. 102070, 2020.
- [16] Y. Zhou, L. Xiaoyue, W. Ran, and dummy, "Bi-objective optimization for battery electric bus deployment considering cost and environmental equity," *IEEE Transactions on Intelligent Transportation Systems*, vol. 22, no. 4, pp. 2487–2497, 2021.
- [17] J. Whitaker, G. Droge, M. Hansen, D. Mortensen, and J. Gunther, "A network flow approach to battery electric bus scheduling, in review," *IEEE Transactions on Intelligent Transportation Systems*.
- [18] R. M. Power, "Rocky mountain power electric service schedule no. 8." [Online]. Available: [https://www.rockymountainpower.net/content/dam/pcorp/documents/en/rockymountainpower/rates-regulation/utah/rates/008\\_Large\\_General\\_Service\\_1\\_000\\_kW\\_and\\_Over\\_Distribution\\_Voltage.pdf](https://www.rockymountainpower.net/content/dam/pcorp/documents/en/rockymountainpower/rates-regulation/utah/rates/008_Large_General_Service_1_000_kW_and_Over_Distribution_Voltage.pdf)
- [19] R.-C. Leou and J.-J. Hung, "Optimal charging schedule planning and economic analysis for electric bus charging stations," *Energies*, vol. 10, no. 4, 2017.
- [20] J. He, N. Yan, J. Zhang, Y. Yu, and T. Wang, "Battery electric buses charging schedule optimization considering time-of-use electricity price," *Journal of Intelligent and Connected Vehicles*, 2022.
- [21] Y. Liu, L. Wang, Z. Zeng, and Y. Bia, "Optimal charging plan for electric bus considering time-of-day electricity tariff," *Journal of Intelligent and Connected Vehicles*, vol. 5, pp. 123–137, 2022.
- [22] I. Ojer, A. Berrueta, J. Pascual, P. Sanchis, and A. Ursua, "Development of energy management strategies for the sizing of a fast charging station for electric buses," in *IEEE International Conference on Environment and Electrical Engineering*, 2020, pp. 1–6.
- [23] N. Qin, A. Gusrialdi, R. Paul Brooker, and A. T-Raissi, "Numerical analysis of electric bus fast charging strategies for demand charge reduction," *Transactions on Research Part A: Policy and Practice*, vol. 94, pp. 386–396, 2016.
- [24] G. Wang, X. Xie, F. Zhang, Y. Liu, and D. Zhang, "Bcharge: Data-driven real-time charging scheduling for large-scale electric bus fleets," *Proceedings - Real-Time Systems Symposium*, pp. 45–55, 2019.
- [25] A. Bagherinezhad, A. D. Palomino, B. Li, and M. Parvania, "Spatio-temporal electric bus charging optimization with transit network constraints," *IEEE Transactions on Industrial Applications*, vol. 56, no. 5, pp. 5741–5749, 2020.

- [26] Y. He, Z. Song, and Z. Liu, "Fast-charging station deployment for battery electric bus systems considering electricity demand charges," *Sustainable Cities and Society*, vol. 48, p. 101530, 2019.
- [27] R. Wei, X. Liu, Y. Ou, and S. Kiavash Fayyaz, "Optimizing the spatio-temporal deployment of battery electric bus system," *Journal of Transport Geography*, 2018.
- [28] Y. Alwesabi, Z. Liu, S. Kwon, and Y. Wang, "A novel integration of scheduling and dynamic wireless charging planning models of battery electric buses," *Energy*, 2021.
- [29] N. I. Nimalsiri, C. P. Mediwaththe, E. L. Ratnam, M. Shaw, D. B. Smith, and S. K. Halgamuge, "A survey of algorithms for distributed charging control of electric vehicles in smart grid," *IEEE Transactions on Intelligent Transportation Systems*, vol. 21, no. 11, pp. 4497–4515, 2020.
- [30] N. El-Taweel and E. Farag, "Incorporation of battery electric buses in the operation of intercity bus services," in *2019 IEEE Transportation Electrification Conference and Expo (ITEC)*, 2019.
- [31] R. Wei, X. Liu, Y. Ou, and S. K. Fayyaz, "Optimizing the spatio-temporal deployment of battery electric bus system," *Journal of Transport Geography*, vol. 68, pp. 160,168, 2018.
- [32] G.-J. Zhou, D.-F. Xie, X.-M. Zhao, and C. Lu, "Collaborative optimization of vehicle and charging scheduling for a bus fleet mixed with electric and traditional buses," *IEEE Access*, 2020.
- [33] J. Whitaker, G. Droge, M. Hansen, D. Mortensen, and J. Gunther, "A network flow approach to battery electric bus scheduling," *IEEE Transactions on Intelligent Transportation Systems*, 2023.
- [34] A. Jahic, M. Eskander, and D. Schulz, "Preemptive vs. non-preemptive charging schedule for large-scale electric bus depots," in *2019 IEEE PES Innovative Smart Grid Technologies Europe*, 2019.
- [35] Q. Gao, Z. Lin, T. Zhu, W. Zhou, G. Wang, T. Zhang, Z. Zhang, M. Waseem, S. Liu, and C. Han, "Charging load forecasting of electric vehicle based on monte carlo and deep learning," in *2019 IEEE Sus. Power and Energy Conf.*, 2019.
- [36] N. El-Taweel, H. Farag, and M. Moataz, "Integrated utility-transit model for optimal configuration of battery electric bus systems," *IEEE Systems Journal*, 2020.
- [37] N. El-Taweel, H. Farag, G. Barai, H. Zeineldin, A. Al-Durra, and E. El-Saadany, "A systematic approach for design and analysis of electrified public bus transit fleets," *IEEE Systems Journal*, 2022.
- [38] A. Houbbadi, E. Redondo-Iglesias, R. Trigui, S. Pelissier, and T. Bouton, "Optimal charging strategy to minimize electricity cost and prolong battery life of electric bus fleet," in *IEEE Vehicle Power and Propulsion Conf.*, 2019, pp. 1–6.

- [39] Gurobi Optimization, LLC, “Gurobi Optimizer Reference Manual,” 2022. [Online]. Available: <https://www.gurobi.com>
- [40] N. Ma and Z. Zhou, “Mixed-integer programming model for two-dimensional non-guillotine bin packing problem with free rotation,” in *Internat. Conf. for Information Science and Control Engineering*, 2017, pp. 456,460.
- [41] J. Ji, Y. Bie, Z. Zeng, and I. Wang, “Trip energy consumption estimation for electric buses,” *Communications in Transportation Research*, vol. 2, p. 100069, 2022.
- [42] X. Rong, B. Wang, C. Shao, G. Yu, Y. Wang, Q. Sun, and Z. Bie, “Coordinated charging strategy of electric vehicle charging station based on combination of linear power flow and genetic algorithm,” in *IEEE Asia-Pacific Power and Energy Engineering Conf.*, 2016, pp. 1772–1776.
- [43] “A branch and bound algorithm for the knapsack problem,” vol. 13, pp. 723–735.
- [44] J. He, N. Yan, J. Zhang, Y. Yu, and T. Wang, “Battery electric buses charging schedule optimization considering time-of-use electricity price,” *Journal of Intelligent and Connected Vehicles*, pp. 138–145, 2022.

## CURRICULUM VITAE

**Daniel T. Mortensen****Published Journal Articles**

- A Network Flow Approach to Battery Electric Bus Scheduling, J. Whitaker, G. Droge, M. Hansen, D. Mortensen, J. Gunther, *IEEE Transactions on Intelligent Transportation Systems*, *Accepted*.

**Published Conference Papers**

- Deep Anomaly Detection for Network Traffic, Eric McKinney and Daniel Mortensen in *Asilomar Conference on Signals, Systems, and Computers*, 2021.